NTNU – Trondheim
Norwegian University of
Science and Technology

Numerical Investigation of Wave-Body Interactions in   Shallow Water

Yi Luo

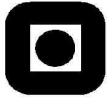Norwegian University of Science and Technology
Department of Marine Technology

MASTER THESIS IN MARINE TECHNOLOGY

SPRING 2013

FOR

Yi Luo

Numerical Investigation of Wave-Body Interactions in Shallow Water
(Numerisk Undersøkelse av Wave-Body Interaksjon i Shallow Water)

Many offshore fields are located in very shallow waters. The investigation of their behavior in such conditions and then the assessment of proper design and operational limits are challenging because non-linear effects typically matter in shallow-water waves and in their interaction with a structure. This requires a non-linear prediction method of the wave-induced loads. Wasim is the non-linear wave load analysis program in the Sesam system, making this a good candidate as a solution tool for this application. The present solver has Airy waves and Stokes 5th order waves as incident wave input. To extend the capability of Wasim an implementation of Stream function wave theory has been made, but this seems to give rise to numerical problems.

The project thesis has confirmed the difficulties in the present Wasim program for the analysis of structures in shallow waters by studying a semi-submersible. It has also examined different wave theories and their applicability in shallow waters.

Objective
The aim of the thesis is to guide toward the extension of WASIM from deep to shallow water applications. The solver will be checked to identify the cause of problems among the possible candidates found during the project thesis. The implementation of other incident-wave theories valid in shallow waters will be also considered, as well as the improvement of the free-surface boundary conditions by introducing nonlinear corrections.

The work should be carried out in steps as follows:

1. Finalize the assessment of the present WASIM implementation by examining the used Stream-function solution for the incident waves and the solver parts where such solution is needed.
2. Assess the influence of nonlinear corrections on the free-surface boundary conditions on the reliability and accuracy of wave-body interaction problems in shallow water.
3. Assess the influence of other more general incident-wave theories, applicable for deep to shallow waters, on the solution for platforms working in different water depths.

The work may show to be more extensive than anticipated. Some topics may therefore be left out after discussion with the supervisor without any negative influence on the grading.

The candidate should in her report give a personal contribution to the solution of the problem formulated in this text. All assumptions and conclusions must be supported by mathematical models and/or references to physical effects in a logical manner.

The candidate should apply all available sources to find relevant literature and information on the actual problem.

The thesis should be organised in a rational manner to give a clear presentation of the work in terms of exposition of results, assessments, and conclusions. It is important that the text is well written and that tables and figures are used to support the verbal presentation. The thesis should be complete, but still as short as possible. In particular, the text should be brief and to the point, with a clear language. Telegraphic language should be avoided.

The thesis must contain the following elements: the text defining the scope (i.e. this text), preface (outlining project-work steps and acknowledgements), abstract (providing the summary), table of contents, main body of thesis, conclusions with recommendations for further work, list of symbols and acronyms, references and (optional) appendices. All figures, tables and equations shall be numerated.

The supervisor may require that the candidate, in an early stage of the work, present a written plan for the completion of the work. The plan should include budget for the use of computer and laboratory resources that will be charged to the department. Overruns shall be reported to the supervisor.

From the thesis it should be possible to identify the work carried out by the candidate and what has been found in the available literature. It is important to give references to the original source for theories and experimental results.

The thesis shall be submitted in two copies:
- The copies must be signed by the candidate.
- This text, defining the scope, must be included.
- The report must appear in a bound volume or a binder.
- Drawings and/or computer prints that cannot be included in the main volume should be organised in a separate folder.
- The bound volume shall be accompanied by a CD or DVD containing the written thesis in World or PDF format. In case computer programs have been made as part of the thesis work, the source codes shall be included. In case of experimental work, the experimental results shall be included in a suitable electronic format.

Supervisor   :Marilena Greco
Submitted   :16 January 2013
Deadline   :10 June 2013

Marilena Greco
Supervisor

Preface

This report is the result of my master thesis written under supervision from both the Department of Marine Technology and Det Norske Veritas. It is a continuation and further study of the project thesis written in the last semester. The project thesis was composed of a literature study of both wave theories and the Rankine panel method and several analyses in Wasim for both learning the program and reproducing the error associated with the stream function method. Then the major work of the master thesis turned to modification and implementation to the source code of the program, and afterwards a significant part of time was used to verify the modification and the new implementations. The update of the program is aimed to provide a combination of the stream function method and proper nonlinear free surface conditions, which should extend the capability of the program dealing with nonlinear problems, especially in shallow water where Stokes 5th wave theory is no longer valid.

The report consists of four chapters. The first chapter includes relevant background theories which are extracted from the project thesis, and most of these theories will be referred later in the rest of the report. Chapter two includes the modification and verification of the stream function method while chapter three includes the implementation and verification of the nonlinear free surface conditions. All the figures, tables and formulas are inserted through the whole report at correct locations instead of being placed in appendix so that readers do not need to flip over pages frequently when reading the paper version.

In final, I would like to give my sincere thanks to my professor Marilena Greco and my supervisor from DNV side, Torgeir Vada, for their guidance, helpful information and valuable availability. Especially Marilena, who spent one hour each week in almost one year to answer my questions and provide me motivations. In addition, I would also like to express my gratitude to Kaijia Han and Jens Bloch Helmers from DNV for their kindly advices and practical support.

Yi Luo

Oslo, June 2013

Abstract

DNV has Wasim (a module of HydroD) as a Rankine panel method potential flow solver originally developed for more concern to deep water analysis. Some attempts have been made to extend the capability of the program in shallow water. The stream function method is chosen and still in development for the current Wasim, but unphysical "pumping" diffractions which may due to numerical problems have been observed. In the previous work, i.e. the project done in the last semester, the error was reproduced and some preliminary possible reasons were proposed.

The main task of this thesis is to fix the bug and test the modification of the program. Then two sets of nonlinear free surface conditions will be implemented which together with the stream function method are purposed to improve the capability of the program when handling nonlinear problems. In final, these two approaches of the nonlinear free surface conditions will be evaluated by comparing with some experiment results. The evaluation process is mainly composed of two parts. Wave diffractions will be tested first by checking the wave loads on a fixed cylinder, and afterwards wave radiations will also be included where the motion responses of a LNG carrier will be studied. The numerical results calculated by Wasim will be compared with the experiment data collected from Huseby & Grue (2000) and the Extreme Seas project respectively.

Contents

List of Symbols

If no explanation is given in the report, the common symbols are defined as following

$H = wave\ height$

$A = wave\ amplitude$

$T = wave\ period$

$\omega = angular\ wave\ frequency = \dfrac{2\pi}{T}$

$L = wave\ length$

$k = wave\ number = \dfrac{2\pi}{L}$

$h = water\ depth$

$t = time\ instant$

$x = horizontal\ coordinate$

$z = vertical\ coordinate$

$\zeta = surface\ elevation$

$c = wave\ celerity\ or\ phase\ speed = \dfrac{L}{T}$

$\phi = water\ velocity\ potential$

$\psi = water\ stream\ function$

$\psi_\zeta = stream\ function\ value\ on\ the\ wave\ profile$

$u = horizontal\ water\ particle\ velocity = \dfrac{\partial \phi}{\partial x} = \dfrac{\partial \psi}{\partial z}$

$w = vertical\ water\ particle\ velocity = \dfrac{\partial \phi}{\partial z} = -\dfrac{\partial \psi}{\partial x}$

$\phi_b = basic\ flow\ potential$

$\phi_l = local\ flow\ potential$

$\phi_m = memory\ flow\ potential$

$\phi_i = incident\ wave\ potential$

$\vec{W} = mean\ velocity\ of\ the\ fluid\ field$

List of Figures

List of Tables

1 Background theory

1.1 Common assumptions and governing equations

i.   The water is homogeneous and incompressible ($\nabla \cdot \boldsymbol{V} = 0$), i.e. ρ is constant if variation of temperature and salinity over water depth are negligible. Thus there is no internal pressure and only surface gravity waves are concerned (e.g. wind-generated waves, but tsunamis or tides are others).

ii. The water is inviscid, i.e. there is no internal shear stresses and no shear stresses on the air-sea interface or on the sea bottom.

iii. The water is initially irrotational, and since it is inviscid it will always be irrotational ($\nabla \times \boldsymbol{V} = 0$). This makes the potential flow theory applicable and together with the first assumption it leads further to a valid Laplace's equation for the velocity potential ($\nabla^2 \phi = 0$).

iv. The wave lengths are at least greater than a few centimeters so that the surface tension becomes unimportant.

v.   The sea bottom is stationary, impermeable and horizontal (also valid for small sloping bottom in shallow water). Therefore the sea bottom is not able to add or absorb any wave energy.

vi. The water pressure is approximated to be equal to the constant atmospheric pressure along the free surface, so the aerostatic pressure difference between the wave crest and trough is negligible.

vii. The water particles on the free surface always remain on the surface. This assumes no particle escaping (no breaking waves).

viii. No stream or current is presented.

These assumptions above will generate the following nonlinear boundary value problem.

$$\frac{\partial^2 \phi}{\partial x^2} + \frac{\partial^2 \phi}{\partial z^2} = 0$$

within the fluid (1)

$$\frac{D(z-\zeta)}{Dt} = \frac{\partial}{\partial t}(z-\zeta) + \nabla\phi \cdot \nabla(z-\zeta) = 0$$

kinematic free surface (2)
condition on $z = \zeta$

$$p - p_{atm} = -\rho(g\zeta + \frac{\partial \phi}{\partial t} + \frac{1}{2}\nabla\phi \cdot \nabla\phi) = 0$$

dynamic free surface (3)
condition on $z = \zeta$

$$\frac{\partial \phi}{\partial z} = 0$$

sea bottom boundary (4)
condition on $z = -h$

If there is no lateral physical boundary nearby, then a periodic boundary condition for the surface waves can be included, i.e. $\frac{\partial \phi(L,z,t)}{\partial x} = \frac{\partial \phi(0,z,t)}{\partial x}$.

A sketch of the boundary value problem is given by following.
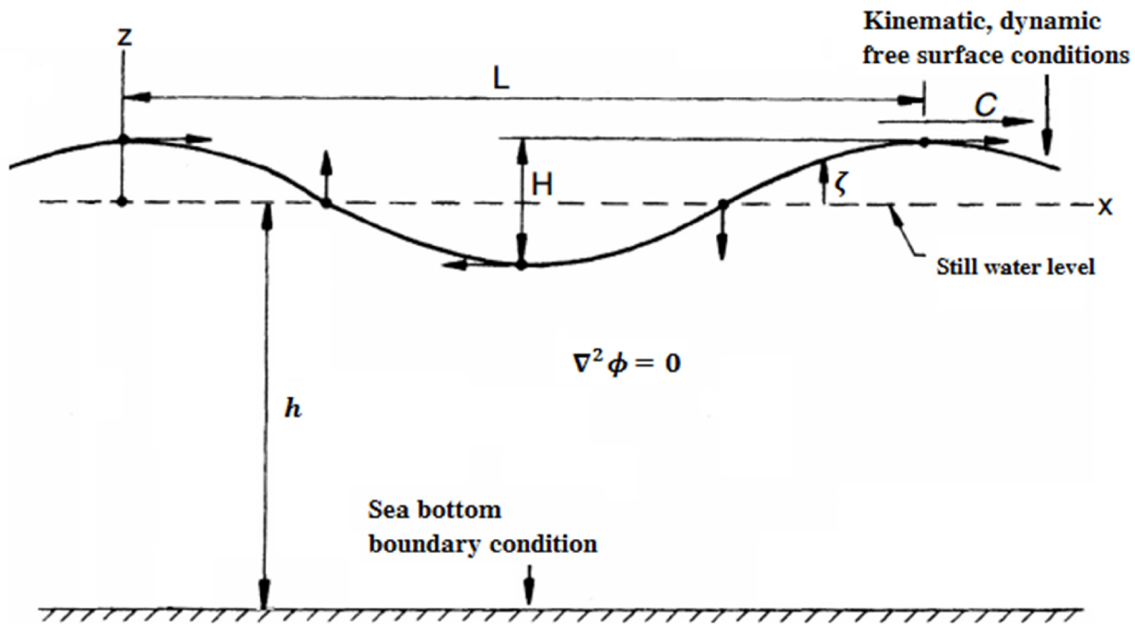
Figure 1-1 Sketch of the general boundary value problem

1.2 Stream function method

The method is mainly based on Fourier series so that each term in the approximated solution already satisfies the field equation, but instead of doing perturbation expansion for the coefficients (as in Stokes wave theory) which will pollute the solution more or less, the coefficients are solved directly by the benefit from development of computer power. The method got its name because stream function is used instead of velocity potential for the purpose of more practical programming. This is due to that the kinematic free surface condition can be satisfied straightforward as the streamline value is constant there, but the velocity potential approach does not implicitly satisfy the kinematic free surface condition so another set of coefficients is required for ζ.

Several approaches can be found as branches of the method. Only Dalrymple's approach (1974) will be explained here as it is which Wasim uses.

First the coordinate system (x, z) is defined to be following the wave and thus have the velocity c relative to the stagnant water. Because of the constant wave shape assumed, the problem becomes steady state and only spatial dependent which results in the benefit that the time-derivatives in the free surface boundary conditions can be taken away. The boundary value problem will be denoted with stream function as given below:

$$\frac{\partial^2 \psi}{\partial x^2} + \frac{\partial^2 \psi}{\partial z^2} = 0 \qquad \text{within the fluid} \qquad (5)$$

(satisfied by default as continuity assumed)

$$\frac{\partial \psi}{\partial x} = -\frac{\partial \psi}{\partial z}\frac{\partial \zeta}{\partial x} \ or \ \psi(x,\zeta) = -Q \qquad \begin{array}{l}\text{kinematic free surface} \\ \text{condition on } z = \zeta\end{array} \qquad (6)$$

(Q is the discharge through a vertical section)

$$\frac{1}{2}\left(\left(\frac{\partial \psi}{\partial x}\right)^2 + \left(\frac{\partial \psi}{\partial z}\right)^2\right) + g\zeta = R \qquad \begin{array}{l}\text{dynamic free surface} \\ \text{condition on } z = \zeta\end{array} \qquad (7)$$

(R is the Bernoulli constant)

$$\frac{\partial \psi}{\partial x} = 0 \ or \ \psi(x,-h) = 0 \qquad \begin{array}{l}\text{sea bottom boundary} \\ \text{condition on } z = -h\end{array} \qquad (8)$$

(satisfied by default because of the term

13

sinh[nk(h+z)])

The lateral boundary condition, $\psi(x,z) = \psi(x+L,z)$, is already hidden in the assumed form of ψ in all those three approaches. In addition to the boundary conditions, we need three more constraints to close the problem when *H, T, h* are input:

$$\bar{\zeta} = \frac{1}{L}\int_0^L \zeta \, dx = 0 \tag{9}$$

(elevations must have a zero mean as incompressibility assumed)

$$H = \zeta_{\max} - \zeta_{min} \tag{5}$$

$$L = cT \tag{11}$$

As no stream is included, the stream function can be assumed as:

$$\psi(x,z) = \frac{X_1 \cdot z}{T} + \sum_{n=2}^{N+1}\{X_n \cdot sinh\frac{2(n-1)\pi}{X_1}(h+z)\cdot cos\frac{2(n-1)\pi}{X_1}x\} \tag{12}$$

where $X_1 = L$, $X_{N+1} = \psi_\zeta$ and there are N+1 unknowns to be solved. The assumed stream function has already taken constraint (11) into account as the wave period should be prescribed. So there is only one boundary condition, the dynamic free surface condition, which is left to be satisfied. This can be done by requiring the following objective function to be zero:

$$O = \frac{1}{I}\sum_{i=1}^{I}(R_i - \bar{R})^2 + \frac{\lambda_1}{I}\sum_{i=1}^{I}\zeta(x_i) + \lambda_2(\zeta(x_1) - \zeta(x_I) - H) = 0 \tag{13}$$

where λ_1 and λ_2 are Lagrange multipliers which can be used to adjust the weight of the last two terms in the objective function, and I is the resolution of the wave profile while N is the order of the stream function. The objective function is a combination of constraint (9), (10) and a fitting of local Bernoulli constants at point i, $R_i = \frac{1}{2}\left(\left(\frac{\partial\psi}{\partial x}\right)_i^2 + \left(\frac{\partial\psi}{\partial z}\right)_i^2\right)$, to the mean Bernoulli constant value $\bar{R} = \frac{1}{I}\sum_{i=1}^{I}R_i$ (Here equidistant points along the wave profile is assumed and $\bar{R}$ is used since no prescribed Bernoulli constant in Dalrymple's approach). Equation (13) is nonlinear and can be solved by use of Newton-Raphson's method, and this yields a linear equation system

consists of N equations with N unknowns (by insert (12) into (13)). The linear system can be pre-sented as:

$$O^{j+1} = O^j + \sum_{n=1}^{N} \frac{\partial O^j}{\partial X_n} \cdot \Delta X_n^j + \sum_{m=1}^{2} \frac{\partial O^j}{\partial \lambda_m} \cdot \Delta \lambda_m^j \tag{14}$$

$$X_n^{j+1} = X_n^j + \Delta X_n^j, \quad \lambda_m^{j+1} = \lambda_m^j + \Delta \lambda_m^j \tag{15}$$

When ΔX_n^j have been solved, the coefficient set X_n at the iteration j+1 will be updated as $X_n^{j+1} = X_n^j + \Delta X_n^j$. Then the wave elevations ζ^{j+1} will be solved based on X_n^{j+1} and X_{N+1}^j (i.e. partly explicit, because $X_{N+1}^{j+1} = \psi_\zeta^{j+1}$ will be updated at last). Insert $z = \zeta$ in (12):

$$\zeta(x)^{j+1} = \frac{T \cdot X_{N+1}^j}{X_1^{j+1}} - \frac{T}{X_1^{j+1}} \sum_{n=2}^{N+1} \{ X_n^{j+1} \cdot \sinh \frac{2(n-1)\pi}{X_1^{j+1}} (h + \zeta(x)^{j+1}) \cdot$$

$$\cos \frac{2(n-1)\pi}{X_1^{j+1}} x \} \tag{6}$$

The wave elevations can be solved by the transcendental equation (16) iteratively. In final X_{N+1}^{j+1} is calculated based on ζ^{j+1} by numerically integrating (16) along the wave profile. Then the left hand side of (16) can be eliminated because of constraint (9), thus X_{N+1}^{j+1} can be solved as:

$$X_{N+1}^{j+1} = \frac{1}{I} \sum_{i=1}^{I} \{ \sum_{n=2}^{N+1} \{ X_n^{j+1} \cdot \sinh \frac{2(n-1)\pi}{X_1^{j+1}} (h + \zeta(x)^{j+1}) \cdot \cos \frac{2(n-1)\pi}{X_1^{j+1}} x \} \} \tag{17}$$

This is the procedure of the method for one iteration and all the N+1 unknowns in (12) plus the wave elevations are computed once. Notice that Δx_i is taken away and use $\frac{1}{I}$ instead of $\frac{1}{L}$ as equidistant points is assumed along the wave profile.

1.3 Basic theory of Wasim

1.3.1 The general model

We consider a body travelling at constant speed with x-component U, y-component V and rotation Ω in the earth fixed coordinate system (x_0, y_0, z_0), i.e. the stagnant fluid will have a mean velocity field $\overrightarrow{W} = (U - \Omega x, V - \Omega y)$ in the body fixed coordinate system (x, y, z). The Galilean transform relates these two coordinate systems can thus be defined as

$$\frac{D}{Dt} = \frac{\partial}{\partial t} - \overrightarrow{W} \cdot \nabla \qquad (18)$$

where $\frac{D}{Dt}$ denotes the time derivative in the earth fixed coordinate system while $\frac{\partial}{\partial t}$ denotes the time derivative in the body fixed coordinate system. The unsteady body motions about its fixed coordinate system is given below

$$\vec{\delta}(\vec{x}, t) = (\xi_1, \xi_2, \xi_3, 0, 0, 0) + (0, 0, 0, \xi_4, \xi_5, \xi_6) \times \vec{x} \qquad (19)$$

where $\vec{x} = (x, y, z)$ and ξ_i are the six degrees of freedom rigid body motions.
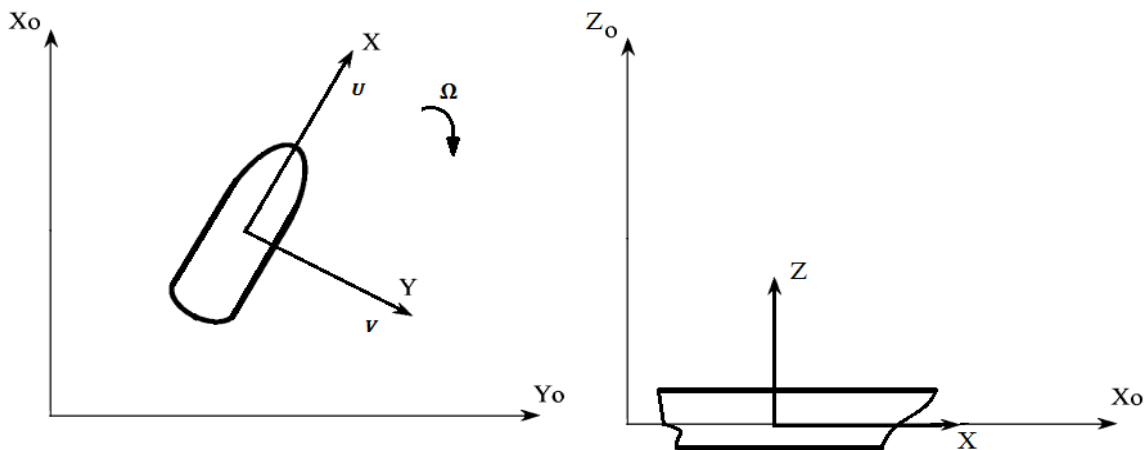
Figure 1-2 Definition of the 3D coordinate systems when a body is presented

1.3.2 Decomposition of the total potential

By linear potential theory, the total fluid potential can be treated as a superposition of several potential components. The classical way is usually to discretize the transient part into a radiation potential and a diffraction potential. In Wasim another alternative is used by introducing so-called local flow and memory flow, and the benefit is better numerical stability. The decomposition is given as $\phi_{tot} = \phi_b + \phi_l + \phi_m + \phi_i$, and the following is a brief explanation.

- ϕ_b is the basis flow potential which is steady state and independent of the other potential components. This component represents the steady flow around the body which is in forward speed. In Wasim, one of the two famous linearization models, the Neumann-Kelvin (where a uniform stream will be used) or the double body flow is available in the graphical user interface of the program. The latter gives more accurate results but may lead to numerical problems in a nonlinear analysis, so the former is set as the default model for nonlinear analyses. In fact Wasim uses a so-called Aspiration model which is a combination of Neumann-Kelvin and double body flow (see the next section for more details). The basis flow is always zero in this project.

- ϕ_l is the local flow potential. It can be understood as the instantaneous response of the surrounding fluid due to a given velocity of the body boundary, i.e. as a pressure release problem, and this further causes disturbance of the free surface. In this way the body forcing is transferred to an inhomogeneity of the fluid, and this inhomogeneity acts as an initial boundary value problem for the memory flow. With other words, in Wasim the classical radiation problem is divided into two parts. The first part is included in the local flow while the rest is put into the memory flow. It is the separation of the local flow added mass from the right hand side of the motion equation which results in the better numerical stability since the remaining force will be independent of the instantaneous acceleration (see the next section for more details). In section 2.3, the local flow will also be zero due to no radiation.

- ϕ_m is the memory flow potential. It represents both a part of the radiation flow and the diffraction flow, i.e. it is the rest of the transient potential. An initial boundary value

problem will be solved at each time step to get the memory flow so this potential component will form the major part of the computation.

- ϕ_i is the incident wave potential. It is given and will be an input, mainly as a Stokes 5th order wave or a stream function wave in this project.

We assume that $\phi_b = O(1)$ while $\phi_l, \phi_m, \phi_i = O(\epsilon)$. Thereby the decomposition is kind of a perturbation expansion (only linear terms are kept) where the parameter ϵ is a measure of the potential magnitude and it is a function of the Froude number. The basis flow is thus the basis for the linearization and it should be the largest of all the potential components (if nonzero forward speed) so that the small body-motions assumption in the body fixed frame will be a good approximation.

1.3.3 The boundary value problems

After the decomposition of the total fluid potential, the whole complex problem is split into several boundary value problems. The advantage is not only the simplification and the practicality to the implementation but also that the results of the different components can be checked and analyzed separately. The boundary value problems together with brief explanations are given below.

i)   Basis flow

$$\nabla^2 \phi_b = 0 \qquad\qquad\qquad \text{within the fluid} \qquad (20)$$

$$\frac{\partial \phi_b}{\partial z} = 0 \qquad\qquad\qquad \text{on } z = 0 \qquad (21)$$

$$\frac{\partial \phi_b}{\partial n} = \left(1 - f(x, y, z)\right) \cdot (\vec{W} \cdot \vec{n}) \qquad \text{on the body boundary} \qquad (22)$$

$$\frac{\partial \phi_b}{\partial z} = 0 \qquad\qquad\qquad \text{on the sea bottom} \qquad (23)$$

The same free surface condition is used as the double body flow modeling. The introduction of function f(x,y,z) is to allow a specified normal flux through the hull. When f(x,y,z)=0, the normal flux equals the free stream, i.e. it gives the Neumann-Kelvin model while f(x,y,z)=1, i.e. no flux

passes through the body, gives the double body flow. By stacking a small amount free stream up to the double body flow, the rectangular wake flow behind a transom stern can be modeled.

ii)   Local flow

$$\nabla^2 \phi_l = 0 \qquad\qquad\qquad \text{within the fluid} \qquad (24)$$

$$\phi_l = 0 \qquad\qquad\qquad \text{on } z = 0 \qquad (25)$$

$$\frac{\partial \phi_l}{\partial n} = \sum_{j=1}^{6} \left(\frac{\partial \xi_j}{\partial t} n_j + \xi_j m_j \right) \qquad \text{on the \textbf{mean} body boundary} \qquad (26)$$

$$\frac{\partial \phi_l}{\partial z} = 0 \qquad\qquad\qquad \text{on the sea bottom} \qquad (27)$$

where

$$(n_1, n_2, n_3) = \vec{n}, \ (n_4, n_5, n_6) = \vec{x} \times \vec{n} \qquad (28)$$

$$(m_1, m_2, m_3) = (\vec{n} \cdot \nabla)(\vec{W} - \nabla\phi_b), \ (m_4, m_5, m_6) = (\vec{n} \cdot \nabla)\left(\vec{x} \times (\vec{W} - \nabla\phi_b)\right) \qquad (29)$$

Since n_j and m_j are time independent while $\frac{\partial \xi_j}{\partial t}$ and ξ_j are spatial independent due to the rigid body motions, equation (26) is similar as so-called "normal modes" approach and n_j, m_j, represent the modal shapes which can be determined before time stepping. The terms m_j give the coupling between the basis flow and unsteady flow, and they may be difficult to compute due to the second order derivative so no further discussion will be included here. We then spatial integrate (26) and assume that ϕ_l is proportional to the instantaneous velocity and the instantaneous displacement which thus can be given as

$$\phi_l(\vec{x}, t) = \sum_{j=1}^{6} N_j(\vec{x}) \frac{\partial \xi_j}{\partial t}(t) + M_j(\vec{x})\xi_j(t) \qquad (30)$$

Therefore N_j and M_j must satisfy the following boundary value problem

$$\nabla^2 N_j = 0, \ \nabla^2 M_j = 0 \qquad\qquad \text{within the fluid} \qquad (31)$$

$$N_j = 0, \ M_j = 0 \qquad\qquad\qquad \text{on } z = 0 \qquad (32)$$

$$\frac{\partial N_j}{\partial n} = n_j, \ \frac{\partial M_j}{\partial n} = m_j \qquad\qquad \text{on the \textbf{mean} body boundary} \qquad (33)$$

$$\frac{\partial N_j}{\partial z} = 0, \ \frac{\partial M_j}{\partial z} = 0 \qquad\qquad \text{on the sea bottom} \qquad (34)$$

By solving N_j and M_j before time stepping, ϕ_l can be simply calculated after solving the motion equation at each time step.

The linearized local flow force (see section 2.1.5 for more details) is assumed to be

$$F_l = \int -\rho\left(\frac{\partial}{\partial t} - \left(\overrightarrow{W} - \nabla\phi_b\right)\cdot\nabla\right)\phi_l\,ds = \sum\sum a_{0jk}\frac{\partial^2\xi_k}{\partial t^2} + b_{0jk}\frac{\partial\xi_k}{\partial t} + c_{0jk}\xi_k \tag{35}$$

By inserting (30) into (35), the local flow added mass, damping and stiffness can be calculated as the following

$$a_{0jk} = \int \rho\,N_k\cdot n_j\,ds \tag{36}$$

$$b_{0jk} = \int \rho\left(-\left(\overrightarrow{W} - \nabla\phi_b\right)\cdot N_k + M_k\right)\cdot n_j\,ds \tag{37}$$

$$c_{0jk} = \int \rho\left(-\left(\overrightarrow{W} - \nabla\phi_b\right)\cdot M_k\right)\cdot n_j\,ds \tag{38}$$

The coefficients are also time independent as expected. Then we move the local flow force to the left hand side of the motion equation so that the rest at right hand side will be memory flow force plus Froude-Krylov force, and both of them are independent of the body instantaneous acceleration. This separation will be unnecessary if the problem is forced oscillations because of no need for solving the motion equation.

    iii)   Memory flow

$$\nabla^2\phi_m = 0 \qquad\qquad\qquad\qquad \text{within the fluid} \qquad (39)$$

$$\frac{\partial\zeta}{\partial t} - \left(\overrightarrow{W} - \nabla\phi_b\right)\nabla\zeta = \frac{\partial^2\phi_b}{\partial z^2}(\zeta + \zeta_i) + \frac{\partial\phi_l}{\partial z} + \frac{\partial\phi_m}{\partial z} - \left(\nabla\phi_b\cdot\nabla\zeta_i\right) \tag{40}$$

$$\frac{\partial\phi_m}{\partial t} - \left(\overrightarrow{W} - \nabla\phi_b\right)\nabla\phi_m = -g\zeta + \left(\overrightarrow{W}\cdot\nabla\phi_b - \frac{1}{2}(\nabla\phi_b)^2\right) - \nabla\phi_b\nabla\phi_i \tag{41}$$

$$\text{on } z = 0$$

$$\frac{\partial\phi_m}{\partial n} = \left(\overrightarrow{W} - \nabla\phi_b\right)\cdot\vec{n} - \frac{\partial\phi_i}{\partial n} \qquad\qquad \text{on the \textbf{mean} body boundary} \qquad (42)$$

$$\frac{\partial\phi_m}{\partial z} = 0 \qquad\qquad\qquad\qquad \text{on the sea bottom} \qquad (43)$$

where ζ_i is the elevation of the incident wave (see Appendix A for more details about the linear-ization of the free surface conditions). On the free surface, known $\frac{\partial\phi_m}{\partial z}$ from the previous time step will be used to calculate ζ at the current time step by explicit Euler time discretization of the kinematic free surface condition, i.e. (40). Then the updated ζ will be used to calculate ϕ_m

at the current time step by implicit Euler time discretization of the dynamic free surface condition, i.e. (41). On the body boundary $\frac{\partial \phi_m}{\partial n}$ is always known since ϕ_b is solved before time stepping while ϕ_i is input.

A combination of Euler schemes is applied because it is proved by von Neumann stability analysis that neither of fully explicit and fully implicit discretization will lead to satisfied numerical properties.

1.3.4 Rankine panel method

To solve the described boundary value problems, a boundary element method will be used. The main idea is to represent the fluid field as superposition of sources (and sometimes also dipoles and vortices). The boundary surfaces are discretized into a finite number of panels where certain number collocation points are distributed depends on the order of the method, and thereby the method is named "panel method". Different source types can be chosen to satisfy certain boundary conditions in advance, e.g. Kelvin or Havelock source satisfies the linear free surface condition, and several source types can be found which satisfy both the free surface and the bottom boundary condition at the same time. The disadvantage for sure is the complicated computation for such multifunctional sources (or Green function). In Wasim, the fundamental Rankine source is used. The cost of using Rankine source is that we have to distribute sources on all the boundaries (except the sea bottom in Wasim) since Rankine source is only solution of Laplace's equation and does not satisfy any boundary conditions, and this will lead to more unknowns and further more memory cost (the increase of CPU cost is less noticeable as it is simple to calculate). The sea bottom boundary condition is satisfied by mirroring so no panel mesh is needed there, but irregular sea bottom (which is more concerned in shallow water) may thus not be allowed in Wasim. Since different boundary value problems with different kind boundary conditions will be solved in Wasim, the use of Rankine source is more general for programming purpose, especially for object oriented language.

If the entire fluid domain considered is denoted as FD, and the corresponding total boundary is denoted as ∂FD. Then by using Green's second identity, the following equation can be derived

$$\int_{FD}(\phi \cdot \nabla^2 G - G \cdot \nabla^2 \phi)dV = \int_{\partial FD}\left(\phi \cdot \frac{\partial G}{\partial n} - G \cdot \frac{\partial \phi}{\partial n}\right)ds \tag{44}$$

where ϕ can be any potential component and G is the Green function. We choose Rankine source as the Green function, i.e.

$$G = \frac{1}{|\vec{x}-\vec{\eta}|} \quad \text{and} \quad \nabla^2 G = -4\pi\delta(\vec{x},\vec{\eta}) \tag{45}$$

where $\vec{\eta}$ is the location of certain collocation point, and δ is the Dirac delta function representing the singularity, i.e.

$$\delta = \begin{cases} +\infty & \vec{x} = \vec{\eta} \\ 0 & \vec{x} \neq \vec{\eta} \end{cases} \tag{46}$$

Then by inserting (45) into (44) we come to the following equation

$$c \cdot \phi(\vec{x}) - \int_{\partial FD} G(\vec{x},\vec{\eta}) \cdot \frac{\partial \phi(\vec{\eta})}{\partial n}d\vec{\eta} + \int_{\partial FD} \phi(\vec{\eta}) \cdot \frac{\partial G(\vec{x},\vec{\eta})}{\partial n}d\vec{\eta} = 0 \tag{47}$$

$$c = \begin{cases} 4\pi & \vec{x} \in FD \\ 2\pi & \vec{x} \in \partial FD \\ 0 & elsewhere \end{cases} \tag{48}$$

In fact, the contribution from the far field boundary can be eliminated so that ∂FD consists only of the free surface and the body boundary (no panel mesh on the sea bottom). And solutions on the free surface and the body boundary are most concerned (where wave elevations or pressures will be computed), i.e. $c = 2\pi$, e.g. when ϕ_m on the free surface is calculated by the dynamic free surface condition and as $\frac{\partial \phi_m}{\partial n}$ on the body boundary is already known (see section 2.1.3), the only unknown will be $\frac{\partial \phi_m}{\partial z}$ on the free surface and ϕ_m on the body boundary. Assume we have N collocation points on the free surface and M collocation points on the body boundary, i.e. we will get N+M unknowns for the concerned example, then by establishing equation (47) at each collocation point we obtain a linear equation system consists of N+M equations, i.e. the problem is closed.

1.3.5 Computation of the pressures

The pressure field can be derived from Bernoulli's equation, i.e.

$$p - p_a = -\rho\left(\frac{D}{Dt}\phi_{tot} + \frac{1}{2}(\nabla\phi_{tot})^2 + gz\right) \tag{49}$$

Assume $p_a \approx 0$ due to relatively small air density and introduce the Galilean transform (18) and the decomposition of the total potential, we can linearize the total pressure by keeping only $O(1)$ and $O(\epsilon)$ terms, which is given as

$$p = -\rho\left(\left(\frac{\partial}{\partial t} - (\vec{W} - \nabla\phi_b)\cdot\nabla\right)(\phi_l + \phi_m + \phi_i) - \nabla\phi_b\left(\vec{W} - \frac{1}{2}\nabla\phi_b\right) + gz\right) \tag{50}$$

Then the total pressure can also be discretized similarly as the total potential, i.e.

Froude-Krylov $\quad p_{FK} = -\rho\left(\frac{\partial}{\partial t} - (\vec{W} - \nabla\phi_b)\cdot\nabla\right)\phi_i$ (51)

Local flow $\quad p_l = -\rho\left(\frac{\partial}{\partial t} - (\vec{W} - \nabla\phi_b)\cdot\nabla\right)\phi_l$ (52)

Memory flow $\quad p_m = -\rho\left(\left(\frac{\partial}{\partial t} - (\vec{W} - \nabla\phi_b)\cdot\nabla\right)\phi_m - \nabla\phi_b\left(\vec{W} - \frac{1}{2}\nabla\phi_b\right)\right)$ (53)

Hydrostatic $\quad p_{stat} = -\rho gz = -\rho g(z_0 - \xi_3 + x\xi_5 - y\xi_4)$ (54)

where z_0 is the mean body position. When the nonlinear analysis option is enabled (see section 2.2 for more details), the $O(\epsilon^2)$ terms will also be included so the nonlinear pressures should be

Froude-Krylov $\quad p_{FK} = -\rho\left(\left(\frac{\partial}{\partial t} - (\vec{W} - \nabla\phi_b)\cdot\nabla\right)\phi_i + \frac{1}{2}(\nabla\phi_i)^2\right)$ (55)

Local flow $\quad p_l = -\rho\left(\left(\frac{\partial}{\partial t} - (\vec{W} - \nabla\phi_b)\cdot\nabla\right)\phi_l + \frac{1}{2}(\nabla\phi_l)^2\right)$ (56)

Memory flow $\quad p_m = -\rho\left(\left(\frac{\partial}{\partial t} - (\vec{W} - \nabla\phi_b)\cdot\nabla\right)\phi_m - \nabla\phi_b\left(\vec{W} - \frac{1}{2}\nabla\phi_b\right) + \frac{1}{2}(\nabla\phi_m)^2\right)$ (57)

Cross coupling $\quad p_{cp} = \nabla\phi_i\nabla\phi_l + \nabla\phi_l\nabla\phi_m + \nabla\phi_i\nabla\phi_m$ (58)

References

Chappelear, J.E. (1961), "Direct numerical calculation of wave properties", Journal of Geophysical Research

Dalrymple, R.A. (1974), "A finite amplitude wave on a linear shear current", Journal of Geophysical Research

Dean, R.G. (1965), "Stream function representation of nonlinear ocean waves", Journal of Geophysical Research

Dean, R.G. & Dalrymple, R.A. (1985), "Water Wave Mechanics for Engineers and Scientists", World Scientific

Greco, Marilena (2011), Lecture Notes "Sea loads", NTNU

Kring, D.C (1994), "Time domain ship motions by a three-dimensional Rankine panel method", MIT

Mei, C. C, Stiassnie, M. & Yue, D. K. P. (2005), "Theory and Applications of Ocean Surface Waves, Part 2", World Scientific

Nakos, D.E. (1990), "Ship wave patterns and motions by a three dimensional Rankine panel method", MIT

Sesam HydroD User Tutorial (2010), "Analysis of a Semi-submersible with anchors by use of Wadam and Wasim", DNV

Sesam User Manual HydroD (2011), "Wave load & stability analysis of fixed and floating structures", DNV

Sesam User Manual Wasim (2011), "Wave Loads on Vessels with Forward Speed", DNV

Svendsen, IB.A. (2006), "Introduction to nearshore hydrodynamics", World Scientific

Vada, Torgeir (1994), DNV Research Report NO.94-2030, DNV

Zhang, Jun (2012), Lecture Notes "Shallow water waves", Texas A&M University

2 Modification of the stream function method

2.1 Review of the error

A semi-sub with six columns is used here. Its length in x-direction is 121.43 meter and breadth in y-direction is 60.44 meter (measured from center of the columns). The diameter of the columns is 20 meter. The semi-sub is sitting fixed on the sea bottom where z=0. The water level is set to z=30 meter, and the height of the columns is 53.35 meter, i.e. 23.35 meter above the still water level. The picture below gives an impression of the model.
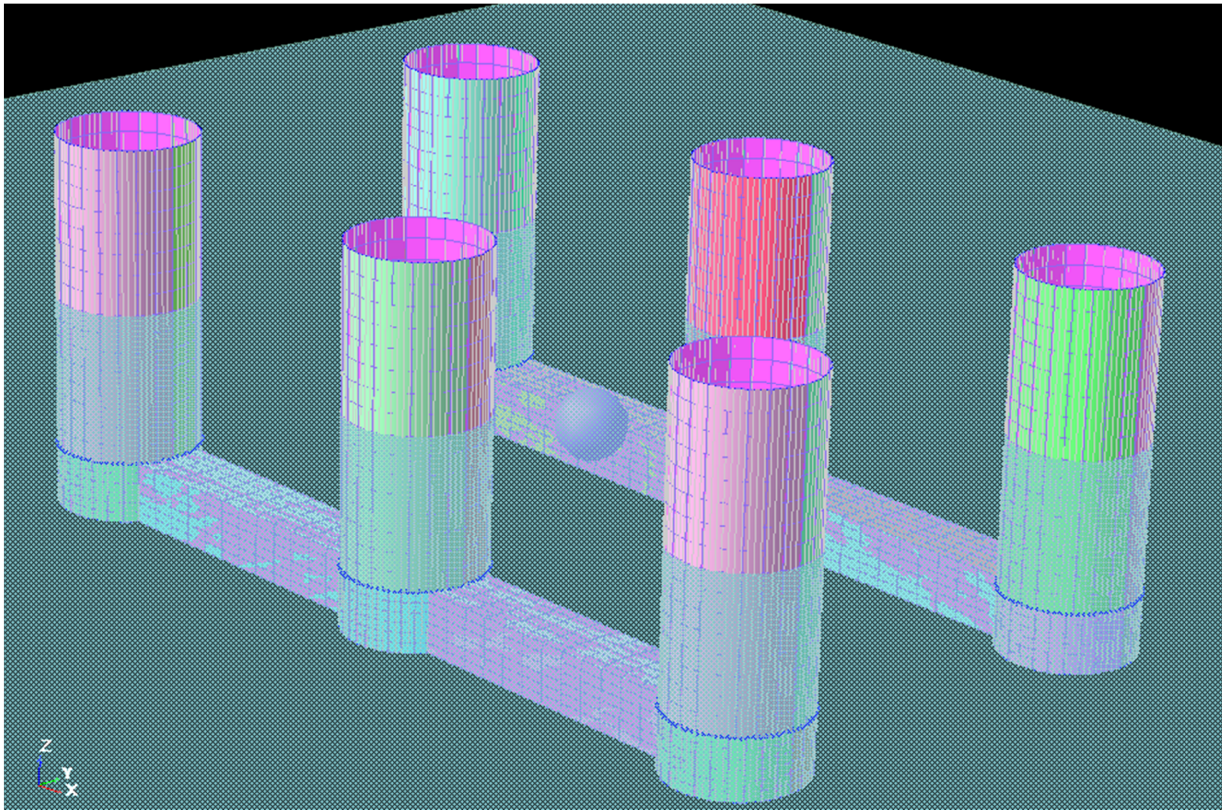
Figure 2-1 The semi-submersible model used to test stream function method

To reproduce the error, we can run two analyses with the model, one of them has a stream function wave with 14 coefficients as incoming wave and the other with a Stokes 5th wave as input. Both input waves have H=12 m and T=15 s, i.e. a wave condition which remains inside of the valid region of Stokes 5th order wave theory. Therefore we expect that both stream function method and Stokes 5th order wave theory will give us almost the same wave profile with very

small deviations in the wave elevations and wave kinematics, and this should further lead to almost the same wave diffractions. But when the incident wave is generated by stream function method, "pumping" wave diffractions can be observed which will not appear if the incident wave is a Stokes 5th wave. The wave diffractions generated by these two analyses are quite different as presented below. The incident wave elevations are already filtered out from the total wave elevations, and since the platform is fixed sitting on the sea bottom there is only diffracted waves left.
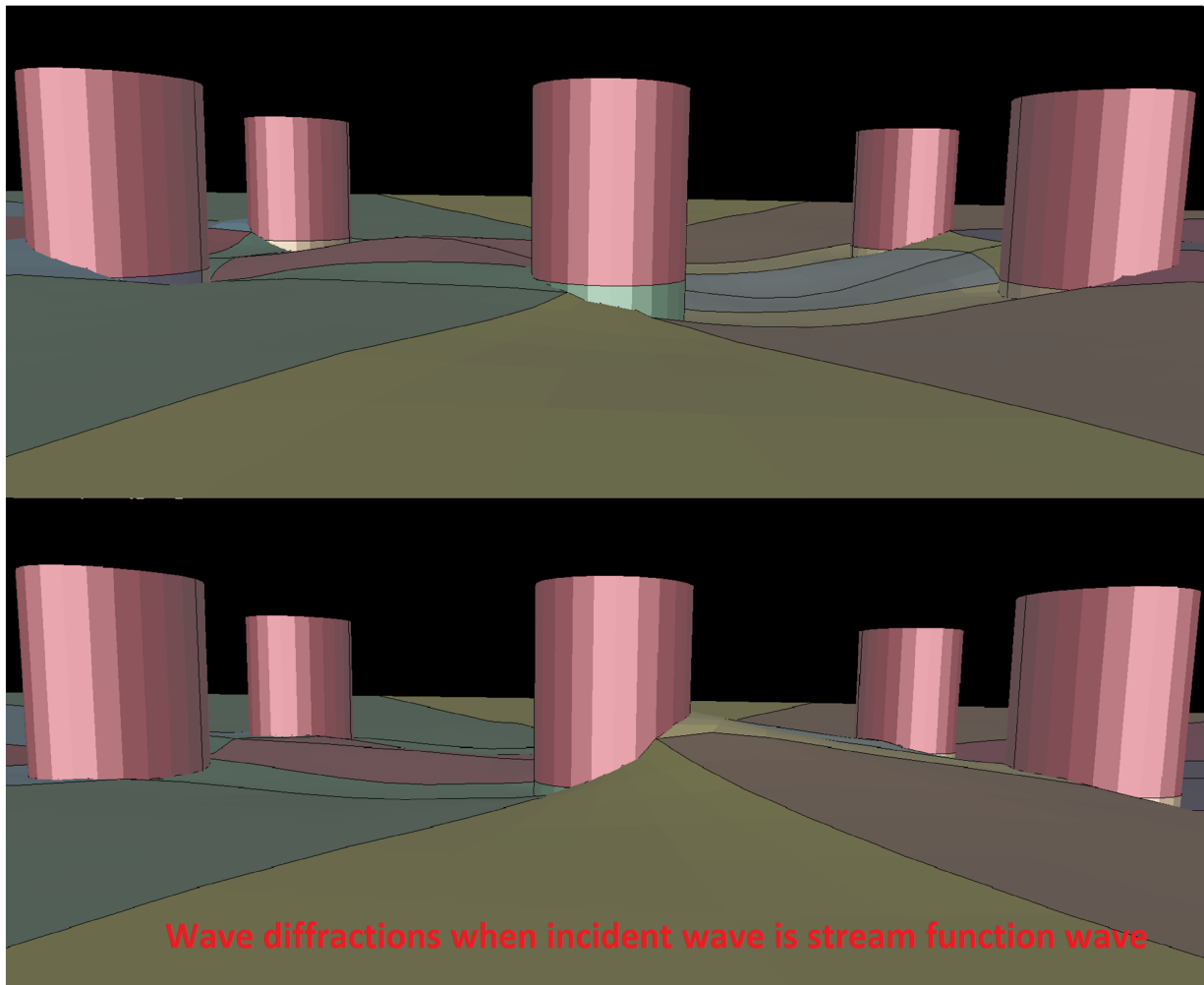
Figure 2-2 The pumping effect shows up when the incident wave is stream function wave

Wave diffractions when incident wave is Stokes 5th wave
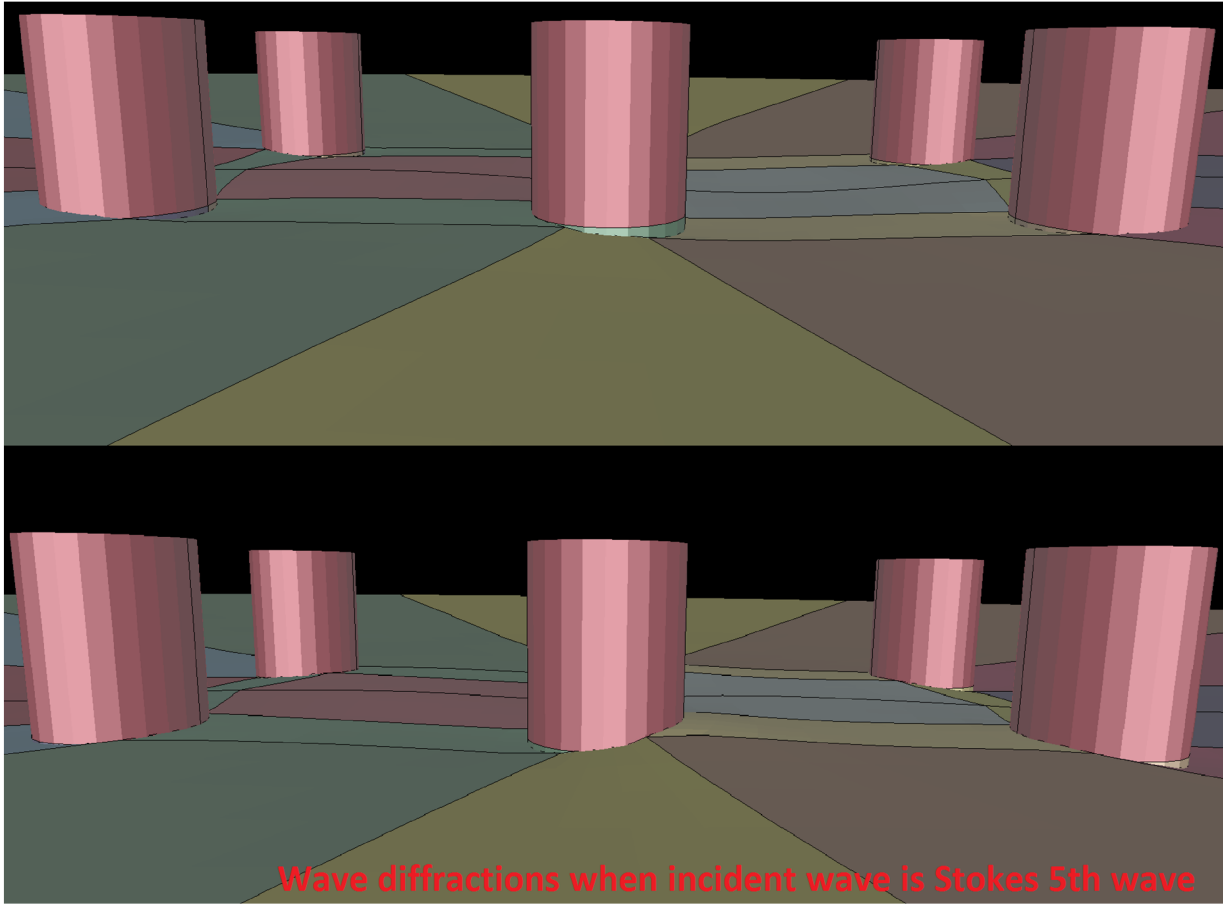
Figure 2-3 The pumping effect disappears when the incident wave is Stokes 5th wave

To present the error even clearer, the time history of the diffraction wave elevations right behind the middle column (where the diffractions are biggest) is plotted.
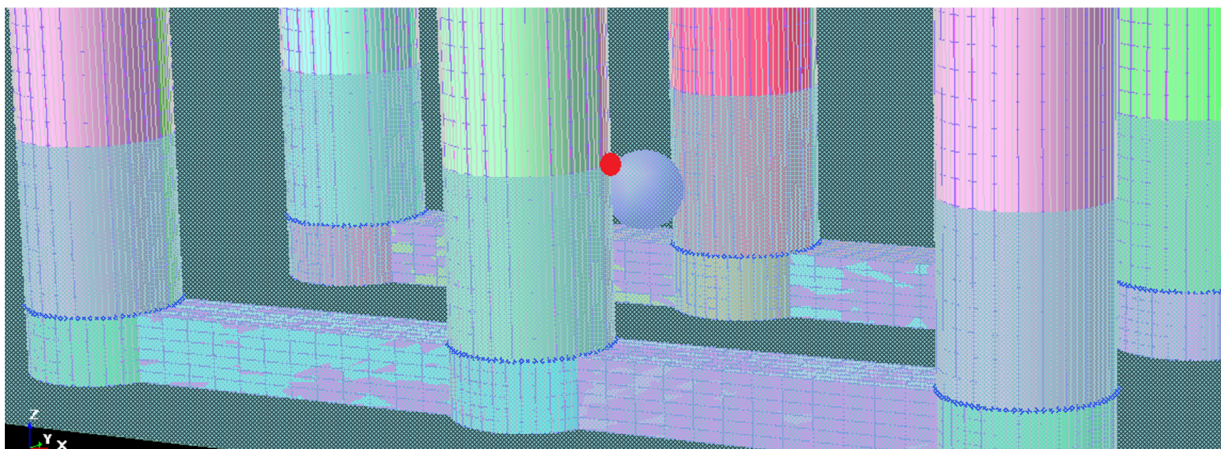
Figure 2-4 Right behind the middle column where the diffraction wave elevation is collected
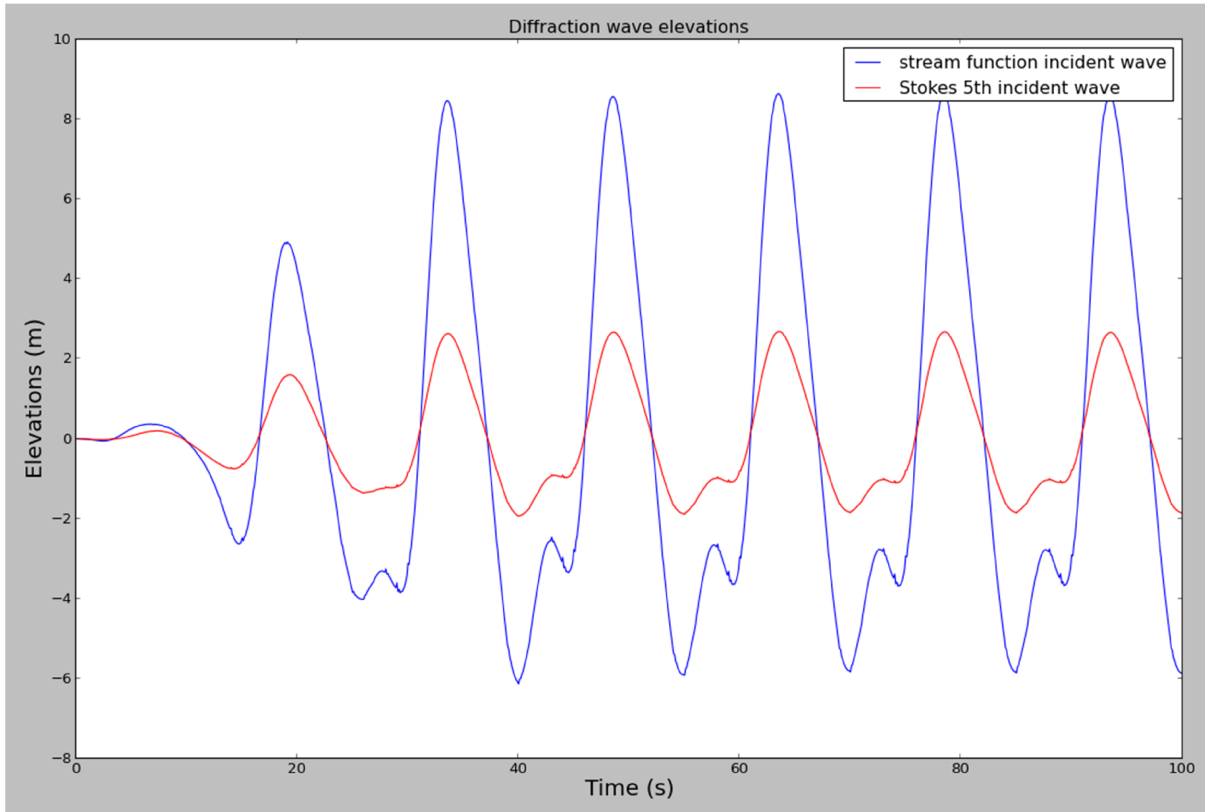
Figure 2-5 Comparison of diffraction wave elevations behind the middle column

Since the Stokes 5th wave in Wasim is well tested and evaluated to be correct, and such phenomenon did not show up during a model test or in a CFD analysis (according to DNV) either. The "pumping" wave diffractions are thus assumed to be unphysical, and there should be some error either inside of the implementation of stream function method itself or associated with the integration of the method into the whole program.

2.2 How the program works

After study the source code of Wasim, one of the possibilities regarding where the error is located can be eliminated now. Because the program does not have an implementation of stream function method internal, but instead an online java application is used to calculate the Fourier coefficients of stream function. The java application is developed by Dalrymple himself at University of Delaware (http://www.coastal.udel.edu/faculty/rad/streamless.html).
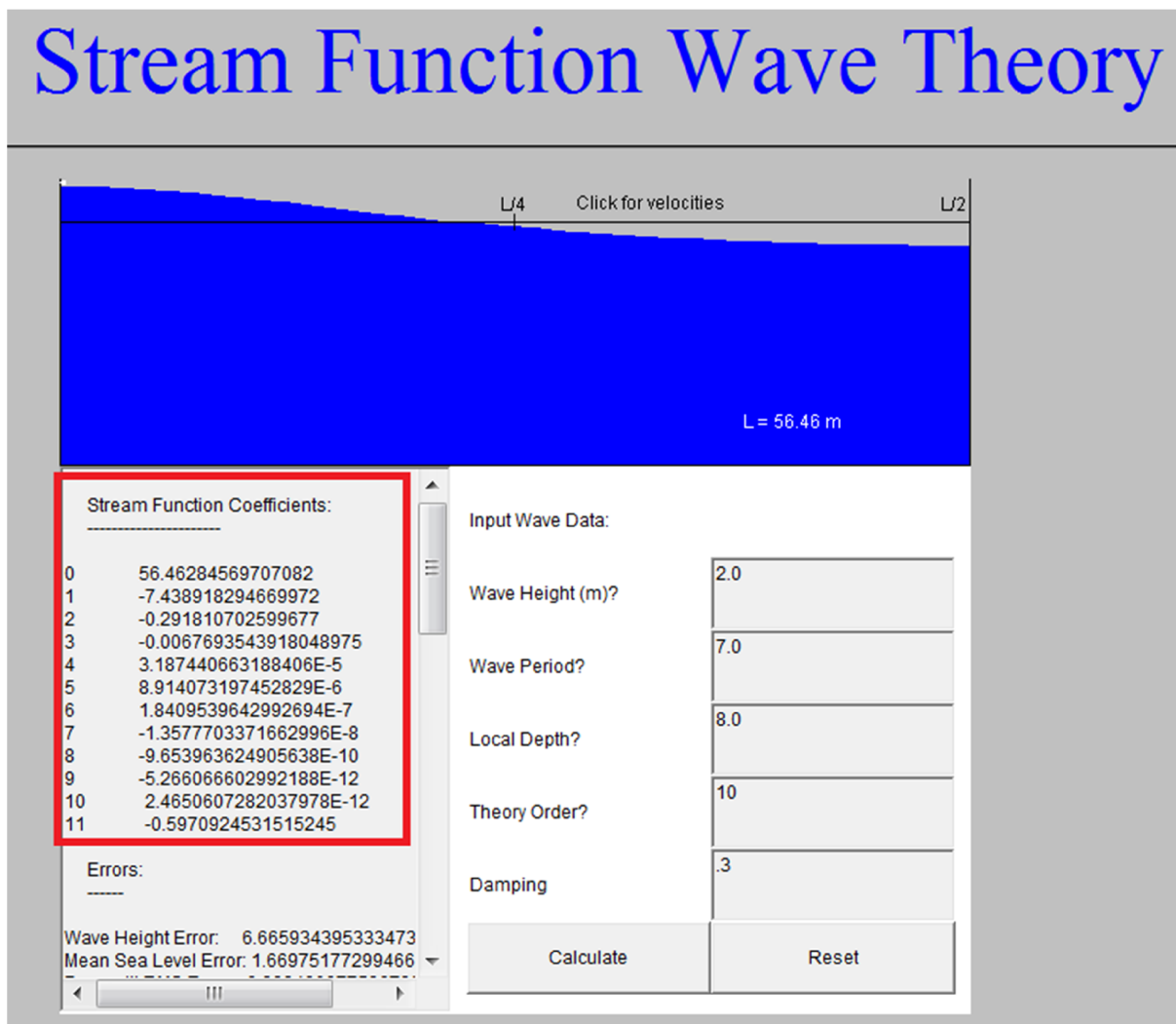
Figure 2-6 Online java application which is used to calculate stream function coefficients for Wasim

After the java application calculated the stream function coefficients, these coefficients will be input to a python script for post-processing. The main task of the python script is to compute a series of wave elevation coefficients so that Wasim can get wave elevation at any point on the

free surface just by summation of some sinus or cosine terms. The script first calculate wave elevations along the wave length in a specified resolution based on the stream function coefficients (more details will be explained later in section 2.4), and then it calculates the wave elevation coefficients by fitting these wave elevation values. The script will in final output a data file includes both the stream function coefficients and the wave elevation coefficients which is input to Wasim, and Wasim uses these coefficients directly to compute wave elevations and wave kinematics.

```
 1  A stream function wave
 2  15.000000      ! Wave period
 3  12.000000      ! Wave height
 4  247.933910     ! Wave length
 5  30.000000      ! Water depth
 6  1025.000000     ! Water density
 7  9.810000      ! Acceleration of gravity
 8  14     ! Number of stream function coefficients
 9  0      2.479339098349e+02
10  1     -9.715809659349e+01
11  2     -8.392909116979e+00
12  3     -5.525710323076e-01
13  4     -2.098057919786e-02
14  5      4.650473839655e-04
15  6      1.236390727965e-04
16  7      3.552543151613e-06
17  8     -1.075231384202e-06
18  9     -1.758216011587e-07
19  10     -1.132228050035e-08
20  11      2.345613274694e-10
21  12      1.195063651166e-10
22  13      2.217465289367e-12
23  20     ! Number of free surface elevation coefficients
24  1      1.153663988866e-05
25  2      5.346188854685e+00
26  3      1.774022057312e+00
27  4      5.644322030014e-01
28  5      1.954928050350e-01
29  6      7.381598941007e-02
30  7      2.969350243352e-02
31  8      1.248421833834e-02
32  9      5.419160596689e-03
33  10      2.409940395655e-03
34  11      1.092307767648e-03
35  12      5.027440026967e-04
36  13      2.343601066173e-04
```

Figure 2-7 A screen capture of an example input file to Wasim

2.3   Fix the wave kinematics

Considering those two analyses in the section 2.1, if we take a look at the linearized Froude-Krylov forces (i.e. the $\frac{1}{2}(\nabla\phi_i)^2$ term is taken away, and as both $\overrightarrow{W}$ and $\nabla\phi_b$ are zero, only $\nabla\phi_i$ is associated), the huge difference tells us that there must be something wrong with the wave kinematics.
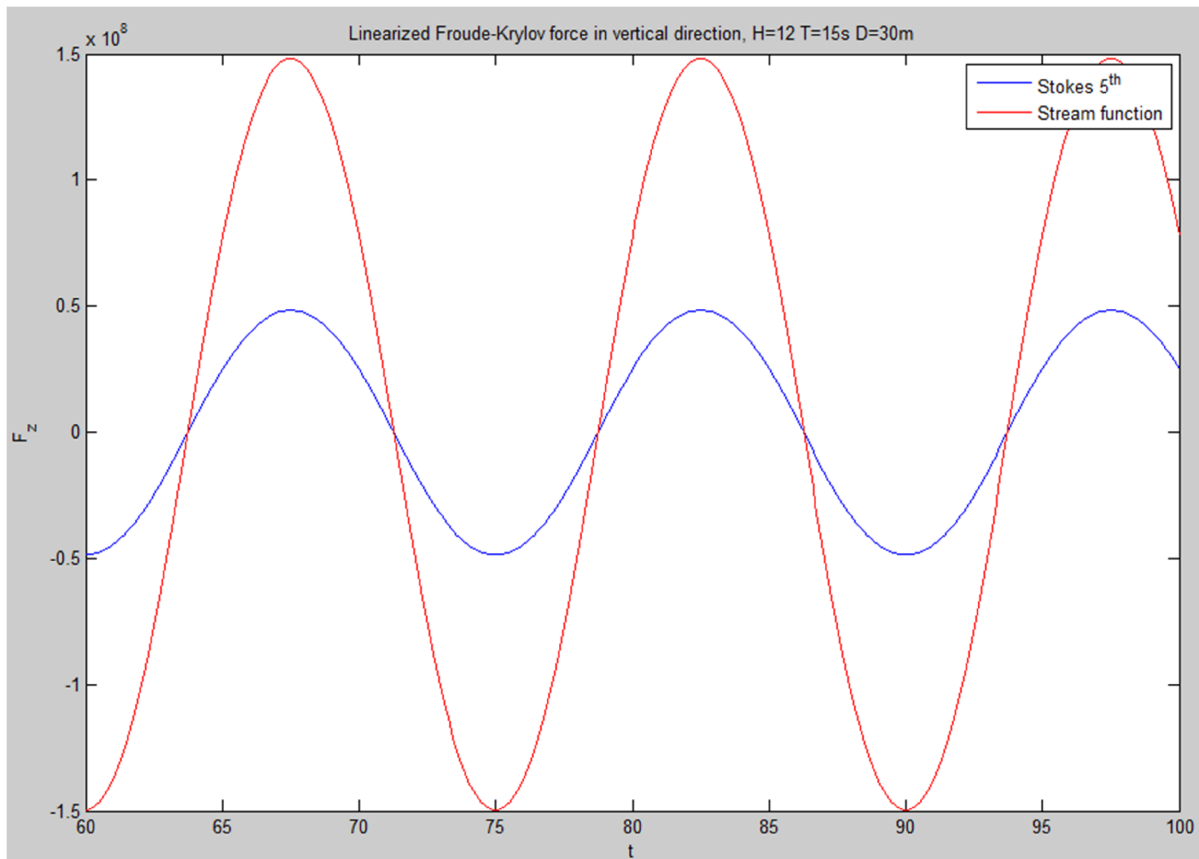
Figure 2-8 Comparison of the linear Froude-Krylov force

After comparing outputs of the stream function wave and the Stokes 5th wave in wasim (the same wave condition as in section 2.1, i.e. H = 12 m, T = 15 s and water depth = 30 m), significant deviations in water particle accelerations and $\frac{d\phi}{dt}$ have been observed.

The wave kinematics are always calculated at point(0,0) while the wave travels in time. This remains in the rest of the report if same kind of comparison is made. If there is no information given, the same wave condition will be used as above.

WAVE NO	WAVE THEORY	WAVE PERIOD ACTUAL	WAVE HEIGHT	WAVE LENGTH	DEPTH TO WAVE LENGTH RATIO	WAVE HEIGHT TO WAVE LENGTH RATIO	WAVE CREST ELEVATION	WAVE TROUGH ELEVATION
1	STOKES 5TH	15.00	12.00	247.5	0.1212	0.4848E-01	7.878	-4.122

get into get_stream_wave...
get out get_stream_wave...

WAVE NO	WAVE THEORY	WAVE PERIOD ACTUAL	WAVE HEIGHT	WAVE LENGTH	DEPTH ACTUAL	WAVE HEIGHT DIMENSIONLESS	DEPTH DIMENSIONLESS
1	Stream	15.00	12.000	247.93	30.00	0.54385E-02	0.13596E-01

time=	elev=	vel-x=	vel-y=	vel-z=	acc-x=	acc-y=	acc-z=	dphidt=
0.00	7.87772	4.34745	0.00000	0.00000	0.00000	0.00000	-1.76608	-71.46369
0.00	7.80846	4.45598	0.00000	0.00000	0.00000	0.00000	-0.61498	-23.51945
0.25	7.75130	4.30195	0.00000	-0.43909	-0.36288	0.00000	-1.73693	-70.71279
0.25	7.67465	4.40437	0.00000	-0.47840	-0.13133	0.00000	-0.60328	-23.24706
0.50	7.38429	4.16716	0.00000	-0.86371	-0.71199	0.00000	-1.65083	-68.48856
0.50	7.29044	4.25194	0.00000	-0.93868	-0.25658	0.00000	-0.56893	-22.44248
0.75	6.81139	3.94821	0.00000	-1.26008	-1.03409	0.00000	-1.51180	-64.87546
0.75	6.70106	4.00568	0.00000	-1.36386	-0.37013	0.00000	-0.51410	-21.14270
1.00	6.08387	3.65339	0.00000	-1.61575	-1.31702	0.00000	-1.32652	-60.01043
1.00	5.96520	3.67672	0.00000	-1.73920	-0.46715	0.00000	-0.44227	-19.40638
1.25	5.26133	3.29383	0.00000	-1.92026	-1.55042	0.00000	-1.10424	-54.07720
1.25	5.14105	3.27950	0.00000	-2.05307	-0.54399	0.00000	-0.35785	-17.30982
1.50	4.40248	2.88296	0.00000	-2.16573	-1.72650	0.00000	-0.85639	-47.29714
1.50	4.27801	2.83083	0.00000	-2.29756	-0.59836	0.00000	-0.26594	-14.94165
1.75	3.55699	2.43575	0.00000	-2.34741	-1.84072	0.00000	-0.59606	-39.91737
1.75	3.41394	2.34868	0.00000	-2.46891	-0.62951	0.00000	-0.17188	-12.39678
2.00	2.75989	1.96783	0.00000	-2.46387	-1.89235	0.00000	-0.33701	-32.19596
2.00	2.57574	1.85103	0.00000	-2.56747	-0.63822	0.00000	-0.08082	-9.77008
2.25	2.02926	1.49452	0.00000	-2.51714	-1.88475	0.00000	-0.09257	-24.38556
2.25	1.78119	1.35466	0.00000	-2.59743	-0.62671	0.00000	0.00270	-7.15012
2.50	1.36751	1.02981	0.00000	-2.51235	-1.82506	0.00000	0.12564	-16.71702
2.50	1.04113	0.87415	0.00000	-2.56616	-0.59831	0.00000	0.07512	-4.61393
2.75	0.76553	0.58548	0.00000	-2.45725	-1.72354	0.00000	0.30885	-9.38496
2.75	0.36121	0.42118	0.00000	-2.48332	-0.55710	0.00000	0.13417	-2.22304
3.00	0.20835	0.17051	0.00000	-2.36128	-1.59240	0.00000	0.45200	-2.53715
3.00	-0.25658	0.00407	0.00000	-2.35983	-0.50740	0.00000	0.17892	-0.02147
3.25	-0.31892	-0.20931	0.00000	-2.23468	-1.44436	0.00000	0.55405	3.73049
3.25	-0.81278	-0.37215	0.00000	-2.20683	-0.45329	0.00000	0.20969	1.96429
3.50	-0.82644	-0.55125	0.00000	-2.08745	-1.29116	0.00000	0.61782	9.37302
3.50	-1.30965	-0.70546	0.00000	-2.03480	-0.39828	0.00000	0.22781	3.72353
3.75	-1.31709	-0.85526	0.00000	-1.92848	-1.14231	0.00000	0.64913	14.38973
3.75	-1.75051	-0.99625	0.00000	-1.85293	-0.34507	0.00000	0.23521	5.25838
4.00	-1.78641	-1.12332	0.00000	-1.76495	-1.00428	0.00000	0.65567	18.81305
4.00	-2.13929	-1.24671	0.00000	-1.66872	-0.29550	0.00000	0.23414	6.58037
4.25	-2.22456	-1.35857	0.00000	-1.60203	-0.88021	0.00000	0.64555	22.69519
4.25	-2.48021	-1.46016	0.00000	-1.48794	-0.25063	0.00000	0.22683	7.70700
4.50	-2.61977	-1.56460	0.00000	-1.44295	-0.77028	0.00000	0.62610	26.09503
4.50	-2.77753	-1.64049	0.00000	-1.31465	-0.21091	0.00000	0.21531	8.65881
4.75	-2.96188	-1.74473	0.00000	-1.28929	-0.67251	0.00000	0.60284	29.06738
4.75	-3.03541	-1.79174	0.00000	-1.15146	-0.17631	0.00000	0.20129	9.45713
5.00	-3.24524	-1.90162	0.00000	-1.14156	-0.58389	0.00000	0.57905	31.65637
5.00	-3.25777	-1.91781	0.00000	-0.99977	-0.14651	0.00000	0.18612	10.12253

Figure 2-9 Comparison of the wave kinematics and dφ/dt between the stream function wave and the Stokes 5th wave

Then we do the same comparison further with a stream function wave calculated by a program based on Fenton's approach (The program is implemented by myself, but it is tested to be correct). We do not use Dalrymple's java application here to do the comparison because the application does not output wave kinematics. Though the wave kinematics can be calculated by the stream function coefficients output of the java application, I preferred to use my program here

33

since it is a good opportunity to extend I/O part of the program and I can modify the source code directly instead of post-process the results of the java application. The velocities and accelerations in y-direction are abandoned below as they are always zero.

Wasim Stream Function						
Fenton Stream Function						
time=	elev=	vel-x=	vel-z=	acc-x=	acc-z=	dphidt=
0.00	7.80846	4.45598	0.00000	0.00000	-0.61498	-23.51945
0.00	8.00570	4.45513	-0.00000	0.00000	-1.92544	-73.62334
0.25	7.67465	4.40437	-0.47840	-0.13133	-0.60328	-23.24706
0.25	7.87042	4.40354	-0.47830	-0.41110	-1.88881	-72.77082
0.50	7.29044	4.25194	-0.93868	-0.25658	-0.56893	-22.44248
0.50	7.48207	4.25117	-0.93849	-0.80321	-1.78128	-70.25272
0.75	6.70106	4.00568	-1.36386	-0.37013	-0.51410	-21.14270
0.75	6.88675	4.00500	-1.36359	-1.15866	-1.60969	-66.18470
1.00	5.96520	3.67672	-1.73920	-0.46715	-0.44227	-19.40638
1.00	6.14425	3.67615	-1.73888	-1.46240	-1.38483	-60.75036
1.25	5.14105	3.27950	-2.05307	-0.54399	-0.35785	-17.30982
1.25	5.31355	3.27908	-2.05272	-1.70297	-1.12059	-54.18841
1.50	4.27801	2.83083	-2.29756	-0.59836	-0.26594	-14.94165
1.50	4.44442	2.83054	-2.29722	-1.87322	-0.83288	-46.77619
1.75	3.41394	2.34868	-2.46891	-0.62951	-0.17188	-12.39678
1.75	3.57501	2.34853	-2.46860	-1.97080	-0.53842	-38.81073
2.00	2.57574	1.85103	-2.56747	-0.63822	-0.08082	-9.77008
2.00	2.73248	1.85101	-2.56721	-1.99816	-0.25334	-30.58885
2.25	1.78119	1.35466	-2.59743	-0.62671	0.00270	-7.15012
2.25	1.93461	1.35474	-2.59724	-1.96219	0.00813	-22.38781
2.50	1.04113	0.87415	-2.56616	-0.59831	0.07512	-4.61393
2.50	1.19198	0.87433	-2.56605	-1.87335	0.23490	-14.44868
2.75	0.36121	0.42118	-2.48332	-0.55710	0.13417	-2.22304
2.75	0.51017	0.42141	-2.48329	-1.74439	0.41982	-6.96406
3.00	-0.25658	0.00407	-2.35983	-0.50740	0.17892	-0.02147
3.00	-0.10884	0.00435	-2.35988	-1.58882	0.55999	-0.07181
3.25	-0.81278	-0.37215	-2.20683	-0.45329	0.20969	1.96429
3.25	-0.66564	-0.37185	-2.20695	-1.41945	0.65641	6.14507
3.50	-1.30965	-0.70546	-2.03480	-0.39828	0.22781	3.72353
3.50	-1.16271	-0.70515	-2.03499	-1.24724	0.71319	11.65299
3.75	-1.75051	-0.99625	-1.85293	-0.34507	0.23521	5.25838
3.75	-1.60851	-0.99595	-1.85315	-1.08064	0.73643	16.45859
4.00	-2.13929	-1.24671	-1.66872	-0.29550	0.23414	6.58037
4.00	-1.99198	-1.24643	-1.66898	-0.92543	0.73314	20.59787
4.25	-2.48021	-1.46016	-1.48794	-0.25063	0.22683	7.70700
4.25	-2.33235	-1.45990	-1.48821	-0.78495	0.71030	24.12558
4.50	-2.77753	-1.64049	-1.31465	-0.21091	0.21531	8.65881
4.50	-2.62901	-1.64025	-1.31493	-0.66057	0.67425	27.10596
4.75	-3.03541	-1.79174	-1.15146	-0.17631	0.20129	9.45713
4.75	-2.88622	-1.79152	-1.15174	-0.55221	0.63037	29.60578
5.00	-3.25777	-1.91781	-0.99977	-0.14651	0.18612	10.12253
5.00	-3.10790	-1.91761	-1.00004	-0.45888	0.58292	31.68943

Figure 2-10 Comparison between the Wasim stream function wave and the Fenton stream function wave

The accelerations and $\frac{d\phi}{dt}$ from the wasim stream function wave seems to be wrong. Both accelerations and $\frac{d\phi}{dt}$ are derivatives by time, which is associated with wave celebrity. Since $\frac{d\phi}{dt} = \frac{\partial\phi}{\partial x} \cdot \frac{\partial x}{dt} = u \cdot c$, if the velocity in x-direction is correct (which has very small deviations compared

both to the Wasim Stokes 5th wave and the Fenton stream function wave), then the wave celebrity should be wrong.

By checking through the source code of Wasim in debug mode, the wave-length, period, height, all the coefficients and etc. are nondimensionalized at once after input, and all the computations are nondimensional, i.e. the results should be redimensionalized before output. After modifying the program so that the results are in correct dimension before output, the results become quite different.

time=	elev=	vel-x=	vel-z=	acc-x=	acc-z=	dphidt=
0.00	7.80846	13.95415	0.00000	0.00000	-6.03092	-230.64705
0.00	8.00570	4.45513	-0.00000	0.00000	-1.92544	-73.62334
0.25	7.67465	13.79253	-1.49815	-1.28788	-5.91616	-227.97575
0.25	7.87042	4.40354	-0.47830	-0.41110	-1.88881	-72.77082
0.50	7.29044	13.31518	-2.93953	-2.51622	-5.57925	-220.08556
0.50	7.48207	4.25117	-0.93849	-0.80321	-1.78128	-70.25272
0.75	6.70106	12.54401	-4.27101	-3.62972	-5.04164	-207.33908
0.75	6.88675	4.00500	-1.36359	-1.15866	-1.60969	-66.18470
1.00	5.96520	11.51385	-5.44641	-4.58118	-4.33715	-190.31161
1.00	6.14425	3.67615	-1.73888	-1.46240	-1.38483	-60.75036
1.25	5.14105	10.26995	-6.42929	-5.33468	-3.50931	-169.75137
1.25	5.31355	3.27908	-2.05272	-1.70297	-1.12059	-54.18841
1.50	4.27801	8.86491	-7.19494	-5.86787	-2.60799	-146.52750
1.50	4.44442	2.83054	-2.29722	-1.87322	-0.83288	-46.77619
1.75	3.41394	7.35504	-7.73153	-6.17335	-1.68554	-121.57092
1.75	3.57501	2.34853	-2.46860	-1.97080	-0.53842	-38.81073
2.00	2.57574	5.79661	-8.04018	-6.25884	-0.79255	-95.81172
2.00	2.73248	1.85101	-2.56721	-1.99816	-0.25334	-30.58885
2.25	1.78119	4.24218	-8.13400	-6.14594	0.02643	-70.11876
2.25	1.93461	1.35474	-2.59724	-1.96219	0.00813	-22.38781
2.50	1.04113	2.73746	-8.03607	-5.86745	0.73664	-45.24722
2.50	1.19198	0.87433	-2.56605	-1.87335	0.23490	-14.44868
2.75	0.36121	1.31894	-7.77665	-5.46332	1.31572	-21.80060
2.75	0.51017	0.42141	-2.48329	-1.74439	0.41982	-6.96406
3.00	-0.25658	0.01274	-7.38993	-4.97587	1.75457	-0.21051
3.00	-0.10884	0.00435	-2.35988	-1.58882	0.55999	-0.07181
3.25	-0.81278	-1.16542	-6.91080	-4.44525	2.05639	19.26314
3.25	-0.66564	-0.37185	-2.20695	-1.41945	0.65641	6.14507
3.50	-1.30965	-2.20918	-6.37210	-3.90579	2.23404	36.51533
3.50	-1.16271	-0.70515	-2.03499	-1.24724	0.71319	11.65299
3.75	-1.75051	-3.11981	-5.80255	-3.38395	2.30664	51.56711
3.75	-1.60351	-0.99595	-1.85315	-1.08064	0.73643	16.45859
4.00	-2.13929	-3.90415	-5.22570	-2.89782	2.29615	64.53140
4.00	-1.99663	-1.24643	-1.66898	-0.92543	0.73314	20.59787
4.25	-2.48021	-4.57258	-4.65956	-2.45785	2.22447	75.57988
4.25	-2.33235	-1.45990	-1.48821	-0.78495	0.71030	24.12558
4.50	-2.77753	-5.13729	-4.11690	-2.06832	2.11146	84.91393
4.50	-2.62901	-1.64025	-1.31493	-0.66057	0.67425	27.10596
4.75	-3.03541	-5.61094	-3.60586	-1.72900	1.97393	92.74272
4.75	-2.88622	-1.79152	-1.15174	-0.55221	0.63037	29.60578
5.00	-3.25777	-6.00572	-3.13085	-1.43674	1.82525	99.26808
5.00	-3.10790	-1.91761	-1.00004	-0.45888	0.58292	31.68943

Figure 2-11 Comparison after modification, the ratio of the values between Wasim and Fenton is about $\sqrt{g}$

If we compare the results carefully, the ratio of all the values from the Wasim stream function wave and the Fenton stream function wave is about $\sqrt{g}$ so it looks like some variable is wrongly nondimensionalized. By further study of the formula which calculates stream function, i.e. equation (12) $\psi(x,z) = \frac{X_1 \cdot z}{T} + \sum_{n=2}^{N+1}\{X_n \cdot \sinh\frac{2(n-1)\pi}{X_1}(h+z) \cdot \cos\frac{2(n-1)\pi}{X_1}x\}$, the Fourier coefficients X_n should have the same dimension as stream function as both *sinh* and *cos* are dimensionless, i.e. the dimension of the Fourier coefficients should be $[\frac{m^2}{s}]$ (or $[\text{alength} * \sqrt{g * \text{alength}}]$ in source code of Wasim, where alength is a reference length, e.g. if we use millimeter as unit in analyses, then alength = 1000), but the coefficients have not been nondimensionlized after input. Since alength=1 as meter is used, the ratio $\sqrt{g}$ then can be explained.

After fixing this bug, the accelerations and $\frac{d\phi}{dt}$ from the wasim stream function wave seems to be correct now.

Wasim Stream Function
Fenton Stream Function

time=	elev=	vel-x=	vel-z=	acc-x=	acc-z=	dphidt=
0.00	7.80846	4.45598	0.00000	0.00000	-1.92585	-73.65251
0.00	8.00570	4.45513	-0.00000	0.00000	-1.92544	-73.62334
0.25	7.67465	4.40437	-0.47840	-0.41126	-1.88921	-72.79948
0.25	7.87042	4.40354	-0.47830	-0.41110	-1.88881	-72.77082
0.50	7.29044	4.25193	-0.93868	-0.80351	-1.78162	-70.27991
0.50	7.48207	4.25117	-0.93849	-0.80321	-1.78128	-70.25272
0.75	6.70106	4.00568	-1.36386	-1.15908	-1.60995	-66.20956
0.75	6.88675	4.00500	-1.36359	-1.15866	-1.60969	-66.18470
1.00	5.96520	3.67672	-1.73920	-1.46291	-1.38498	-60.77219
1.00	6.14425	3.67615	-1.73888	-1.46240	-1.38483	-60.75036
1.25	5.14105	3.27950	-2.05306	-1.70352	-1.12063	-54.20669
1.25	5.31355	3.27908	-2.05272	-1.70297	-1.12059	-54.18841
1.50	4.27801	2.83083	-2.29756	-1.87379	-0.83281	-46.79062
1.50	4.44442	2.83054	-2.29722	-1.87322	-0.83288	-46.77619
1.75	3.41394	2.34868	-2.46891	-1.97134	-0.53824	-38.82124
1.75	3.57501	2.34853	-2.46860	-1.97080	-0.53842	-38.81073
2.00	2.57574	1.85103	-2.56747	-1.99863	-0.25309	-30.59555
2.00	2.73248	1.85101	-2.56721	-1.99816	-0.25334	-30.58885
2.25	1.78119	1.35466	-2.59743	-1.96258	0.00844	-22.39102
2.25	1.93461	1.35474	-2.59724	-1.96219	0.00813	-22.38781
2.50	1.04113	0.87415	-2.56616	-1.87365	0.23523	-14.44879
2.50	1.19198	0.87433	-2.56605	-1.87335	0.23490	-14.44868
2.75	0.36121	0.42118	-2.48332	-1.74460	0.42015	-6.96158
2.75	0.51017	0.42141	-2.48329	-1.74439	0.41982	-6.96406
3.00	-0.25658	0.00407	-2.35982	-1.58895	0.56029	-0.06722
3.00	-0.10884	0.00435	-2.35988	-1.58882	0.55999	-0.07181
3.25	-0.81278	-0.37215	-2.20683	-1.41950	0.65667	6.15130
3.25	-0.66564	-0.37185	-2.20695	-1.41945	0.65641	6.14507
3.50	-1.30965	-0.70546	-2.03480	-1.24724	0.71340	11.66044
3.50	-1.16271	-0.70515	-2.03499	-1.24724	0.71319	11.65299
3.75	-1.75051	-0.99625	-1.85293	-1.08060	0.73658	16.46692
3.75	-1.60351	-0.99595	-1.85315	-1.08064	0.73643	16.45859
4.00	-2.13929	-1.24671	-1.66872	-0.92536	0.73323	20.60681
4.00	-1.99198	-1.24643	-1.66898	-0.92543	0.73314	20.59787

36

4.25	-2.48021	-1.46016	-1.48794	-0.78487	0.71034	24.13492
4.25	-2.33235	-1.45990	-1.48821	-0.78495	0.71030	24.12558
4.50	-2.77753	-1.64049	-1.31465	-0.66048	0.67425	27.11556
4.50	-2.62901	-1.64025	-1.31493	-0.66057	0.67425	27.10596
4.75	-3.03541	-1.79174	-1.15146	-0.55212	0.63034	29.61553
4.75	-2.88622	-1.79152	-1.15174	-0.55221	0.63037	29.60578
5.00	-3.25777	-1.91781	-0.99977	-0.45880	0.58286	31.69927
5.00	-3.10790	-1.91761	-1.00004	-0.45888	0.58292	31.68943

Figure 2-12 Comparison after bug fixing, the accelerations and dφ/dt seems to be correct now

Since the program can calculate the wave kinematics properly, the huge deviation in Froude-Krylov force will disappear at once.
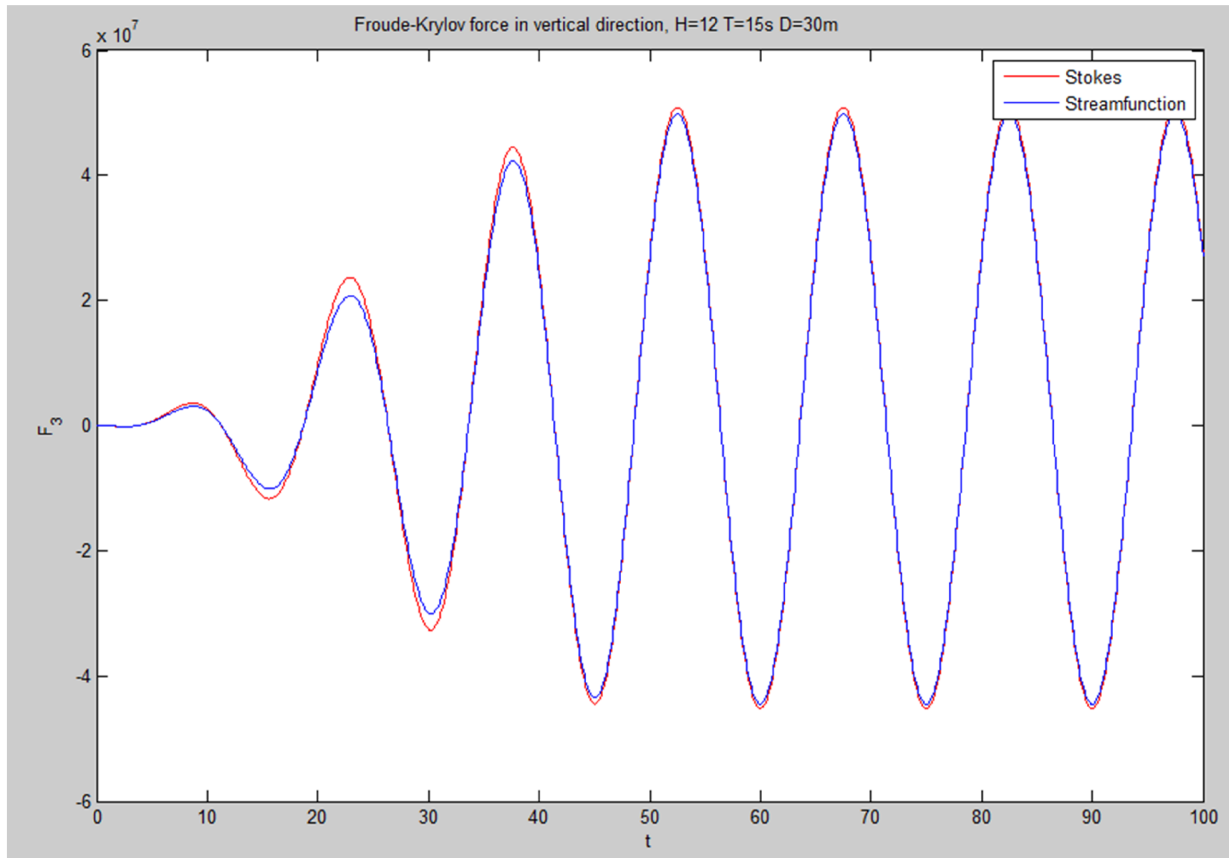
Figure 2-13 Comparison of the Froude-Krylov force after bug fixing

And this leads further to vanished "pumping effect". The diffraction wave elevations right behind the middle column are very close to the analysis where the incident wave is Stokes 5th wave.
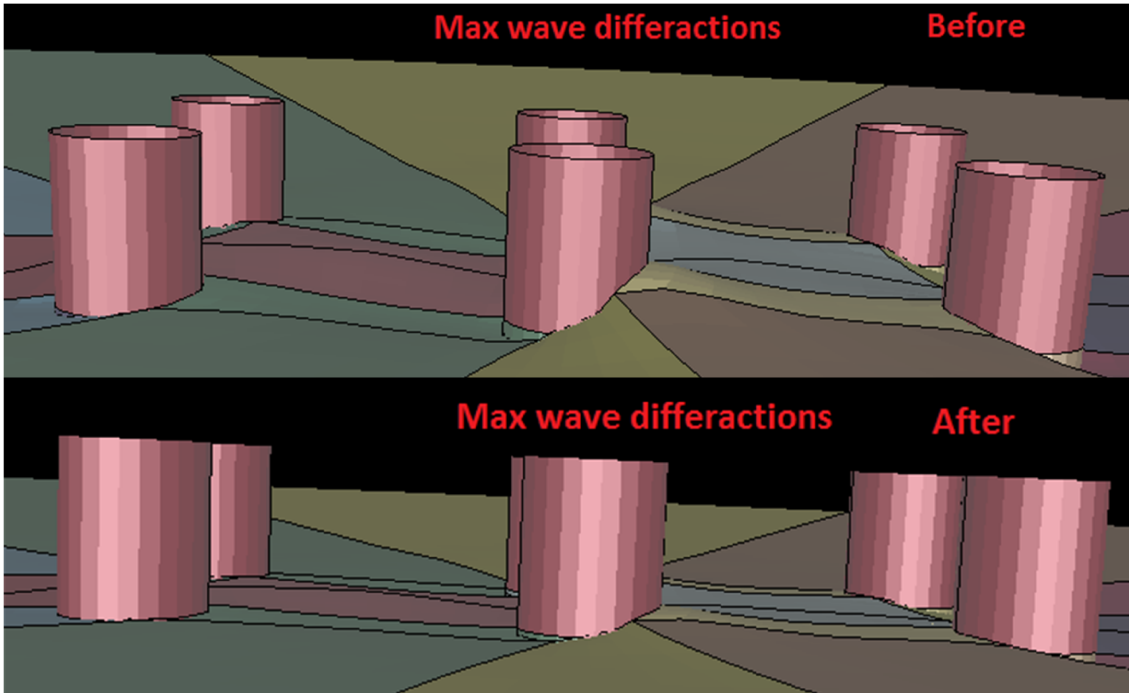
Figure 2-14 "pumping effect" disappears after bug fixing
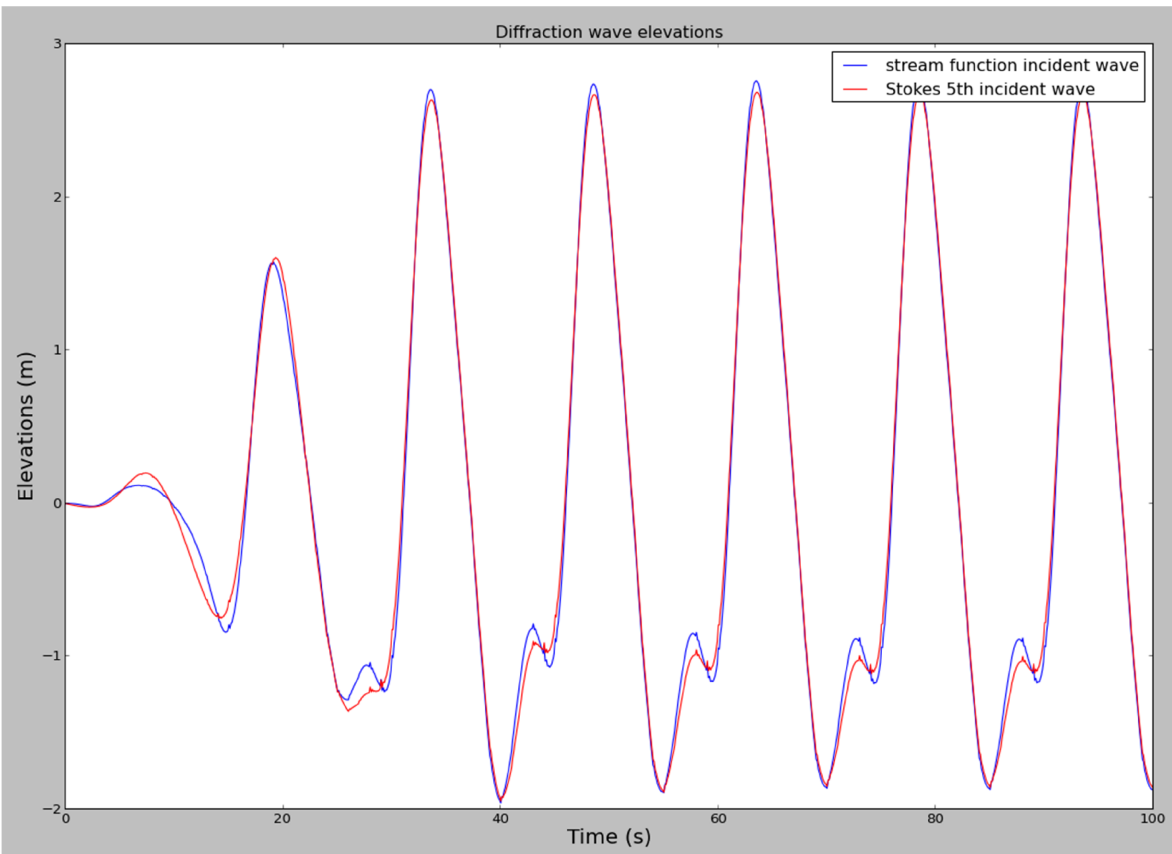
Figure 2-15 Comparison of diffraction wave elevations behind the middle column after bug fixing

2.4 Fix the wave elevations

Another strange thing observed when doing the analyses is about the wave elevations of the Wasim stream function wave. When we zoom in around the crest, the stream function wave generated by Wasim gives a lower crest (7.8084 m) than the Stokes wave (7.8777 m). And the trough (-4.1482 m) of the Wasim stream function wave is lower than the Stokes wave (-4.1222 m). What we expected is that the stream function wave should have a higher crest and also a flatter trough due to higher order nonlinearity. The stream function wave generated by using Fenton's approach gives more reasonable results where the highest elevation is 8.0069 m and the lowest elevation is -3.9929 m. See the pictures below.
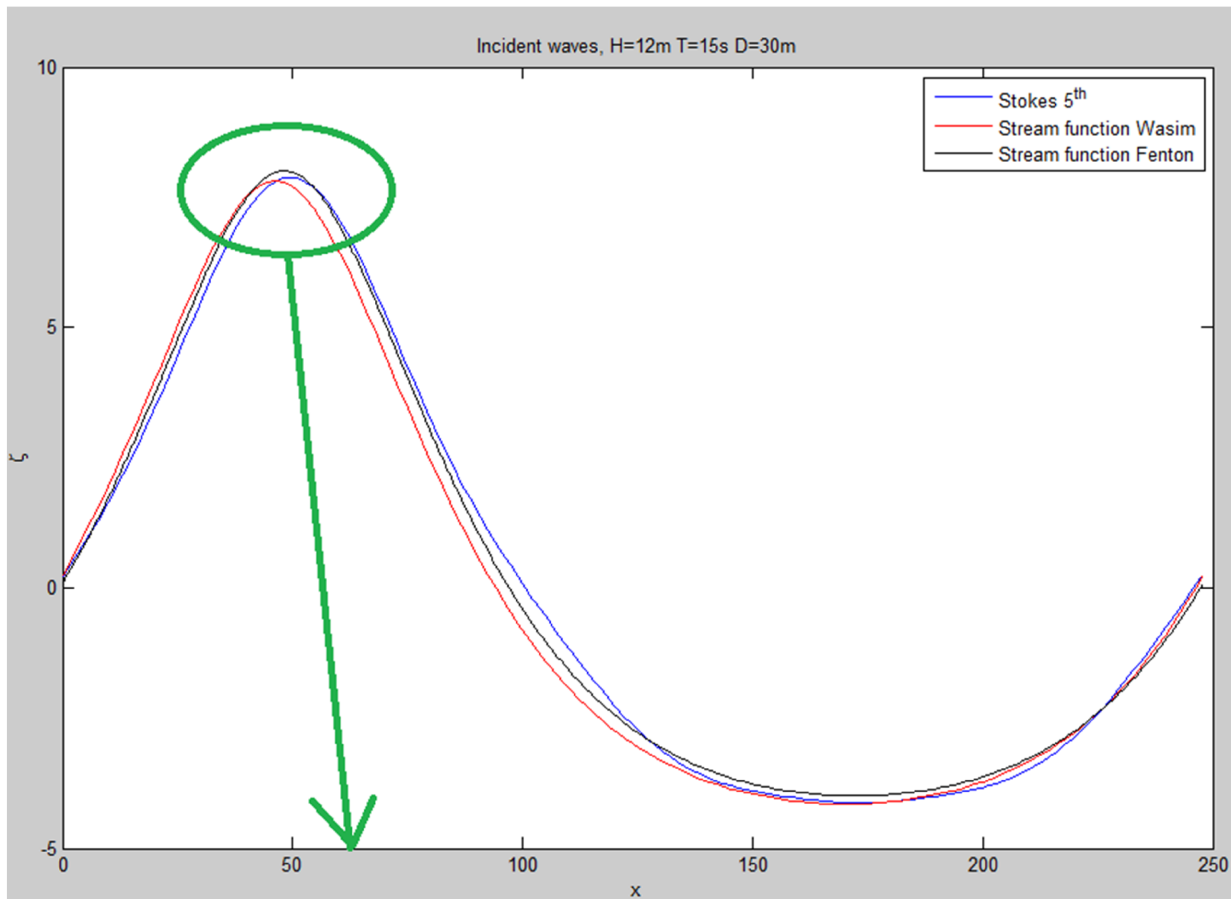
Figure 2-16 Comparison of the incident wave profiles
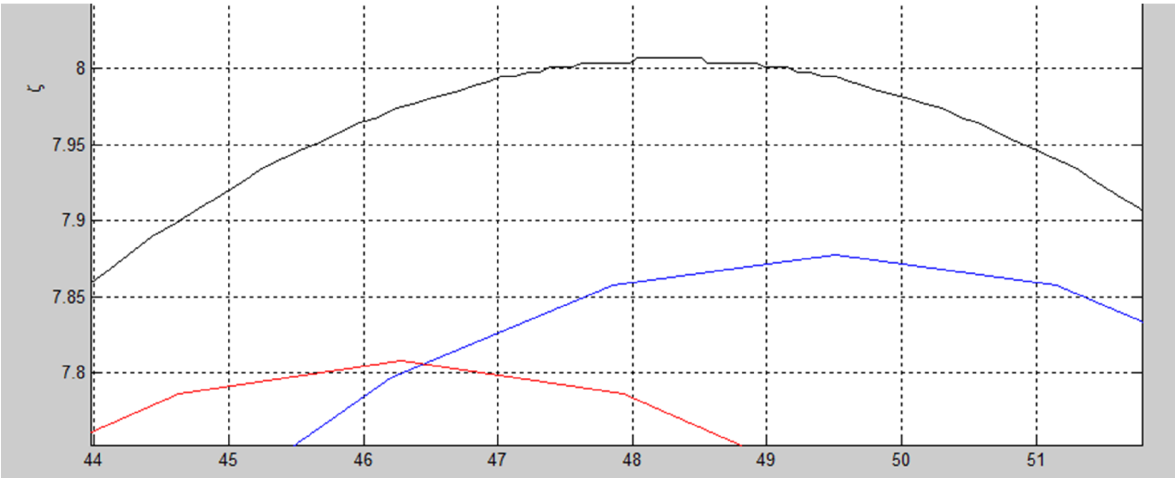
Figure 2-17 Comparison of the wave crests after zoomed in

Similar results as Fenton's approach can be obtained by using Dalrymple's java application.
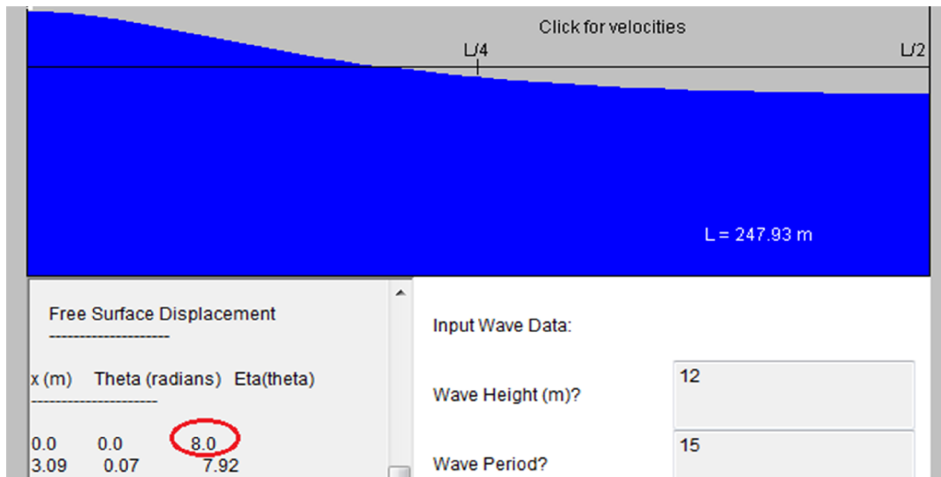
Figure 2-18 Wave elevation at crest from Dalrymple's java application
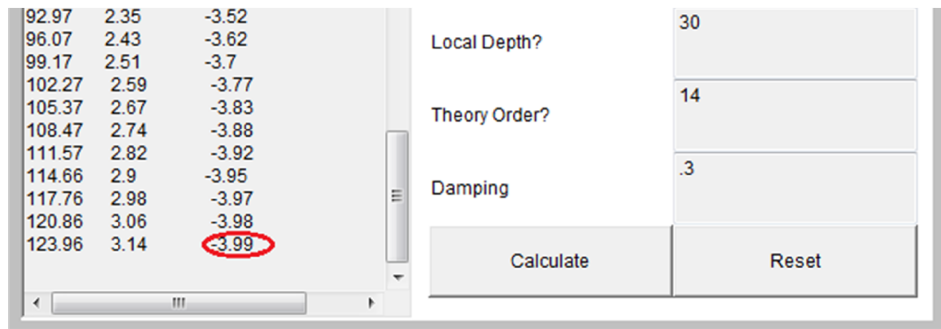
Figure 2-19 Wave elevation at trough from Dalrymple's java application

Since Wasim calculates wave elevations by using the wave elevation coefficients output by the python script, so there must be some error in the script. The python script first calculates exact

elevation values at some collocation points in a predefined resolution (let us denote these val-
ues as elev_exact), then the script calculates the wave elevation coefficients (let us denote
these coefficients as elev_coeff) based on these elev_exact values by least square fitting. In final
the script can interpolate approximated elevation values (let us denote these values as
elev_approx) at any point by series summation of these elevation_coeff. The problem looks like
that the elev_exact values are already not so accurate while the least squares fitting works per-
fectly, i.e. very little difference between elev_exact values and elev_approx values at the collo-
cation points.

Python				Dalrymple	Fenton
x	elev_exact	elev_approx		elev	elev
0.00	7.811772	7.811771		8.00	8.005705
3.10	7.736088	7.736088		7.92	7.929232
6.20	7.514654	7.514655		7.70	7.705514
9.30	7.163071	7.163071		7.35	7.350414
12.40	6.703732	6.703731		6.88	6.886747
15.50	6.161995	6.161995		6.34	6.340328
18.60	5.562907	5.562908		5.73	5.736547
21.69	4.929059	4.929058		5.09	5.098177
24.79	4.279532	4.279531		4.44	4.444416
27.89	3.629673	3.629673		3.79	3.790729
30.99	2.991322	2.991322		3.14	3.149079
34.09	2.373272	2.373271		2.52	2.528305
37.19	1.781780	1.781779		1.93	1.934606
40.29	1.221054	1.221054		1.37	1.372088
43.39	0.693680	0.693681		0.84	0.843278
46.49	0.200988	0.200987		0.34	0.349511
49.59	-0.256659	-0.256660		-0.10	-0.108836
52.69	-0.679619	-0.679619		-0.53	-0.532158
55.79	-1.068784	-1.068783		-0.92	-0.921439
58.88	-1.425423	-1.425423		-1.27	-1.278035

Figure 2-20 Comparison of the wave elevation values indicates elev_exact may already be wrong

I was expecting in the beginning that the script would calculate elev_exact by solving the tran-
scendental equation (16) iteratively based on the stream function coefficients output of the java
application, i.e. physically by requiring $\psi(z = \zeta) = \psi_\zeta = X_{N+1}$. But the script solves the prob-
lem in a smarter way, by requiring local pressure equals to zero along the wave surface, i.e. to
increase or decrease wave elevation iteratively at a collocation point so that the local pressure

there will converge to zero. This approach takes fewer iterations since the local pressure can be calculated straightforward after wave kinematics are known. But the disadvantage is that Dalrymple's approach is mainly based on least square fitting the objective function $O = \frac{1}{I}\sum_{i=1}^{I}(R_i - \bar{R})^2 + \frac{\lambda_1}{I}\sum_{i=1}^{I}\zeta(x_i) + \lambda_2(\zeta(x_1) - \zeta(x_I) - H)$, and the local Bernoulli constant R_i will be slightly different at the collocation points, then solving elev_exact from the dynamic F.S:

condition $\frac{1}{2}\left(\left(\frac{\partial\psi}{\partial x}\right)^2 + \left(\frac{\partial\psi}{\partial z}\right)^2\right) + g\zeta = R$ should refer to those local R_i so that the whole method will be consistent. So long these R_i values are not available from the online java application, solving the transcendental equation will give better solutions, though a bit slower when the script is used to calculate a series of waves.

time=	elev=	vel-x=	vel-z=	acc-x=	acc-z=	dphidt=
Wasim Stream Function						
Fenton Stream Function						
0.00	8.00601	4.45598	0.00000	0.00000	-1.92585	-73.65251
0.00	8.00570	4.45513	0.00000	-0.00000	-1.92544	-73.62334
0.25	7.87069	4.40437	-0.47840	-0.41126	-1.88921	-72.79948
0.25	7.87042	4.40354	0.47830	0.41110	-1.88881	-72.77082
0.50	7.48228	4.25193	-0.93868	-0.80351	-1.78162	-70.27991
0.50	7.48207	4.25117	0.93849	0.80321	-1.78128	-70.25272
0.75	6.88691	4.00568	-1.36386	-1.15908	-1.60995	-66.20956
0.75	6.88675	4.00500	1.36359	1.15866	-1.60969	-66.18470
1.00	6.14428	3.67672	-1.73920	-1.46291	-1.38498	-60.77219
1.00	6.14425	3.67615	1.73888	1.46240	-1.38483	-60.75036
1.25	5.31339	3.27950	-2.05306	-1.70352	-1.12063	-54.20669
1.25	5.31355	3.27908	2.05272	1.70297	-1.12059	-54.18841
1.50	4.44418	2.83083	-2.29756	-1.87379	-0.83281	-46.79062
1.50	4.44442	2.83054	2.29722	1.87322	-0.83288	-46.77619
1.75	3.57480	2.34868	-2.46891	-1.97134	-0.53824	-38.82124
1.75	3.57501	2.34853	2.46860	1.97080	-0.53842	-38.81073
2.00	2.73221	1.85103	-2.56747	-1.99863	-0.25309	-30.59555
2.00	2.73248	1.85101	2.56721	1.99816	-0.25334	-30.58885
2.25	1.93423	1.35466	-2.59743	-1.96258	0.00844	-22.39102
2.25	1.93461	1.35474	2.59724	1.96219	0.00813	-22.38781
2.50	1.19158	0.87415	-2.56616	-1.87365	0.23523	-14.44879
2.50	1.19198	0.87433	2.56605	1.87335	0.23490	-14.44868
2.75	0.50985	0.42118	-2.48332	-1.74460	0.42015	-6.96158
2.75	0.51017	0.42141	2.48329	1.74439	0.41982	-6.96406
3.00	-0.10910	0.00407	-2.35982	-1.58895	0.56029	-0.06722
3.00	-0.10884	0.00435	2.35988	1.58882	0.55999	-0.07181
3.25	-0.66593	-0.37215	-2.20683	-1.41950	0.65667	6.15130
3.25	-0.66564	-0.37185	2.20695	1.41945	0.65641	6.14507
3.50	-1.16299	-0.70546	-2.03480	-1.24724	0.71340	11.66044
3.50	-1.16271	-0.70515	2.03499	1.24724	0.71319	11.65299
3.75	-1.60369	-0.99625	-1.85293	-1.08060	0.73658	16.46692
3.75	-1.60351	-0.99595	1.85315	1.08064	0.73643	16.45859
4.00	-1.99207	-1.24671	-1.66872	-0.92536	0.73323	20.60681
4.00	-1.99198	-1.24643	1.66898	0.92543	0.73314	20.59787

Figure 2-21 Comparison of the wave elevation values after modification

2.5 Test the modifications

The modification of both Wasim source code and the python script should be tested. The wave elevation, kinematics and $\frac{d\phi}{dt}$ will be compared with results from other programs according to the following figure and table.
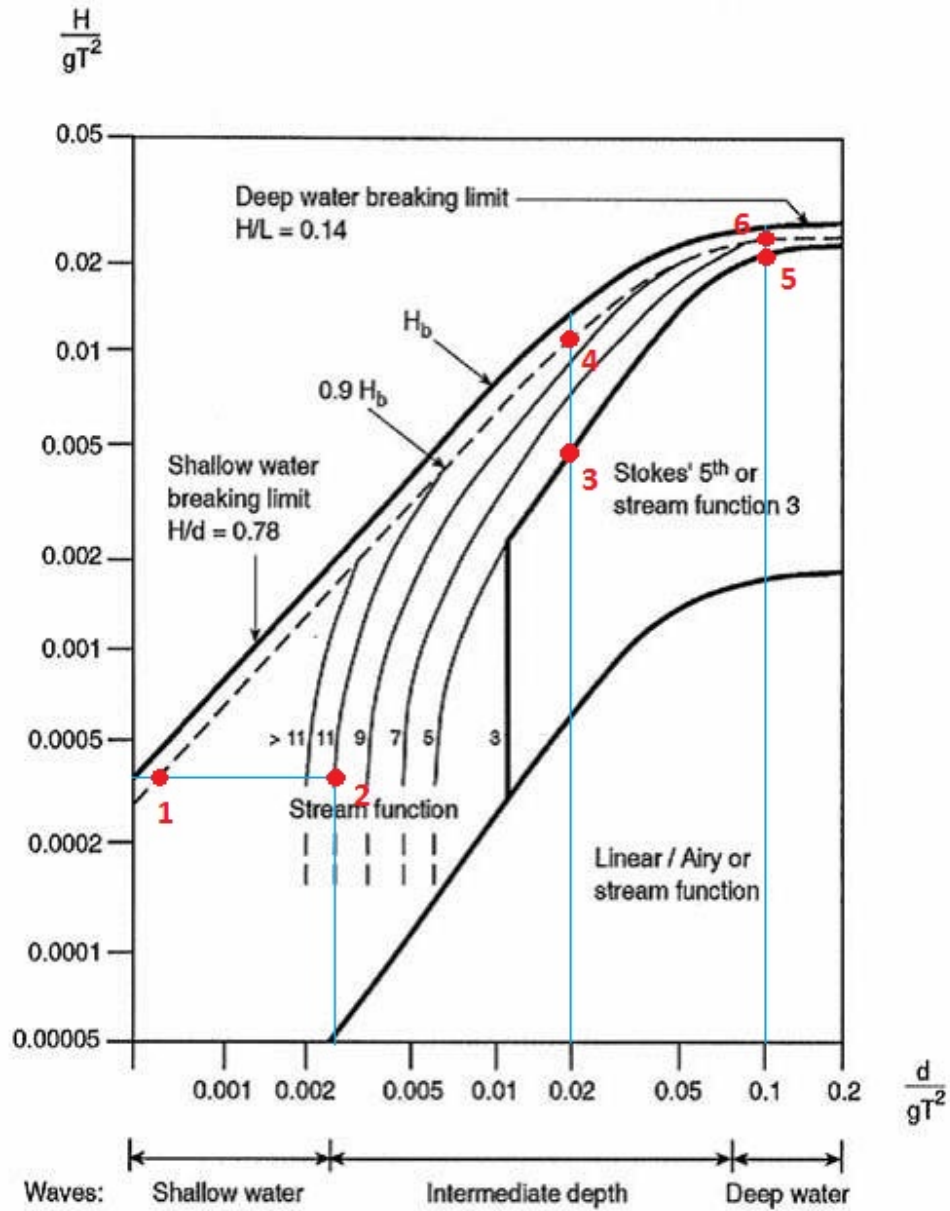
Figure 2-22 Wave conditions which will be used for testing

Point	$\dfrac{d}{gT^2}$	$\dfrac{H}{gT^2}$	T (s)	H (m)	Program	Order
Shallow water (D=30m)						
1	0.0006	0.0004	71.4043	20.0000	WasimStream WajacStream FentonStream	varies
2	0.0026	0.0004	34.3015	4.6154	WasimStream WajacStream FentonStream	11
Intermediate water (D=100m)						
3	0.0200	0.0048	22.5800	24.0000	WasimStream WajacStream FentonStream WasimStokes WajacStokes FentonStokes	5
4	0.0020	0.0100	22.5800	50.0000	WasimStream WajacStream FentonStream	11
Deep water (D=300m)						
5	0.1000	0.0199	17.4904	59.6998	WasimStream WajacStream FentonStream WasimStokes WajacStokes FentonStokes	5
6	0.1000	0.0220	17.4904	65.9998	WasimStream WajacStream FentonStream	11

Table 2-1 Parameters to the wave conditions which will be used for testing

Program	Theory
WasimStream	Dalrymple's approach
WajacStream	Dean's approach
FentonStream (my implementation)	Fenton's approach
WasimStokes	Fenton's approach
WajacStokes	Skjelbreia and Hendrickson's approach
FentonStokes (my implementation)	Fenton's approach

Table 2-2 Information about the programs which will be used for testing

2.5.1 Wave condition 2

Point 2 Wasim Stream Function
Point 2 Wajac Stream Function
Point 2 Fenton Stream Function

time=	elev=	vel-x=	vel-z=	acc-x=	acc-z=	dphidt=
0.00	3.30382	1.90459	0.00000	0.00000	-0.30533	-32.93270
0.00	3.30310	1.90382	0.00000	0.00000	-0.27151	32.91311
0.00	3.30372	1.90423	-0.00000	0.00000	-0.30525	-32.92056
0.25	3.29154	1.89775	-0.07612	-0.05461	-0.30278	-32.81449
0.25	3.29084	1.89699	-0.07607	-0.04990	-0.26913	32.79502
0.25	3.29145	1.89740	-0.07610	-0.05458	-0.30271	-32.80242
0.50	3.25500	1.87738	-0.15097	-0.10814	-0.29522	-32.46215
0.50	3.25432	1.87663	-0.15087	-0.09889	-0.26205	32.44308
0.50	3.25492	1.87703	-0.15094	-0.10810	-0.29515	-32.45030
0.75	3.19502	1.84386	-0.22333	-0.15959	-0.28290	-31.88254
0.75	3.19439	1.84314	-0.22318	-0.14609	-0.25051	31.86412
0.75	3.19496	1.84352	-0.22328	-0.15952	-0.28284	-31.87104
1.00	3.11292	1.79784	-0.29206	-0.20799	-0.26621	-31.08681
1.00	3.11235	1.79716	-0.29186	-0.19069	-0.23488	31.06926
1.00	3.11288	1.79752	-0.29199	-0.20790	-0.26616	-31.07578
1.25	3.01048	1.74019	-0.35612	-0.25251	-0.24569	-30.08994
1.25	3.00998	1.73956	-0.35588	-0.23196	-0.21564	30.07348
1.25	3.01046	1.73989	-0.35604	-0.25241	-0.24565	-30.07949
1.50	2.88981	1.67196	-0.41464	-0.29246	-0.22196	-28.91027
1.50	2.88940	1.67140	-0.41436	-0.26927	-0.19339	28.89507
1.50	2.88981	1.67170	-0.41455	-0.29235	-0.22193	-28.90049
1.75	2.75327	1.59438	-0.46689	-0.32730	-0.19573	-27.56879
1.75	2.75296	1.59389	-0.46659	-0.30215	-0.16878	27.55501
1.75	2.75329	1.59414	-0.46680	-0.32718	-0.19571	-27.55976

Figure 2-23 Comparison of wave elevation, kinematics and dφ/dt in wave condition 2

Wasim stream function seems to work well. Acc-z from Wajac stream function seems to have

lower absolute value, and $\frac{d\phi}{dt}$ has opposite sign (may due to different definition). The absolute

value of $\frac{d\phi}{dt}$ in Wajac stream function is a little lower which may due to the lower absolute value

of vel-x.

2.5.2 Wave condition 3

Point 3 Wasim Stream Function						
Point 3 Wajac Stream Function						
Point 3 Fenton Stream Function						
Point 3 Wasim Stokes 5th						
Point 3 Wajac Stokes 5th						
Point 3 Fenton Stokes 5th						
time=	elev=	vel-x=	vel-z=	acc-x=	acc-z=	dphidt=
0.00	13.96025	4.71898	0.00000	0.00000	-1.19688	-131.06857
0.00	13.95837	4.71746	0.00000	0.00000	-0.99316	130.99767
0.00	13.95998	4.71825	-0.00000	0.00000	-1.19676	-131.01974
0.00	13.95547	4.71440	0.00000	0.00000	-1.19496	-130.96103
0.00	13.94746	4.71777	0.00000	0.00000	-1.19522	130.99048
0.00	13.95547	4.71669	0.00000	0.00000	-1.19506	-130.97122
0.25	13.90310	4.70308	-0.29877	-0.12704	-1.19148	-130.62712
0.25	13.90124	4.70158	-0.29865	-0.11827	-0.98800	130.55658
0.25	13.90308	4.70236	-0.29874	-0.12701	-1.19136	-130.57848
0.25	13.89868	4.69857	-0.29830	-0.12653	-1.18963	-130.52148
0.25	13.89108	4.70193	-0.29836	-0.12658	-1.18988	130.55077
0.25	13.89867	4.70086	-0.29832	-0.12655	-1.18972	-130.53159
11.50	-10.02903	-3.60578	0.12684	0.03560	0.60409	100.14982
11.50	-10.02871	-3.39854	0.11397	0.03810	0.60930	-94.37280
11.50	-10.02930	-3.60550	0.12686	0.03560	0.60417	100.12011
11.50	-10.03376	-3.61078	0.12729	0.03597	0.60621	100.19062
11.50	-10.04221	-3.40080	0.11416	0.03608	0.54361	-94.42445
11.50	-10.03367	-3.60843	0.12785	0.03613	0.60626	100.19750
11.75	-9.98853	-3.59157	0.27792	0.07815	0.60460	99.75508
11.75	-9.98819	-3.38499	0.24978	0.08354	0.61006	-93.99660
11.75	-9.98855	-3.59129	0.27795	0.07814	0.60468	99.72547
11.75	-9.99284	-3.59642	0.27888	0.07893	0.60658	99.79196
11.75	-10.00089	-3.38721	0.25019	0.07914	0.54398	-94.04712
11.75	-9.99263	-3.59403	0.27946	0.07910	0.60663	99.79766
12.00	-9.91771	-3.56668	0.42917	0.12106	0.60543	99.06372
12.00	-9.91734	-3.36128	0.38591	0.12919	0.61135	-93.33832
12.00	-9.91736	-3.56640	0.42922	0.12105	0.60551	99.03432
12.00	-9.92136	-3.57129	0.43060	0.12222	0.60718	99.09406
12.00	-9.92873	-3.36343	0.38653	0.12245	0.54458	-93.38689
12.00	-9.92102	-3.56885	0.43118	0.12240	0.60723	99.09850

Figure 2-24 Comparison of wave elevation, kinematics and dφ/dt in wave condition 3

Wasim stream function works well. Wajac stream function has the same problem as observed at point 2, but vel-x and $\frac{d\phi}{dt}$ varies more. In addition $\frac{d\phi}{dt}$ from Wajac stokes 5th also has also opposite sign and lower absolute value, and the other parameters have more or less deviations.

2.5.3 Wave condition 4

Point 4 Wasim Stream Function						
Point 4 Wajac Stream Function						
Point 4 Fenton Stream Function						
time=	elev=	vel-x=	vel-z=	acc-x=	acc-z=	dphidt=
0.00	33.93060	9.86690	0.00000	0.00000	-3.03107	-292.59091
0.00	33.92268	9.86304	0.00000	0.00000	-2.02128	292.41141
0.00	33.93020	9.86516	-0.00000	0.00000	-3.03055	-292.47687
0.25	33.59167	9.81734	-0.75569	-0.39574	-3.00622	-291.12128
0.25	33.58380	9.81353	-0.75517	-0.34098	-1.99967	290.94363
0.25	33.59603	9.81561	-0.75556	-0.39562	-3.00570	-291.00795
0.50	32.61351	9.66977	-1.49904	-0.78264	-2.93256	-286.74521
0.50	32.60645	9.66612	-1.49800	-0.67499	-1.93561	286.57321
0.50	32.62634	9.66808	-1.49878	-0.78242	-2.93207	-286.63409
0.75	31.09796	9.42746	-2.21812	-1.15234	-2.81271	-279.55972
0.75	31.09293	9.42406	-2.21662	-0.99539	-1.83135	279.39685
0.75	31.11155	9.42584	-2.21775	-1.15201	-2.81226	-279.45217
1.00	29.17714	9.09566	-2.90188	-1.49735	-2.65079	-269.72067
1.00	29.17441	9.09260	-2.89997	-1.29621	-1.69043	269.57010
1.00	29.17872	9.09413	-2.90140	-1.49693	-2.65038	-269.61803
1.25	26.98077	8.68137	-3.54045	-1.81137	-2.45208	-257.43542
1.25	26.97966	8.67872	-3.53818	-1.57235	-1.51743	257.29971
1.25	26.96455	8.67996	-3.53987	-1.81085	-2.45172	-257.33878
11.00	-16.04970	-5.38916	-0.17479	-0.03282	0.60457	159.80890
11.00	-16.05138	-5.08139	-0.15465	-0.04651	0.62658	-150.64905
11.00	-16.05027	-5.38884	-0.17483	-0.03278	0.60471	159.76557
11.25	-16.06853	-5.39382	-0.02407	-0.00451	0.60185	159.94710
11.25	-16.07014	-5.08704	-0.02130	-0.00640	0.62389	-150.81635
11.25	-16.06943	-5.39350	-0.02408	-0.00451	0.60198	159.90357
11.50	-16.05883	-5.39142	0.12648	0.02373	0.60325	159.87596
11.50	-16.06048	-5.08413	0.11191	0.03365	0.62528	-150.73021
11.50	-16.05955	-5.39110	0.12651	0.02370	0.60339	159.83254
11.75	-16.02061	-5.38192	0.27789	0.05233	0.60877	159.59441
11.75	-16.02232	-5.07265	0.24587	0.07400	0.63074	-150.38986
11.75	-16.02081	-5.38162	0.27796	0.05228	0.60894	159.55133

Figure 2-25 Comparison of wave elevation, kinematics and dφ/dt in wave condition 4

Wasim stream function works well. Wajac stream function has the same problem, and the deviations become larger as steepness increases.

2.5.4 Wave condition 5

time=	elev=	vel-x=	vel-z=	acc-x=	acc-z=	dphidt=
	Point 5 Wasim Stream Function					
	Point 5 Wajac Stream Function					
	Point 5 Fenton Stream Function					
	Point 5 Wasim Stokes 5th					
	Point 5 Wajac Stokes 5th					
	Point 5 Fenton Stokes 5th					
0.00	36.24900	9.71073	0.00000	0.00000	-3.71611	-298.92221
0.00	36.24652	9.70856	0.00000	0.00000	-2.54322	298.76367
0.00	36.24722	9.71222	-0.00000	0.00000	-3.71765	-298.90862
0.00	35.96840	9.67220	0.00000	0.00000	-3.68944	-298.98502
0.00	35.60236	9.76096	0.00000	0.00000	-3.65997	299.10669
0.00	35.96839	9.75683	0.00000	0.00000	-3.69962	-299.80946
0.25	35.86460	9.66273	-0.92710	-0.38339	-3.69306	-297.44470
0.25	35.86203	9.66057	-0.92692	-0.37420	-2.52166	297.28687
0.25	35.90022	9.66420	-0.92749	-0.38360	-3.69462	-297.43063
0.25	35.65931	9.62619	-0.92068	-0.36764	-3.66933	-297.57513
0.25	35.31226	9.71604	-0.91340	-0.35898	-3.64086	297.73019
0.25	35.65761	9.71056	-0.92321	-0.36967	-3.67934	-298.38790
0.50	34.75391	9.51963	-1.84274	-0.75969	-3.62464	-293.03961
0.50	34.75119	9.51749	-1.84238	-0.74161	-2.45764	292.88382
0.50	34.87991	9.52101	-1.84353	-0.76017	-3.62626	-293.02380
0.50	34.74686	9.48880	-1.83134	-0.73022	-3.60938	-293.36499
0.50	34.45468	9.58186	-1.81727	-0.71334	-3.58389	293.61835
0.50	34.74021	9.57242	-1.83632	-0.73422	-3.61889	-294.14296
9.00	-23.38080	-6.71617	0.59541	0.20124	2.84169	-206.67807
9.00	-23.38553	-8.73211	0.76787	0.25636	3.00678	268.74413
9.00	-23.65775	-8.89816	0.77234	0.25522	3.02456	270.07739
9.00	-24.02231	-6.82396	0.60698	0.20678	2.37462	-209.10771
9.00	-23.64273	-8.80683	0.84744	0.28082	3.03088	270.61787
9.25	-23.20602	-8.64008	1.51810	0.50891	2.97990	265.96475
9.25	-23.19870	-6.65462	1.17743	0.39801	2.82465	-204.78397
9.25	-23.19127	-8.63672	1.51623	0.50641	2.97690	265.80832
9.25	-23.44423	-8.80317	1.52526	0.50435	2.99569	267.16672
9.25	-23.80432	-6.76378	1.20080	0.40922	2.35568	-207.26350
9.25	-23.41475	-8.70529	1.60169	0.53113	2.99992	267.49784
9.50	-22.90409	-8.48178	2.25717	0.75681	2.92942	261.09186
9.50	-22.89673	-6.55252	1.75606	0.59378	2.79643	-201.64221
9.50	-22.87475	-8.47914	2.25469	0.75359	2.92754	260.95870
9.50	-23.09615	-8.64619	2.26861	0.75095	2.94792	262.35635
9.50	-23.44800	-6.66343	1.79205	0.61110	2.32407	-204.18857
9.50	-23.05214	-8.54149	2.34582	0.77876	2.94993	262.46443

Figure 2-26 Comparison of wave elevation, kinematics and dφ/dt in wave condition 5

Wasim stream function works well! Wajac stream function and stokes 5th in Wajac are still not so accurate, especially at wave trough.

2.5.5 Wave condition 6

Point 6 Wasim Stream Function						
Point 6 Wajac Stream Function						
Point 6 Fenton Stream Function						
time=	elev=	vel-x=	vel-z=	acc-x=	acc-z=	dphidt=
0.00	41.06444	10.51933	0.00000	0.00000	-4.12604	-330.47858
0.00	41.06204	10.51678	0.00000	0.00000	-2.74381	330.29971
0.00	41.06899	10.51854	-0.00000	0.00000	-4.12618	-330.36681
0.25	40.51025	10.46298	-1.02898	-0.44982	-4.09570	-328.70844
0.25	40.50696	10.46045	-1.02875	-0.43407	-2.71625	328.53043
0.25	40.52254	10.46218	-1.02901	-0.44994	-4.09582	-328.59663
0.50	38.94825	10.29535	-2.04291	-0.88847	-4.00619	-323.44217
0.50	38.94455	10.29285	-2.04246	-0.85765	-2.63489	323.26678
0.50	38.96781	10.29450	-2.04296	-0.88869	-4.00623	-323.33034
0.75	36.61962	10.02053	-3.02749	-1.30580	-3.86173	-314.80826
0.75	36.61649	10.01808	-3.02681	-1.26118	-2.50352	314.63724
0.75	36.62451	10.01962	-3.02754	-1.30610	-3.86167	-314.69662
8.25	-24.69270	-9.06779	-1.54363	-0.50578	3.09198	284.87674
8.25	-24.68506	-6.92593	-1.18936	-0.39499	2.92282	-217.52203
8.25	-24.68832	-9.06603	-1.54325	-0.50554	3.09130	284.74638
8.50	-24.87498	-9.16244	-0.76667	-0.25107	3.12052	287.85019
8.50	-24.86713	-6.98638	-0.58941	-0.19568	2.93853	-219.42075
8.50	-24.87113	-9.16063	-0.76647	-0.25092	3.11975	287.71747
8.75	-24.93426	-9.19322	0.01502	0.00492	3.12980	288.81723
8.75	-24.92618	-7.00598	0.01203	0.00399	2.94362	-220.03624
8.75	-24.93078	-9.19139	0.01502	0.00492	3.12899	288.68370
9.00	-24.87024	-9.15998	0.79662	0.26088	3.11978	287.77295
9.00	-24.86221	-6.98475	0.61345	0.20366	2.93811	-219.36943
9.00	-24.86638	-9.15817	0.79642	0.26073	3.11901	287.64034
9.25	-24.68325	-9.06289	1.57331	0.51552	3.09050	284.72272
9.25	-24.67523	-6.92266	1.21331	0.40295	2.92197	-217.41933
9.25	-24.67887	-9.06113	1.57292	0.51527	3.08983	284.59249
9.50	-24.37333	-8.90244	2.34028	0.76756	3.04213	279.68195
9.50	-24.36508	-6.81962	1.81005	0.60148	2.89522	-214.18341
9.50	-24.36971	-8.90075	2.33974	0.76729	3.04154	279.55507

Figure 2-27 Comparison of wave elevation, kinematics and dφ/dt in wave condition 6

Wasim stream function works well while Wajac stream function has still the same problem especially at wave trough. One possibility could be that when wave is below the still water level, Wajac will output the wave kinematics at $(0,\zeta)$ instead of at $(0,0)$ (where no water can be found actually) while the other programs will always calculate the wave kinematics at $(0,0)$. But this cannot explain the deviations when wave is above the still water level, though they are smaller but still visiable. Further study or modification of Wajac program will not be included in this report.

2.5.6 Wave condition 1

i) WasimStream

The online java application works only up to order 40, otherwise it will return NaN results. Order 40 is for sure enough for the most waves, but maybe not enough for wave condition 1.
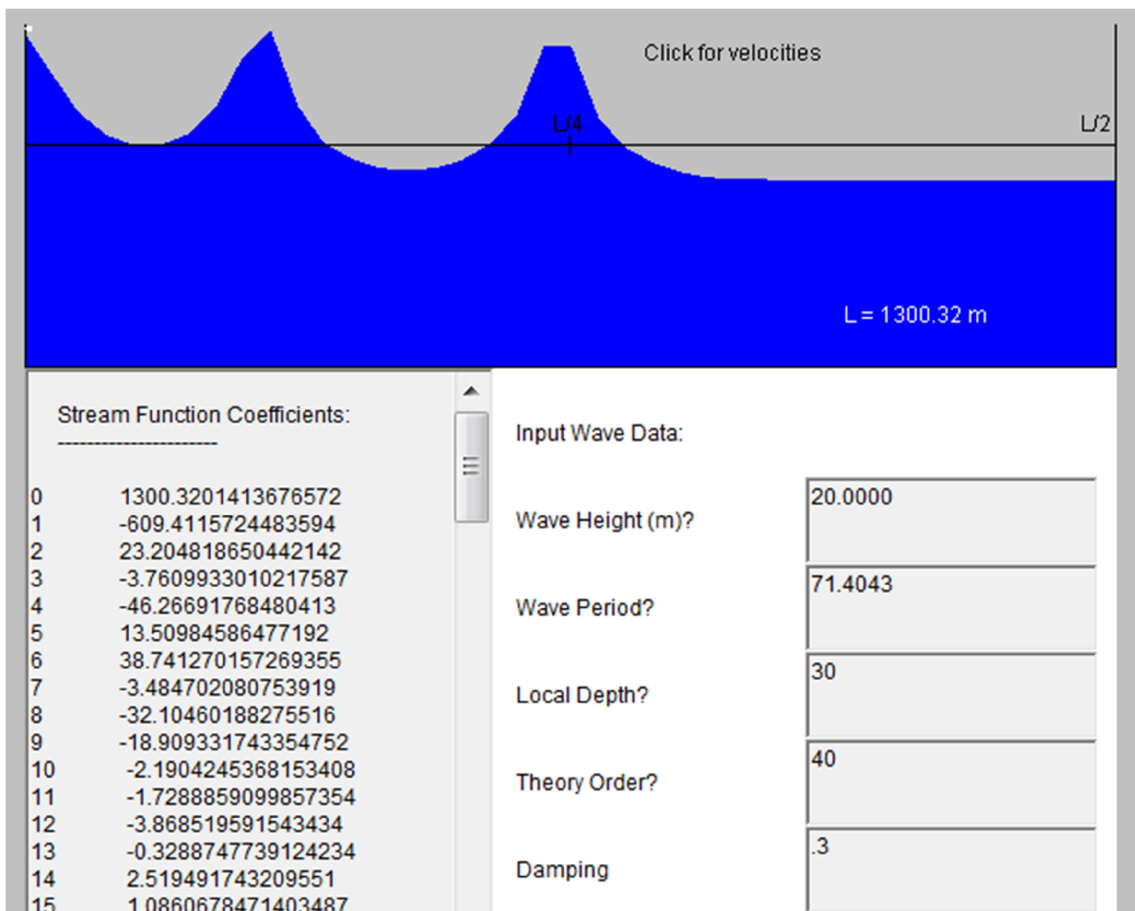

Figure 2-28 Dalrymple's approach to wave condition 1

Dalrymple's approach cannot even converge to the correct wave height and wave length as the oscillations are global. This is due to that the wave is too long (Dalrymple & Solana 1986).

ii) WajacStream

The max order the program allows is 24, and when order 24 is used the program will not give any output. It seems that Dean's approach cannot converge either.

iii) FentonStream

For such long waves, Fenton's approach can solve the problem stepwise, i.e. by first divide the wave height into several parts, and then solve a lower wave with the same wave length and step upwards in wave height after convergence.

When 10 steps in wave height and order 40 are used, the method can converge to the correct wave height and wave length, though we can still observe small local oscillations due to lack of more higher order terms.
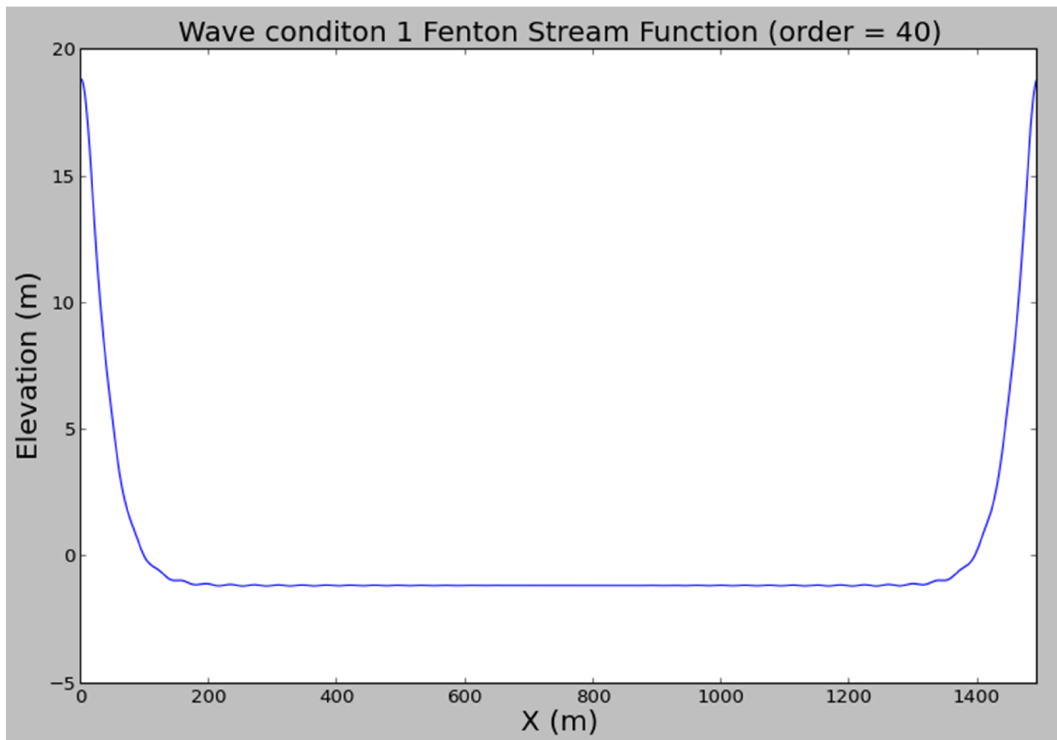

Figure 2-29 Fenton's approach to wave condition 1 when order = 40

If we set order = 100, the small local oscillations will disappear which gives a perfect wave profile.
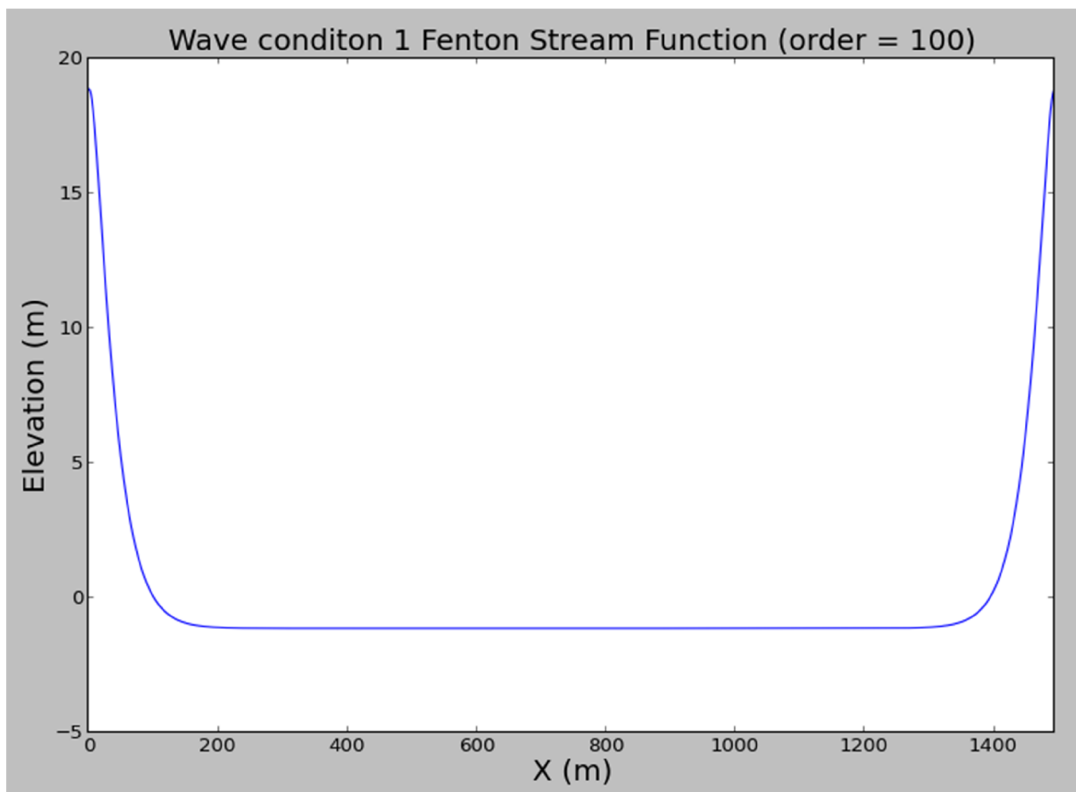
Figure 2-30 Fenton's approach to wave condition 1 when order = 100

After all, it seems that Fenton's approach is more robust when waves are extremely long. At least it can handle solitary waves which Dean or Dalrymple's approach cannot. On the other side, Wasim after modification and cooperating with Dalrymple's java application works well except for the limitation to deal with extremely long waves. But the stream function method is both general enough to replace the Stokes 5th and it extends even more the validity range for input waves to Wasim, especially waves in shallow water.

References

Dalrymple, R.A. (1974), "A finite amplitude wave on a linear shear current", Journal of Geophysical Research

Dalrymple, R.A. & Solana, P. (1986), "Nonuniqueness in Stream Function Wave Theory", Journal of Waterway, Port, Coastal and Ocean Engineering

Dean, R.G. & Dalrymple, R.A. (1985), "Water Wave Mechanics for Engineers and Scientists", World Scientific

Fenton, J.D. (1980), "Accurate numerical solutions for nonlinear waves", Proceedings of the 17th ICCE, Sydney

Fenton, J. D. (1985), "A fifth-order Stokes theory for steady waves", Journal of Waterway, Port, Coastal, and Ocean Engineering

Fenton, J.D.(1988), "The numerical solution of steady water wave problems", Computers & Geoscience

Fenton, J.D. (1990), "Nonlinear wave theories", The Sea - Ocean Engineering Science

Fenton, J.D. (1999), "Numerical methods for nonlinear waves", Advances In Coastal And Ocean Engineering

Helmers, J.B. (2011), '' Stream Function Waves in NTANO362'', DNV

Intel® Fortran Compiler XE 12.1 User and Reference Guides

Numpy and Scipy documentation, Numpy 1.7 reference

Python 2.7.5 documentation, the python language reference

Rienecker, M.M. & Fenton, J.D. (1981), "A Fourier approximation method for steady water waves", Journal of Fluid Mechanics

Skjelbreia, L. & Hendrickson, J. (1961), "Fifth order gravity wave theory", Proceedings of 7th Conference on Coastal Engineering

3 Nonlinear free surface conditions

3.1 Theoretical derivation

After the implementation of stream function method is included in Wasim, it is reasonable to have nonlinear free surface conditions which combined with stream function method can improve the capability of Wasim to handle nonlinear problems. Some free surface conditions with strong nonlinear coupling terms were once attempted to be implemented in Wasim, but the results were not satisfying. This may due to that the program as a whole is a weakly nonlinear potential solver (the strongest limitation may be that when the program solves the memory flow potential in time domain, the left hand side matrix of the linear system which is derived from equation (44) will not be updated). Fully or strongly nonlinear analysis without parallel computing at present is too far to commercial softwares. In the rest of the report, only weakly nonlinear free surface conditions based on perturbation theory will be discussed.

3.1.1 Kinematic free surface condition

We start from the most derived kinematic free surface condition:

$$\left(\frac{D}{Dt} + \nabla \phi_{tot} \cdot \nabla \right) \cdot [z - \zeta_{tot}] = 0 \qquad \text{on z= } \zeta + \zeta_i \quad (59)$$

Introduce Galilean transform (18), $\phi_{tot} = \phi_b + \phi_l + \phi_m + \phi_i$ and $\zeta_{tot} = \zeta + \zeta_i$ where ζ is wave radiation and diffraction elevation while ζ_i is incident wave elevation. Then we come to the fully nonlinear kinematic free surface condition:

$$\frac{\partial}{\partial z}(\phi_b + \phi_l + \phi_m + \phi_i) = \left(\frac{\partial}{\partial t} - \vec{W} \cdot \nabla \right) \cdot (\zeta + \zeta_i) + \nabla(\phi_b + \phi_l + \phi_m + \phi_i) \cdot \qquad (60)$$

$$\nabla(\zeta + \zeta_i) \qquad \qquad \text{on z= } \zeta + \zeta_i$$

i) Alternative 1

Move terms only including ζ_i and ϕ_i without coupling with other variables to the right hand side of (60) and leave all the other terms at the left hand side, then we come to equation (61).

$$\left[\frac{\partial \zeta}{\partial t} - (\vec{W} - \nabla \phi_b) \cdot \nabla \zeta + \nabla(\phi_l + \phi_m + \phi_i) \cdot \nabla \zeta + \nabla(\phi_b + \phi_l + \phi_m) \cdot \nabla \zeta_i - \right. \tag{61}$$
$$\left. \frac{\partial}{\partial z}(\phi_b + \phi_l + \phi_m)\right] = \left[\frac{\partial \phi_i}{\partial z} - \left(\frac{\partial}{\partial t} - \vec{W} \cdot \nabla\right) \cdot \zeta_i - \nabla \phi_i \cdot \nabla \zeta_i\right] \qquad \text{on } z = \zeta + \zeta_i$$

Taylor expand left hand side of (61) about z=0 and keep only terms up to $O(\epsilon)$. Assume $O(\phi_b) = O(1)$ while $O(\phi_l) = O(\phi_m) = O(\phi_i) = O(\zeta) = O(\zeta_i) = O(\epsilon)$, and introduce $\frac{\partial \phi_b}{\partial z} = 0$ on $z = 0$. Right hand side of the equation remains the same. This yields equation (62)

$$\left[\frac{\partial \zeta}{\partial t} - (\vec{W} - \nabla \phi_b) \cdot \nabla \zeta + \nabla \phi_b \cdot \nabla \zeta_i - \frac{\partial^2 \phi_b}{\partial z^2} \cdot (\zeta + \zeta_i) - \frac{\partial}{\partial z}(\phi_l + \phi_m)\right]_{z=0} \tag{62}$$
$$= \left[\frac{\partial \phi_i}{\partial z} - \left(\frac{\partial}{\partial t} - \vec{W} \cdot \nabla\right) \cdot \zeta_i - \nabla \phi_i \cdot \nabla \zeta_i\right]_{z=\zeta+\zeta_i}$$

Equation (62) is identical to Sunhui's approach (D-4.1-DNV, see reference list). The left hand side of (62) is what we have in the current Wasim, i.e. the linear kinematic free surface condition (see Appendix A).

ii) Alternative 2

We start from equation (61). Taylor expand left hand side of the eqution. about z=0 and keep only terms up to $O(\epsilon)$. But now we assume $O(\phi_b) = O(\phi_i) = O(\zeta_i) = O(1)$ while $O(\phi_l) = O(\phi_m) = O(\zeta) = O(\epsilon)$. At the same time we Taylor expand right hand side of the equation. about $z=\zeta_i$. This gives us equation (63)

$$\left[\frac{\partial \zeta}{\partial t} - (\vec{W} - \nabla \phi_b) \cdot \nabla \zeta + \nabla \phi_i \cdot \nabla \zeta + \nabla \phi_b \cdot \nabla \zeta_i + \nabla(\phi_l + \phi_m) \cdot \nabla \zeta_i - \frac{\partial^2 \phi_b}{\partial z^2} \cdot \right. \tag{63}$$
$$\left. (\zeta + \zeta_i) - \frac{\partial}{\partial z}(\phi_l + \phi_m)\right]_{z=0}$$
$$= \left[\frac{\partial \phi_i}{\partial z} + \frac{\partial^2 \phi_i}{\partial z^2} \cdot \zeta - \left(\frac{\partial}{\partial t} - \vec{W} \cdot \nabla\right) \cdot \zeta_i - \nabla \phi_i \cdot \nabla \zeta_i - \frac{\partial}{\partial z}(\nabla \phi_i \cdot \nabla \zeta_i) \cdot \zeta\right]_{z=\zeta_i}$$

Since the kinematic free surface condition $\frac{\partial \psi_i}{\partial x} = -\frac{\partial \psi_i}{\partial z}\frac{\partial \zeta_i}{\partial x}$ is applied when we solved the stream

function incident wave (see section 1.2), rewrite the condition by using velocity potential gives

$\frac{\partial \phi_i}{\partial z} = \frac{\partial \phi_i}{\partial x}\frac{\partial \zeta_i}{\partial x}$. Then transform the equation to the 3D body fixed coordinate (figure 1.2) and in-

troduce Galilean transform (18), which leads to equation (64).

$$\left(\frac{\partial}{\partial t} - \vec{W}\cdot\nabla\right)\cdot\zeta_i + \nabla\phi_i\cdot\nabla\zeta_i = \frac{\partial\phi_i}{\partial z} \qquad\qquad \text{on z= } \zeta_i \qquad (64)$$

Insert equation (64) into the right hand side of equation (63):

$$\left[\frac{\partial\zeta}{\partial t} - \left(\vec{W} - \nabla\phi_b\right)\cdot\nabla\zeta + \nabla\phi_i\cdot\nabla\zeta + \nabla\phi_b\cdot\nabla\zeta_i + \nabla(\phi_l + \phi_m)\cdot\nabla\zeta_i - \frac{\partial^2\phi_b}{\partial z^2}\cdot \qquad (65)\right.$$

$$\left.(\zeta + \zeta_i) - \frac{\partial}{\partial z}(\phi_l + \phi_m)\right]_{z=0} = \left[\frac{\partial^2\phi_i}{\partial z^2}\cdot\zeta - \frac{\partial}{\partial z}(\nabla\phi_i\cdot\nabla\zeta_i)\cdot\zeta\right]_{z=\zeta_i}$$

If we further Taylor expand the right hand side of (65) and reorganize the equation, which gives:

$$\left[\frac{\partial\zeta}{\partial t} - \left(\vec{W} - \nabla\phi_b\right)\cdot\nabla\zeta + \nabla\phi_b\cdot\nabla\zeta_i - \frac{\partial^2\phi_b}{\partial z^2}\cdot(\zeta + \zeta_i) - \frac{\partial}{\partial z}(\phi_l + \phi_m)\right] \qquad (66)$$

$$= \left[\frac{\partial^2\phi_i}{\partial z^2}\cdot\zeta - \frac{\partial}{\partial z}(\nabla\phi_i\cdot\nabla\zeta_i)\cdot\zeta - \nabla\phi_i\cdot\nabla\zeta - \nabla(\phi_l + \phi_m)\cdot\nabla\zeta_i\right] \qquad \text{on z=0}$$

Then the left hand side of (66) is what we have in the current Wasim.

3.1.2 Dynamic free surface condition

We start from the the most derived dynamic F.S. condition.

$$\frac{D\phi_{tot}}{Dt} = -g\zeta_{tot} - \frac{1}{2}(\nabla\phi_{tot})^2 \qquad\qquad \text{on z= } \zeta + \zeta_i \quad (67)$$

Introduce Galilean transform (18), $\phi_{tot} = \phi_b + \phi_l + \phi_m + \phi_i$ and $\zeta_{tot} = \zeta + \zeta_i$. Then we come to

the fully nonlinear dynamic free surface condition:

$$\left(\frac{\partial}{\partial t} - \vec{W}\cdot\nabla\right)(\phi_b + \phi_l + \phi_m + \phi_i) = -g(\zeta + \zeta_i) - \frac{1}{2}\left(\nabla(\phi_b + \phi_l + \phi_m + \right. \qquad (68)$$

$$\left.\phi_i)\right)^2 \qquad\qquad \text{on z= } \zeta + \zeta_i$$

i) Alternative 1

Move terms only including ζ_i and ϕ_i without coupling with other variables to the right hand side of (68) and leave all the other terms at the left hand side, then we come to equation (69).

$$\left[\left(\frac{\partial}{\partial t} - \vec{W} \cdot \nabla\right)(\phi_b + \phi_l + \phi_m) + g\zeta + \frac{1}{2}\left(\nabla(\phi_b + \phi_l + \phi_m)\right)^2 + (\nabla\phi_i \cdot \nabla\phi_b + \quad (69)\right.$$

$$\left.\nabla\phi_i \cdot \nabla\phi_l + \nabla\phi_i \cdot \nabla\phi_m)\right] = \left[-\left(\frac{\partial}{\partial t} - \vec{W} \cdot \nabla\right)\phi_i - g\zeta_i - \frac{1}{2}(\nabla\phi_i)^2\right] \text{ on z= } \zeta + \zeta_i$$

Taylor expand left hand side of (69) about z=0 and keep only terms up to $O(\epsilon)$. Assume $O(\phi_b) = O(1)$ while $O(\phi_l) = O(\phi_m) = O(\phi_i) = O(\zeta) = O(\zeta_i) = O(\epsilon)$, and introduce $\frac{\partial \phi_b}{\partial z} = 0$ on $z = 0, \frac{\partial \phi_b}{\partial t} = 0$. Right hand side of the equation remains the same. This yields equation (70).

$$\left[\left(\frac{\partial}{\partial t} - (\vec{W} - \nabla\phi_b) \cdot \nabla\right)(\phi_l + \phi_m) - \vec{W} \cdot \nabla\phi_b + g\zeta + \frac{1}{2}(\nabla\phi_b)^2 + \nabla\phi_b \cdot \quad (70)\right.$$

$$\left.\nabla\phi_i\right]_{z=0} = \left[-\left(\frac{\partial}{\partial t} - \vec{W} \cdot \nabla\right)\phi_i - g\zeta_i - \frac{1}{2}(\nabla\phi_i)^2\right]_{z=\zeta+\zeta_i}$$

Equation (70) is identical to Sunhui's approach (D-4.1-DNV, see reference list). The left hand side of (70) is what we have in the current Wasim, i.e. the linear dynamic free surface condition (see Appendix A).

ii) Alternative 2

We start from equation (69). Taylor expand left hand side about z=0 and keep only terms up to $O(\epsilon)$. But now assume $O(\phi_b) = O(\phi_i) = O(\zeta_i) = O(1)$ while $O(\phi_l) = O(\phi_m) = O(\zeta) = O(\epsilon)$. At the same time we Taylor expand right hand side about $z=\zeta_i$. This gives us equation (71).

$$\left[\left(\frac{\partial}{\partial t} - (\vec{W} - \nabla\phi_b) \cdot \nabla\right)(\phi_l + \phi_m) - \vec{W} \cdot \nabla\phi_b + g\zeta + \frac{1}{2}(\nabla\phi_b)^2 + \nabla\phi_b \cdot \quad (71)\right.$$

$$\left.\nabla\phi_i + \frac{\partial}{\partial z}(\nabla\phi_b \cdot \nabla\phi_i) \cdot (\zeta + \zeta_i) + \nabla\phi_i \cdot \nabla\phi_l + \nabla\phi_i \cdot \nabla\phi_m\right]_{z=0}$$

$$= \left[-\left(\frac{\partial}{\partial t} - \vec{W} \cdot \nabla\right)\phi_i - \zeta \cdot \frac{\partial}{\partial z}\left(\left(\frac{\partial}{\partial t} - \vec{W} \cdot \nabla\right)\phi_i\right) - g\zeta_i - \frac{1}{2}(\nabla\phi_i)^2 - \right.$$

$$\left.\frac{\partial}{\partial z}\left(\frac{1}{2}(\nabla\phi_i)^2\right) \cdot \zeta\right]_{z=\zeta_i}$$

Introduce the fully nonlinear dynamic free surface condition of incident wave $\left(\frac{\partial}{\partial t} - \vec{W} \cdot \nabla\right)\phi_i +$ $g\zeta_i + \frac{1}{2}(\nabla\phi_i)^2 = 0$ into (71) and further Taylor expand right hand side of the equation about z=0, which leads to equation (72).

$$\left[\left(\frac{\partial}{\partial t} - (\vec{W} - \nabla\phi_b) \cdot \nabla\right)(\phi_l + \phi_m) - \vec{W} \cdot \nabla\phi_b + g\zeta + \frac{1}{2}(\nabla\phi_b)^2 + \nabla\phi_b \cdot \nabla\phi_i\right] \quad (72)$$

$$= \left[-\zeta \cdot \left(\left(\frac{\partial}{\partial t} - \vec{W} \cdot \nabla\right) \cdot \frac{\partial\phi_i}{\partial z}\right) - \nabla\phi_i \cdot \frac{\partial(\nabla\phi_i)}{\partial z} \cdot \zeta - \frac{\partial}{\partial z}(\nabla\phi_b \cdot \nabla\phi_i) \cdot (\zeta + \zeta_i) - \right.$$

$$\left. \nabla\phi_i \cdot \nabla\phi_l - \nabla\phi_i \cdot \nabla\phi_m\right]$$

Then the left hand side of (72) is what we have in the current Wasim.

The advantage of alternative 1 is that the update with regards to what already included in the current Wasim, is only associated with ϕ_i and ζ_i, which is not difficult to be implemented. The disadvantage may be the inconsistence of the approach since different parts of the free surface conditions are evaluated differently. Whether this approach will converge to acceptable results should be tested. Comparing with alternative 1, the disadvantage of alternative 2 is the extra terms required to be calculated, e.g. the terms where ϕ_i or ζ_i has coupling with ϕ_m, especially the last term in (72) which can cause problems as the dynamic free surface condition is used to solve ϕ_m implicitly (see section 1.3.3). The advantage of alternative 2 is assumed to be a better consistence with linear theory , which will be tested later.

3.2 Discretization and implementation of the free surface conditions

Because the basis flow is steady state and the local flow potential can be calculated straightforward after solving the motion equation (see section 1.3.3), the main computation in time marching will be the memory flow, i.e. to solve the boundary value problem which includes equations (40) (or (62)/(66)), (41) (or (70)/(72)) and (42), where the three unknows ϕ_m, ζ and $\frac{\partial \phi_m}{\partial n}$ are approximated in Wasim as follows:

$$\phi_m^n(\vec{x}) = \sum a_j^n \cdot B_j(\vec{x}) \tag{73}$$

$$\frac{\partial}{\partial n}\phi_m^n(\vec{x}) = \sum b_j^n \cdot B_j(\vec{x}) \tag{74}$$

$$\zeta^n(\vec{x}) = \sum c_j^n \cdot B_j(\vec{x}) \tag{75}$$

B_j is the quadratic spline centered at $\vec{x}_j$, and the superscript denotes time step, i.e. $a_j^n = a_j(n\Delta t)$.

Consider the initial value problem $\frac{dy}{dt} = f(t, y)$ where the function f and the initial data t_0, $y(t_0)$ are known. Several time discretization schemes which are used in Wasim are presented below.

i) Explicit (forward) Euler

$$\frac{1}{\Delta t}(y^{n+1} - y^n) = f^n \Rightarrow y^{n+1} = y^n + \Delta t \cdot f(t^n, y^n)$$

ii) Implicit (backward) Euler

$$\frac{1}{\Delta t}(y^{n+1} - y^n) = f^{n+1} \Rightarrow y^{n+1} = y^n + \Delta t \cdot f(t^{n+1}, y^{n+1})$$

iii) Explicit Leap-Frog scheme

$$\frac{1}{2\Delta t}(y^{n+1} - y^{n-1}) = f^n \Rightarrow y^{n+1} = y^{n-1} + 2\Delta t \cdot f(t^n, y^n)$$

iv) Trapzoidal scheme

$$\frac{1}{\Delta t}(y^{n+1} - y^n) = \frac{1}{2}(f^{n+1} + f^n) \Rightarrow y^{n+1} = y^n + \frac{\Delta t}{2} \cdot (f(t^{n+1}, y^{n+1}) + f(t^n, y^n))$$

3.2.1 Implementation of the kinematic free surface condition

i) Linear kinematic free surface condition (available in the offical Wasim version)

First order: apply explicit Euler scheme to (40)

$$B_j \cdot c_j^{n+1} = \zeta^n + \Delta t \left[\left(\vec{W} - \nabla \phi_b \right) \cdot \sum c_j^n \cdot \nabla B_j + \frac{\partial \phi_l^n}{\partial z} + \frac{\partial \phi_m^n}{\partial n} \right] \qquad \text{on z= 0} \qquad (76)$$

Second order: apply explicit Leap-Frog scheme to (40)

$$B_j \cdot c_j^{n+1} = \zeta^{n-1} + 2\Delta t \left[\left(\vec{W} - \nabla \phi_b \right) \cdot \sum c_j^n \cdot \nabla B_j + \frac{\partial \phi_l^n}{\partial z} + \frac{\partial \phi_m^n}{\partial n} \right] \qquad \text{on z= 0} \qquad (77)$$

Note:

- Term $\frac{\partial^2 \phi_b}{\partial z^2} \cdot (\zeta + \zeta_i)$ is neglected due to the difficulty of 2nd order derivation calculation, but $-\nabla \phi_b \cdot \nabla \zeta_i$ can be included as an option (in source code if ifscond=1 or ilin_surf>1, where ifscond is a variable depends on whether the base flow is inhomogeneous, i.e. ifscond=1 indicates $\nabla \phi_b \neq 0$, and ilin_surf is a variable depends on what nonlinearity should be included in the free surface conditions).
- If ilin_surf=2 or 3, a nonlinear term $-\nabla(\phi_m + \phi_i) \cdot \nabla(\zeta + \zeta_i)$ will be included. But this option gives unsatisfying results and will not be discussed in the report.
- If ilin_surf=5 and the incident wave is generated by stream function method, extra terms $-\left[(\nabla \phi_i)_{z=\zeta+\zeta_i} \cdot \zeta_i - (\nabla \phi_i)_{z=\zeta_i} \cdot \zeta_i \right] + \left[\left(\frac{\partial \phi_i}{\partial z} \right)_{z=\zeta+\zeta_i} - \left(\frac{\partial \phi_i}{\partial z} \right)_{z=\zeta_i} \right]$ will be included. Then it will be identical to the approach alternative 1.

ii) Alternative 1

First order: apply explicit Euler scheme to (62)

$$B_j \cdot c_j^{n+1} = \zeta^n + \Delta t \left[\left(\vec{W} - \nabla \phi_b \right) \cdot \sum c_j^n \cdot \nabla B_j + \frac{\partial \phi_l^n}{\partial z} + \frac{\partial \phi_m^n}{\partial n} \right] + \Delta t \left[\frac{\partial \phi_l^n}{\partial z} - \right. \qquad (78)$$

$$\left. \left(\frac{\partial}{\partial t} - \vec{W} \cdot \nabla \right) \cdot \zeta_i^n - \nabla \phi_i^n \cdot \nabla \zeta_i^n \right]_{z= \zeta+\zeta_i} \qquad \text{on z= 0}$$

Second order: apply explicit Leap-Frog scheme to (62)

$$B_j \cdot c_j^{n+1} = \zeta^{n-1} + 2\Delta t \left[(\overrightarrow{W} - \nabla \phi_b) \cdot \sum c_j^n \cdot \nabla B_j + \frac{\partial \phi_l^n}{\partial z} + \frac{\partial \phi_m^n}{\partial n} \right] + \tag{79}$$

$$2\Delta t \left[\frac{\partial \phi_i^n}{\partial z} - \left(\frac{\partial}{\partial t} - \overrightarrow{W} \cdot \nabla \right) \cdot \zeta_i^n - \nabla \phi_i^n \cdot \nabla \zeta_i^n \right]_{z = \zeta + \zeta_i} \qquad \text{on } z= 0$$

Note:

- Term $\frac{\partial^2 \phi_b}{\partial z^2} \cdot (\zeta + \zeta_i)$ is neglected.
- This approach can be switched on when ilin_surf=5

iii) Alternative 2

First order: apply explicit Euler scheme to (66)

$$B_j \cdot c_j^{n+1} = \left[1 + \Delta t \cdot \frac{\partial^2 \phi_i^n}{\partial z^2} - \Delta t \cdot \frac{\partial}{\partial z} (\nabla \phi_i^n \cdot \nabla \zeta_i^n) \right] \cdot \zeta^n + \Delta t \left[(\overrightarrow{W} - \nabla \phi_b - \tag{80} \right.$$

$$\left. \nabla \phi_i^n) \sum c_j^n \cdot \nabla B_j + \frac{\partial \phi_l^n}{\partial z} + \frac{\partial \phi_m^n}{\partial n} - \nabla(\phi_b + \phi_l^n + \phi_m^n) \cdot \nabla \zeta_i^n \right] \qquad \text{on } z= 0$$

Second order: apply explicit Leap-Frog scheme to (66)

$$B_j \cdot c_j^{n+1} = \zeta^{n-1} + 2\Delta t \left[\frac{\partial^2 \phi_i^n}{\partial z^2} - \frac{\partial}{\partial z} (\nabla \phi_i^n \cdot \nabla \zeta_i^n) \right] \cdot \zeta^n + 2\Delta t \left[(\overrightarrow{W} - \nabla \phi_b - \tag{81} \right.$$

$$\left. \nabla \phi_i^n) \sum c_j^n \cdot \nabla B_j + \frac{\partial \phi_l^n}{\partial z} + \frac{\partial \phi_m^n}{\partial n} - \nabla(\phi_b + \phi_l^n + \phi_m^n) \cdot \nabla \zeta_i^n \right] \qquad \text{on } z= 0$$

Note:

- Term $\frac{\partial^2 \phi_b}{\partial z^2} \cdot (\zeta + \zeta_i)$ is neglected.
- This approach can be switched on when ilin_surf=6

3.2.2 Implementation of the dynamic free surface condition

i) Linear kinematic free surface condition (available in the offical Wasim version)

First order: apply implicit Euler scheme to (41)

$$\left[B_j - \Delta t(\overrightarrow{W} - \nabla\phi_b) \cdot \nabla B_j\right] \cdot a_j^{n+1} = \phi_m^n - \Delta t(g\zeta^{n+1}) - \Delta t\left(\left(\frac{\partial}{\partial t} - \overrightarrow{W} \cdot \right.\right. \tag{82}$$

$$\left.\left.\nabla\right)\phi_i^{n+1} + g\zeta_i^{n+1}\right) \qquad\qquad \text{on z= 0}$$

Second order: apply trapzoidal scheme to (41)

$$\left[B_j - \frac{1}{2}\Delta t(\overrightarrow{W} - \nabla\phi_b) \cdot \nabla B_j\right] \cdot a_j^{n+1} = \phi_m^n + \frac{\Delta t}{2}\left[(\overrightarrow{W} - \nabla\phi_b)\Sigma\, a_j^n \cdot \nabla B_j - \right. \tag{83}$$

$$\left. g(\zeta^{n+1} + \zeta^n)\right] - \Delta t\left(\left(\frac{\partial}{\partial t} - \overrightarrow{W} \cdot \nabla\right)\phi_i^{n+1} + g\zeta_i^{n+1}\right) \qquad \text{on z= 0}$$

Note:

- Term $\left(\overrightarrow{W} \cdot \nabla\phi_b - \frac{1}{2}(\nabla\phi_b)^2\right)$ is neglected, but $-\nabla\phi_b \cdot \nabla\phi_i$ can be included as an option.
- The linear dynamic free surface condtion of the incident wave, i.e. the last term in (83) remains to be subtracted Euler implicitly in the trapezoidal-scheme.
- If ilin_surf=1, 3 or 5, the linear dynamic free surface condition of incident wave will be evaluated on z= $\zeta + \zeta_i$

ii) Alternative 1

First order: apply implicit Euler scheme to (70) and consider only the memory flow

$$\left[B_j - \Delta t(\overrightarrow{W} - \nabla\phi_b) \cdot \nabla B_j\right] \cdot a_j^{n+1} = \phi_m^n - \Delta t(g\zeta^{n+1}) + \Delta t\left[-\left(\frac{\partial}{\partial t} - \overrightarrow{W} \cdot \right.\right. \tag{84}$$

$$\left.\left.\nabla\right)\phi_i^{n+1} - g\zeta_i^{n+1} - \frac{1}{2}(\nabla\phi_i^{n+1})^2\right]_{z=\zeta+\zeta_i} \qquad \text{on z= 0}$$

Second order: apply trapzoidal scheme to (70) and consider only the memory flow

$$\left[B_j - \frac{1}{2}\Delta t(\overrightarrow{W} - \nabla\phi_b) \cdot \nabla B_j\right] \cdot a_j^{n+1} = \phi_m^n + \frac{\Delta t}{2}\left[(\overrightarrow{W} - \nabla\phi_b)\sum a_j^n \cdot \nabla B_j - \right. \quad (85)$$

$$\left. g(\zeta^{n+1} + \zeta^n)\right] + \Delta t\left[\left(\frac{\partial}{\partial t} - \overrightarrow{W} \cdot \nabla\right)\phi_i^{n+1} + g\zeta_i^{n+1} - \frac{1}{2}(\nabla\phi_i^{n+1})^2\right]_{z=\zeta+\zeta_i}$$

<div align="right">on z= 0</div>

Note:

- Term $\left(\overrightarrow{W} \cdot \nabla\phi_b - \frac{1}{2}(\nabla\phi_b)^2\right)$ is neglected, but $-\nabla\phi_b \cdot \nabla\phi_i$ can be included as an option.
- This approach can be switched on when ilin_surf=5

iii) Alternative 2

First order: apply implicit Euler scheme to (72) and consider only the memory flow

$$\left[B_j - \Delta t(\overrightarrow{W} - \nabla\phi_b) \cdot \nabla B_j\right] \cdot a_j^{n+1} = \phi_m^n + \Delta t\left[-g\zeta^{n+1} + \left(\overrightarrow{W} - \frac{1}{2}\nabla\phi_b - \right.\right. \quad (86)$$

$$\left. \nabla\phi_i^{n+1}\right) \cdot \nabla\phi_b - \zeta^{n+1} \cdot \left(\left(\frac{\partial}{\partial t} - \overrightarrow{W} \cdot \nabla\right) \cdot \frac{\partial\phi_i^{n+1}}{\partial z} + \nabla\phi_i^{n+1} \cdot \frac{\partial(\nabla\phi_i^{n+1})}{\partial z}\right) -$$

$$\left. \left(\nabla\phi_b \cdot \frac{\partial}{\partial z}(\nabla\phi_i^{n+1})\right) \cdot (\zeta^{n+1} + \zeta_i^{n+1})\right] \qquad \text{on z= 0}$$

Second order: apply trapzoidal scheme to (72) and consider only the memory flow

$$\left[B_j - \frac{\Delta t}{2}(\overrightarrow{W} - \nabla\phi_b) \cdot \nabla B_j\right] \cdot a_j^{n+1} = \phi_m^n + \frac{\Delta t}{2}\left\{(\overrightarrow{W} - \nabla\phi_b)\sum a_j^n \cdot \nabla B_j - \right. \quad (87)$$

$$g(\zeta^{n+1} + \zeta^n) + \left(2\overrightarrow{W} - \nabla\phi_b - (\nabla\phi_i^{n+1} + \nabla\phi_i^n)\right) \cdot \nabla\phi_b - \left[\zeta^{n+1} \cdot\right.$$

$$\left(\left(\frac{\partial}{\partial t} - \overrightarrow{W} \cdot \nabla\right) \cdot \frac{\partial\phi_i^{n+1}}{\partial z} + \nabla\phi_i^{n+1} \cdot \frac{\partial(\nabla\phi_i^{n+1})}{\partial z}\right) + \zeta^n \cdot \left(\left(\frac{\partial}{\partial t} - \overrightarrow{W} \cdot \nabla\right) \cdot \frac{\partial\phi_i^n}{\partial z} + \nabla\phi_i^n \cdot\right.$$

$$\left.\left.\frac{\partial(\nabla\phi_i^n)}{\partial z}\right)\right] - \left[\left(\nabla\phi_b \cdot \frac{\partial}{\partial z}(\nabla\phi_i^{n+1})\right) \cdot (\zeta^{n+1} + \zeta_i^{n+1}) + \left(\nabla\phi_b \cdot \frac{\partial}{\partial z}(\nabla\phi_i^n)\right) \cdot\right.$$

$$\left.\left. (\zeta^n + \zeta_i^n)\right]\right\} \qquad \text{on z= 0}$$

Note:

- $$\frac{\partial}{\partial z}(\nabla\phi_b \cdot \nabla\phi_i) \cdot (\zeta + \zeta_i) = \left(\frac{\partial^2\phi_b}{\partial z^2} \cdot \frac{\partial\phi_i}{\partial z} + \nabla\phi_b \cdot \frac{\partial}{\partial z}(\nabla\phi_i)\right) \cdot (\zeta + \zeta_i) \approx \left(\nabla\phi_b \cdot \frac{\partial}{\partial z}(\nabla\phi_i)\right) \cdot$$

  $(\zeta + \zeta_i)$ as terms associated with $\frac{\partial^2\phi_b}{\partial z^2}$ are omitted.

- Term $\nabla\phi_i \cdot \nabla\phi_m$ is neglected. If we include it implicitly, the term will be moved to the left hand side, then Wasim needs to update the coefficients matrix at the left hand side due to $\nabla\phi_i$, which is not allowed at present. If we include it explicitly, then the dynamic free surface condition will be discretized emplicitly, which leads to unsatisfying results and sometimes the method loses its numerical stability.

- This approach can be switched on when ilin_surf=6

3.3 Wave loads on a fixed cylinder

The main task of this section is to test the wave diffractions with the implemented nonlinear free surface conditions by studying the wave loads on a fixed body. A series of analyses are done in Wasim, and the numerical results will be compared with the experimental results in Huseby & Grue (2000). A fixed cylinder with a 3cm radius in 0.6m water depth is set up in Wasim which is identical to the model and environmental condition used in the mentioned experiment.
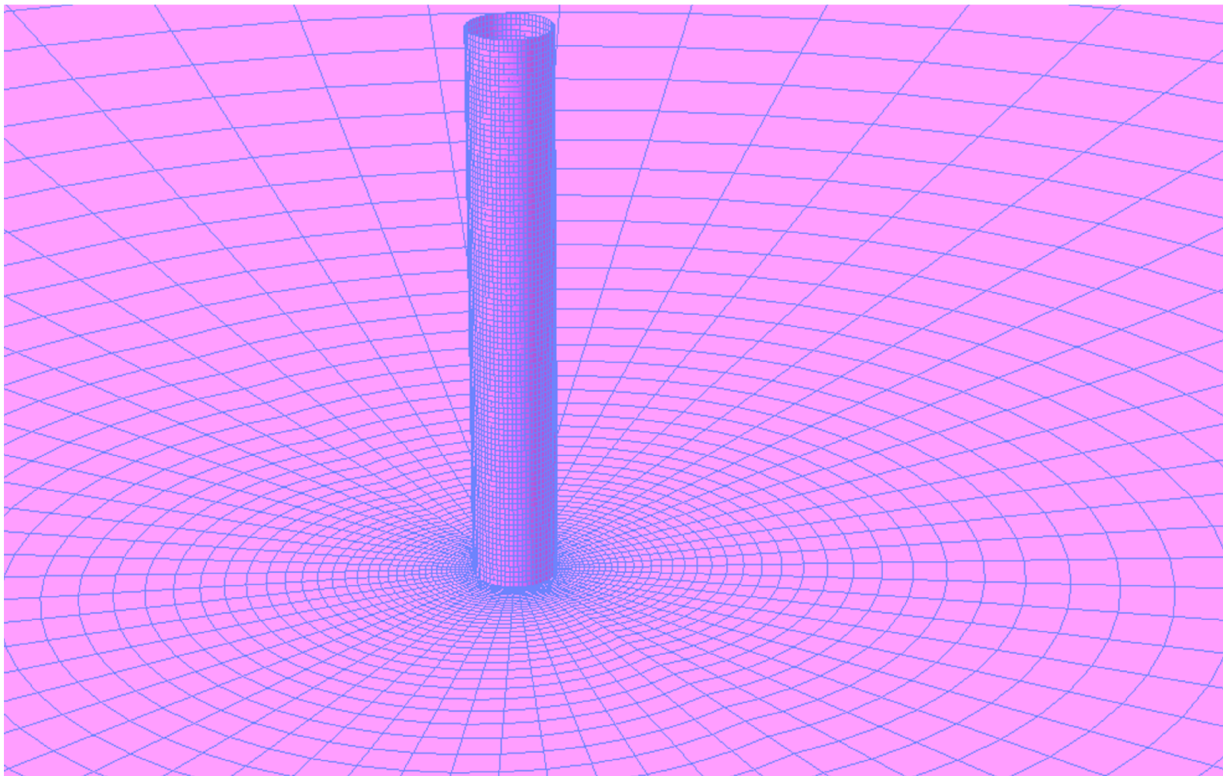

Figure 3-1 The fixed cylinder model in Wasim

We keep kR=0.245, where k is the wave number and R is the cylinder radius. The dimension of the cylinder will not be changed during all the analyses so the wave number will also be constant. Then we increase kA from 0.00245 up to 0.245, where A is the wave amplitude.

kA	0.00245	0.0245	0.049	0.0735	0.098	0.1225	0.147	0.1715	0.196	0.2205	0.245
A (m)	0.0003	0.003	0.006	0.009	0.012	0.015	0.018	0.021	0.024	0.027	0.03

Table 3-1 Wave steepness and corresponding wave amplitudes which will be used

The horizontal wave loads calculated by Wasim will be decomposed into five harmonic components by a small python script which is mainly based on least squares fitting, i.e.

$$F(t) \approx \sum_{i=1}^{5} A_i \sin(i\omega t) + B_i \cos(i\omega t) \qquad (88)$$

$$|F_i| = \sqrt{A_i^2 + B_i^2} \qquad (89)$$

$$\theta_i = \arctan\left(\frac{B_i}{A_i}\right) \qquad (90)$$

where $|F_i|$ is the amplitude of the ith order horizontal load and θ_i is the phase angle between the ith order horizontal load and the total horizontal load. Regarding decomposition of the results, we have also considered to use FFT which is quite traditional for post-processing. But in this case FFT decomposition will give a bit smaller 1st order loads because FFT principally includes infinitive number of harmonic components and is sensitive to small local oscillations. Since the results are always steady state and quite regular, the harmonic Fourier analysis should be a better choice.

The first and second order numerical results compared with corresponding experimental results are presented on the next pages. The mesh resolution is fine enough. There are 62 elements (along the circumference) × 100 elements (along the height) on the cylinder boundary and 62 × 154 elements on the free surface. This fine mesh requires a time step down to 0.001s (1st order time integration), and one analysis of 10s duration will take about 3 hours. The results can be improved slightly if we put more elements on the free surface, but it is little worth considering the corresponding time costage.

Legend label	Description
Experiment	Experiment data from Huseby & Grue (2000)
Ferrant	Fully nonlinear numerical results from Ferrant (1998)
McCamy-Fuchs	Theoretical solutions from McCamy & Fuchs (1954)
Airy	Wasim results, Airy incident wave

Streamfunction	Wasim results, stream function incident wave with 11 coefficients
ilin = 0	Wasim results, linear analysis
ilin =3	Wasim results, nonlinear analysis (more non-linearity will be included in force integration, details can be found in my project thesis P39)
ilin_surf = 0	Wasim results, linear free surface condtions
ilin_surf = 5	Wasim results, nonlinear free surface conditions alternative 1
ilin_surf = 6	Wasim results, nonlinear free surface conditions alternative 2

Table 3-2 Description to the legend labels used in the plots
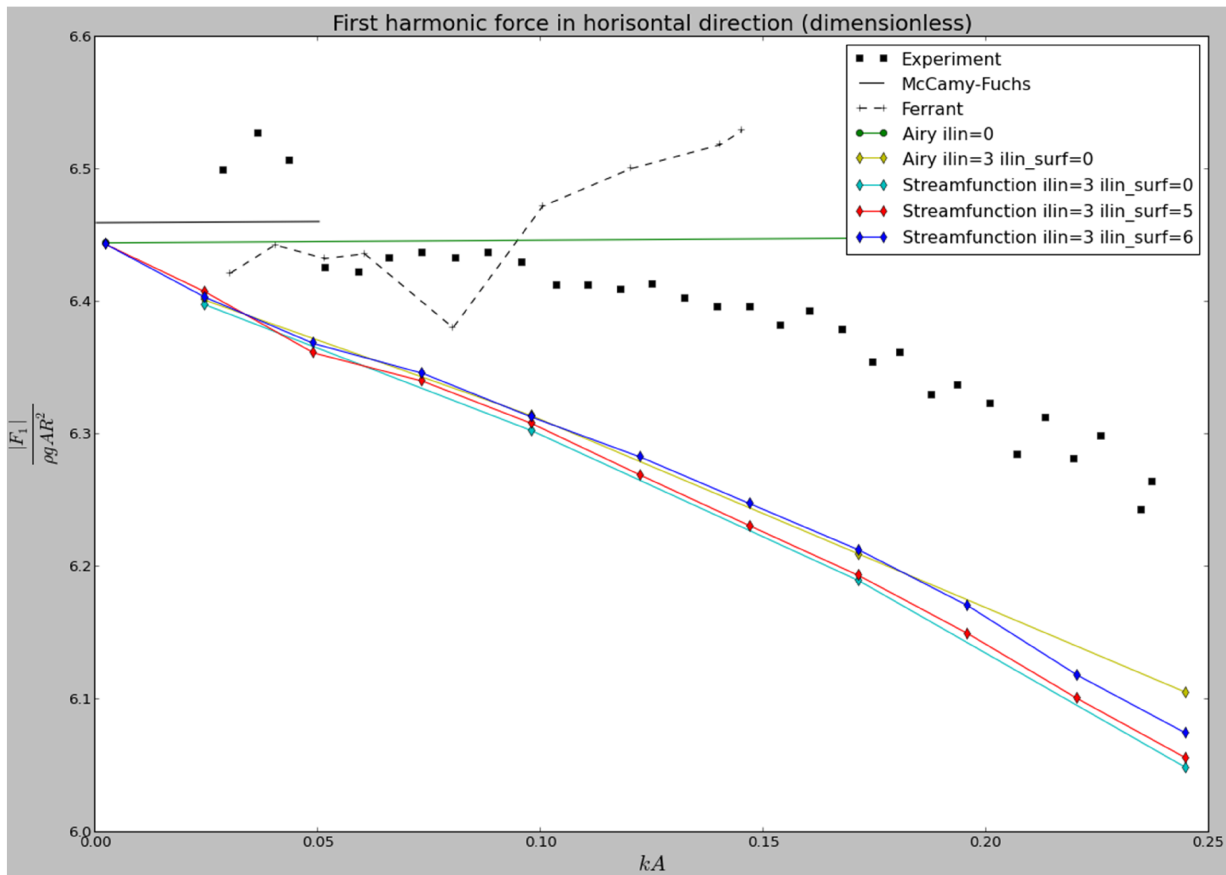
Figure 3-2 First order horizontal force on the cylinder
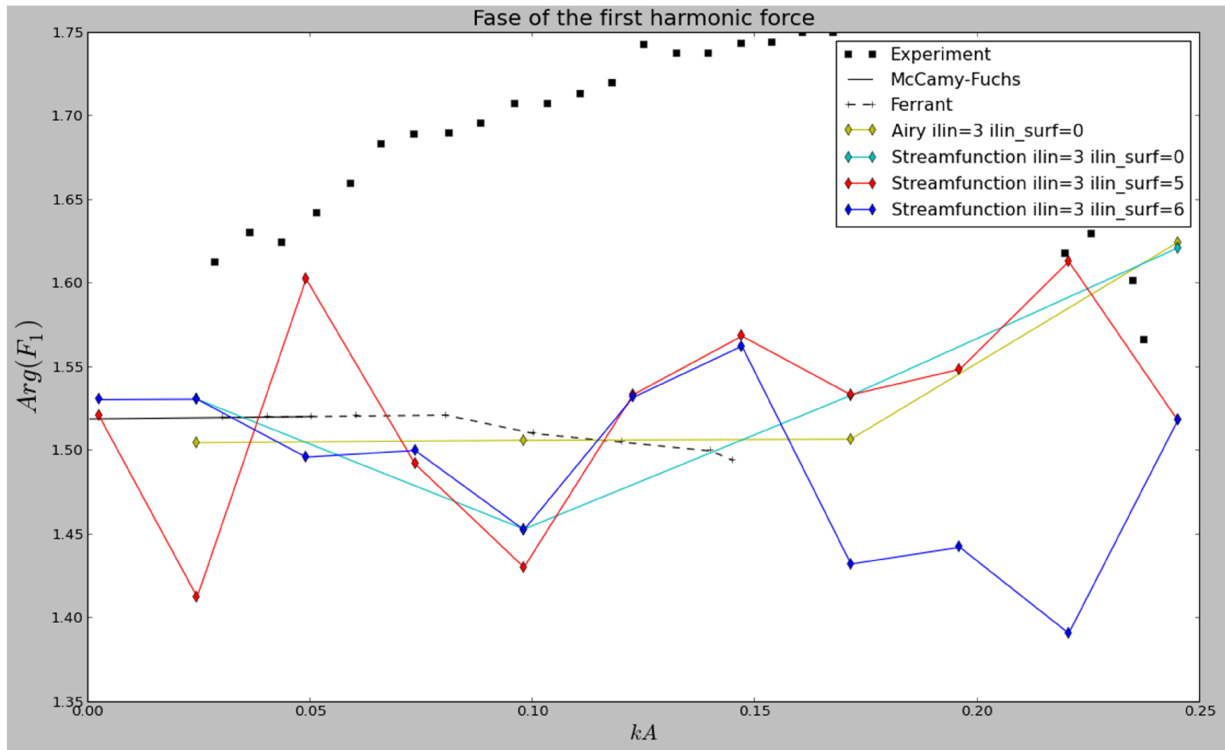
Figure 3-3 Phase angle of the first order horizontal force
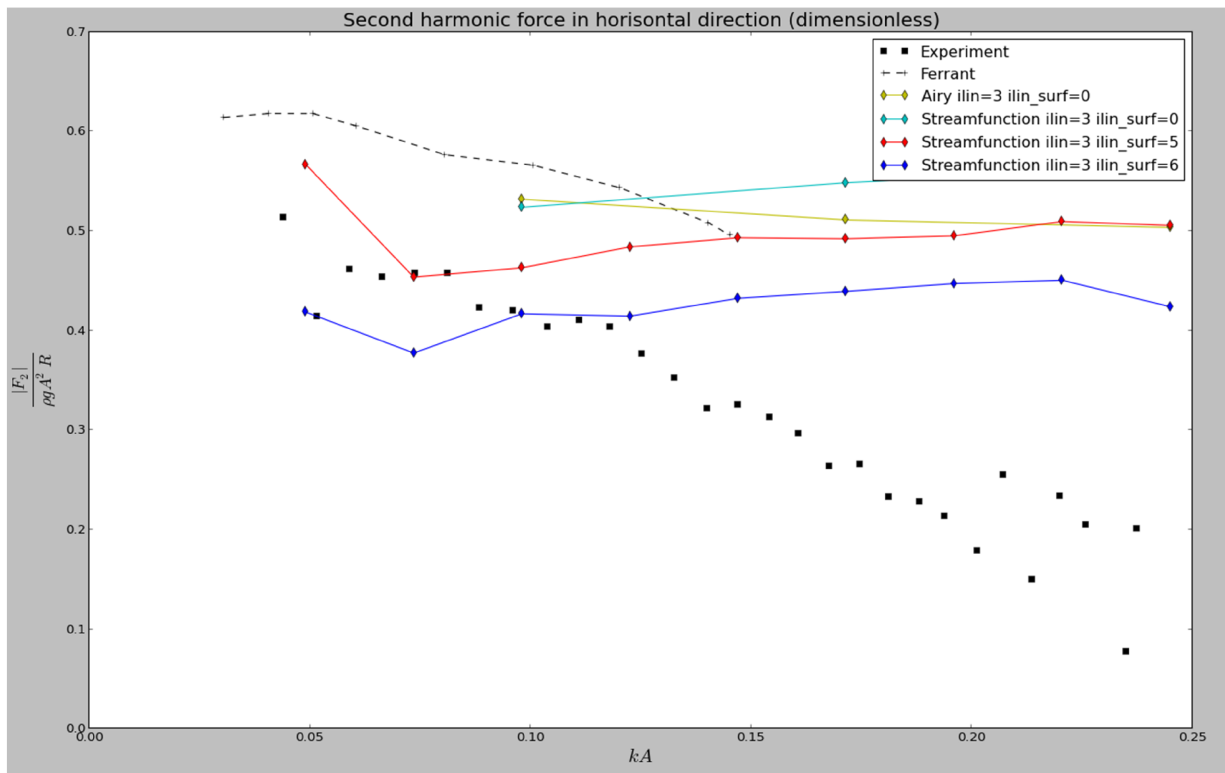
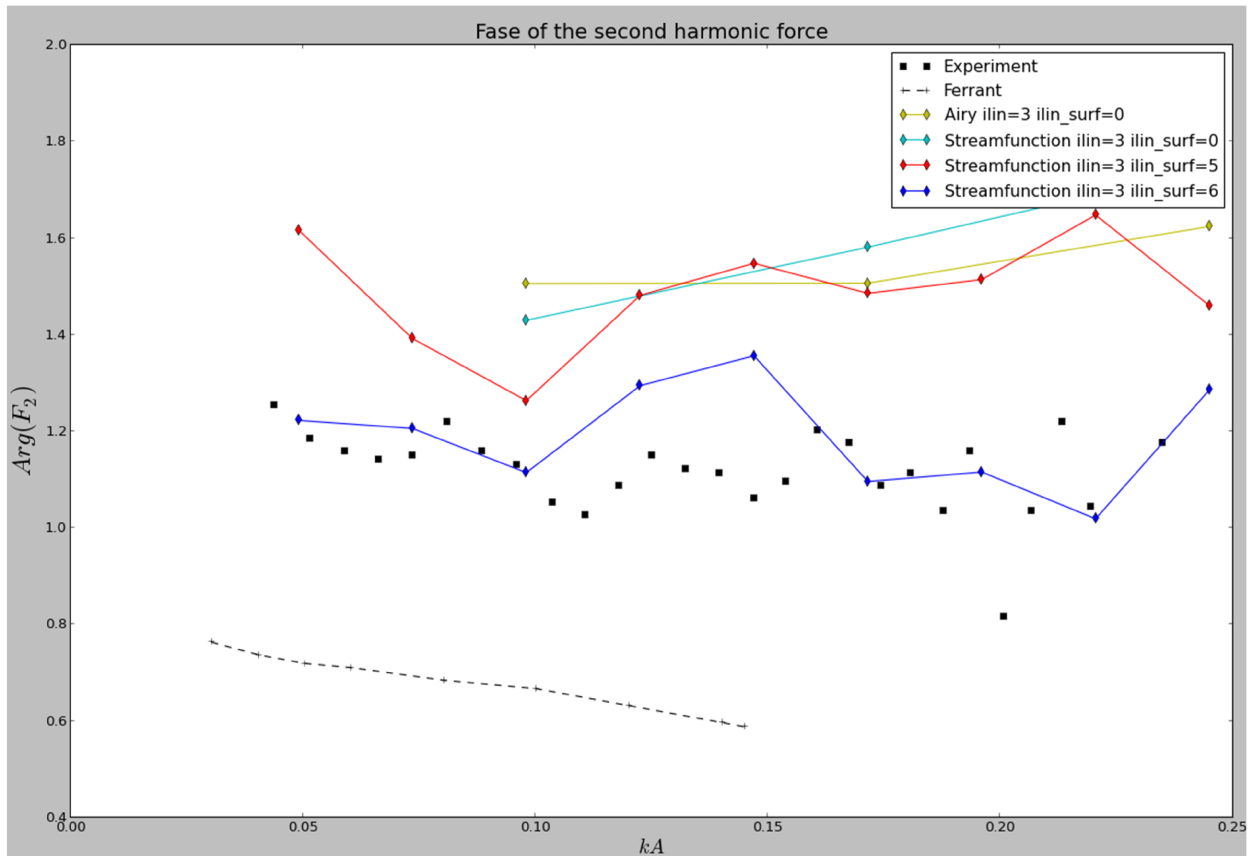**Figure 3-4 Second order horizontal force on the cylinder**

Figure 3-5 Phase angle of the second order horizontal force

- Figure 3.2: all the 1st order loads calculated by Wasim converge to the linear solution when kA is small, even the approach alternative 1, which considered to be theoretically inconsistent, does so as well when the incident wave becomes small.

- Figure 3.2: all the 1st order loads calculated by Wasim are close to each other. They seems to be better than the fully nonlinear results from Ferrant (1998). Though a noticeable nearly constant deviation can be observed comparing with the experiment results, but at least the tendency is correct when kA becomes large.

- Figure 3.3: the phase angles of the 1st order loads from Wasim oscillate a lot around 90 degree (theoretical solution) when the nonlinear free surface conditions are applied (both alternative 1 and 2). All the numerical results tend to be close to the theoretical solution, but the most experiment results are far from 90 degree.

- Figure 3.4: Stream function incident wave combined with nonlinear free surface conditions alternative 2 seems to be a little closer to the experiment results. But all the results from Wasim give larger estimation when kA increases. The fully nonlinear analysis from Ferrant (1998) gives better results at this stage.

- Figure 3.5: Stream function incident wave combined with nonlinear free surface conditions alternative 2 seems to give the best results.

- The yellow line and the cyan line are always close to each other, but the cyan line has quite different pattern than the red/blue line. For this diffraction problem, it seems that the free surface conditions can influence the results more than the incident wave model. Therefore, to update Wasim with some nonlinear free surface conditions will be important for this kind of analyses.

A certain amount of time has been used to figure out the deviations in the 1st order load amplitudes. At first, the deviations were attempted to be explained by some viscous force. The non-dimensional Morison drag was estimated and the magnitude of the drag force was a bit larger than the deviations, so I was hoping there could be found some 1st order viscous force in the same order of magnitude. The viscous force might be skin drag which is associated with KC-number. But according to Huseby & Grue (2000), KC-number was between 1 and 3.6 and Re-number was around 20000 when the experiments were done, therefore the viscous drag force should be very small even when kA is large.

If we further take a look at figure 3.2-3.5, the results from Wasim have lower 1st order amplitudes but higher 2nd order amplitudes when kA becomes large. This could be caused by that the horizontal load time histories from Wasim have higher crests and flatter troughs, i.e. the pattern of the load time histories from Wasim should be more asymmetric about x-axis comparing with the experiment results. The picture below gives an illustration of this phenomenon. The magnitudes in the picture are just for a clear demonstration so they are meaningless.
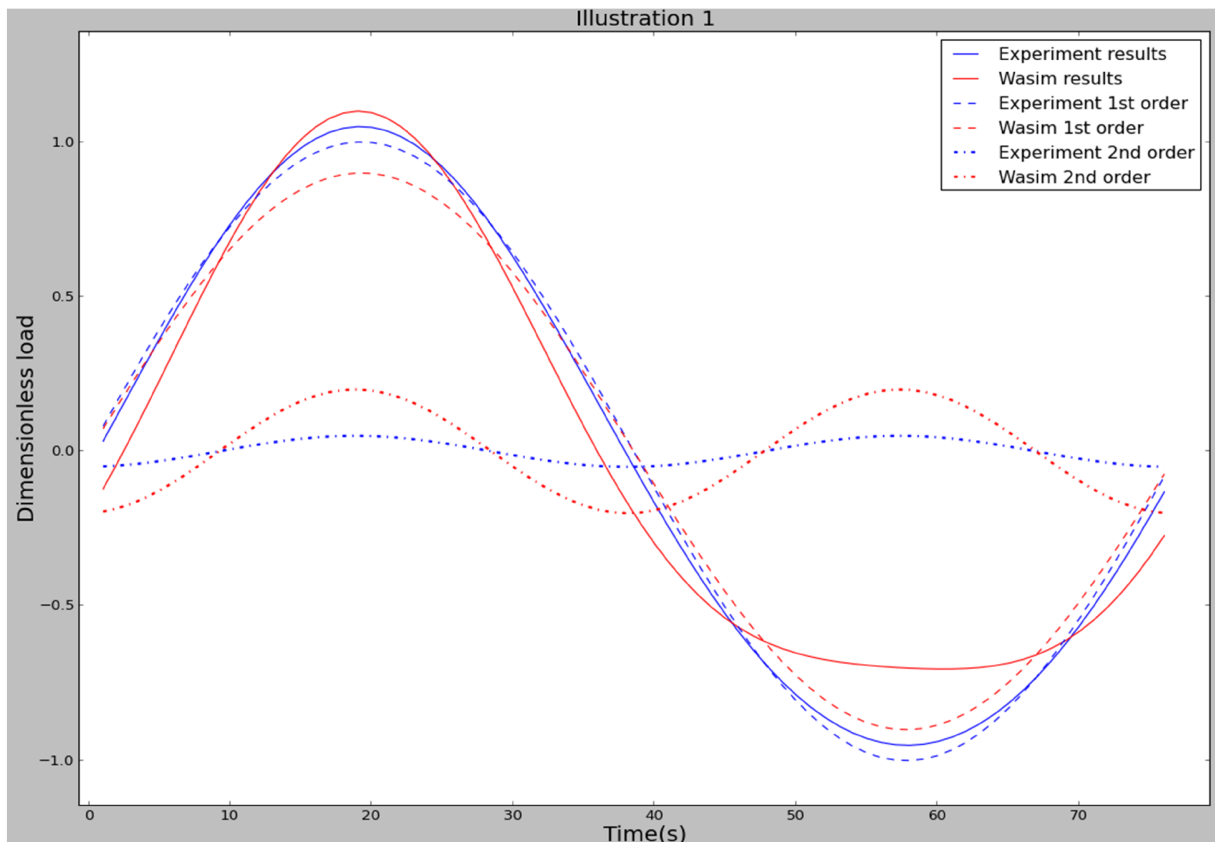
Figure 3-6 Illustration1: Asymmetry about x-axis causes lower 1st order amplitude and higher 2nd order amplitude

Another observation is that the phase angles of the 1ˢᵗ order loads from the experiment results have values father away from 90 degree, which could cause the 1ˢᵗ order load amplitudes from the experiment results to be larger than those which have phase angles closer to 90 degree, see figure 3.7 (apologize for my painting skills…). This may due to that the load time histories from the experiments are more asymmetric about some axis at x=$2n\pi + \frac{\pi}{2}$. This asymmetry can also make the least squares fitting converge to more than one possible solutions Figure 3.8 gives an illustration of this phenomenon. Both two solutions have almost the same sum of squared residuals, i.e. both of them are numerically correct. But if only one of them is physically correct, then we need some physics law as constraint when we least squares fit the objective function, which may be expressed as:

$$O = |Norm_2(load_{exact}) - Norm_2(load_{approx})| + \sum \lambda_i \cdot law_i = 0 \qquad (91)$$

The problem is that the constraints and the Lagrange multipliers are unknown, then the convergence direction of the least squares fitting works like which direction a pen tends to fall down when you balance it on fingertip. This may also explain why the phase angle of the 1st order loads from Wasim oscillates around 90 degree after harmonic Fourier analysis.
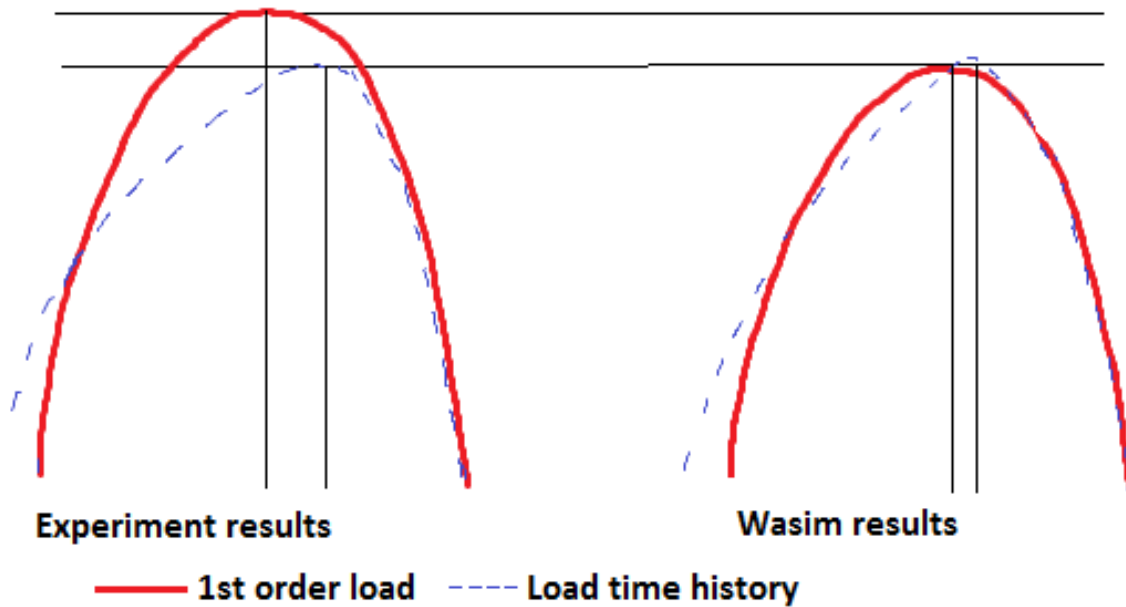

Figure 3-7 Illustration 2: Phase angle closer to 90 degree causes lower 1st order amplitude
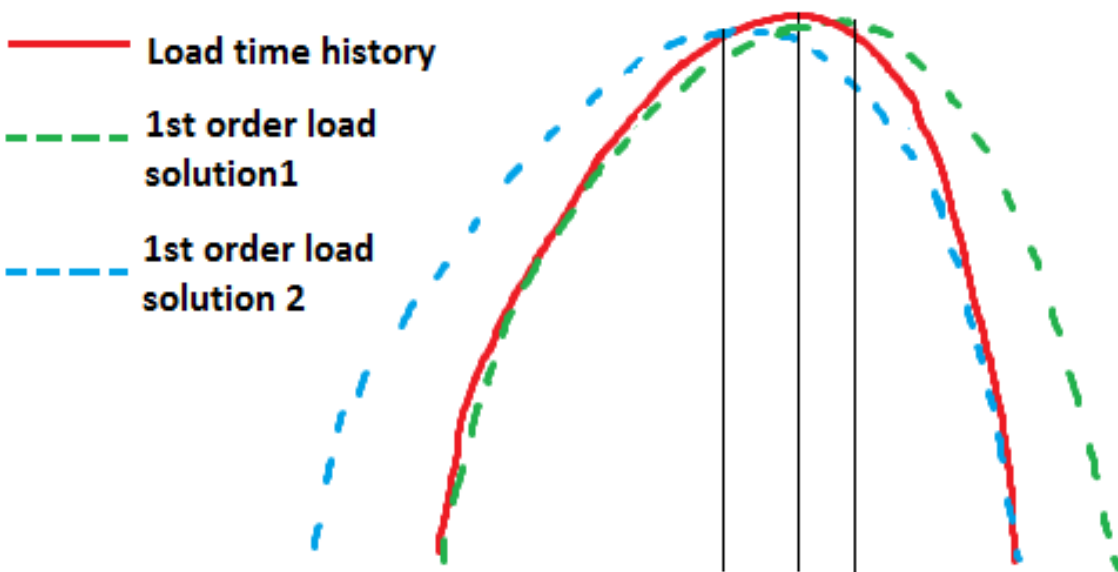

Figure 3-8 Illustration 3: Horizontal asymmetry causes more than one possible solutions

The load time histories should have both vertical and horizontal asymmetry when kA becomes large. But for practical problems, the maximum and minimum load values are more important than the exact load profile. Since the values of both harmonic amplitudes and phase angles up to 6th order are available from Huseby & Grue (2000), to reproduce the time history of the total horizontal wave load would not be difficult. The maximum and minimum values from the load time histories are picked up and compared with the results calculated by Wasim.
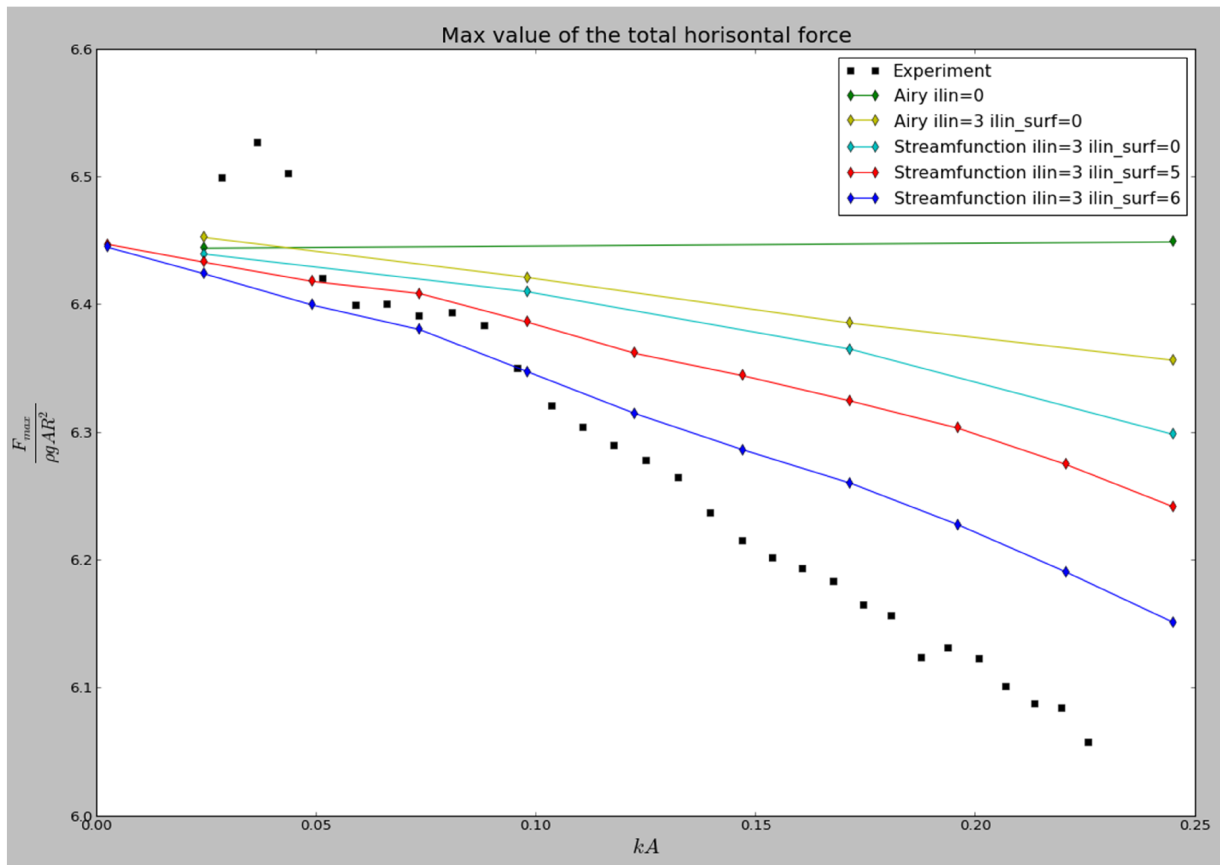

Figure 3-9 Maximum value of the dimensionless horizontal wave load on the cylinder

The load profiles from the experiments seems to have lower maximum magnitudes and higher minimum magnitudes. The implementation of the nonlinear free surface conditions alternative 2, which may due to more nonlinear terms as $O(\phi_i) = O(\zeta_i) = O(1)$ is assumed, seems to give results more compatible to the experiment data. When the linear free surface conditions (ilin_surf=0) are applied, the nonlinear analyses give underestimated minimum load values but acceptable and conservative load amplitudes. On the other side, the linear solutions (ilin=0),
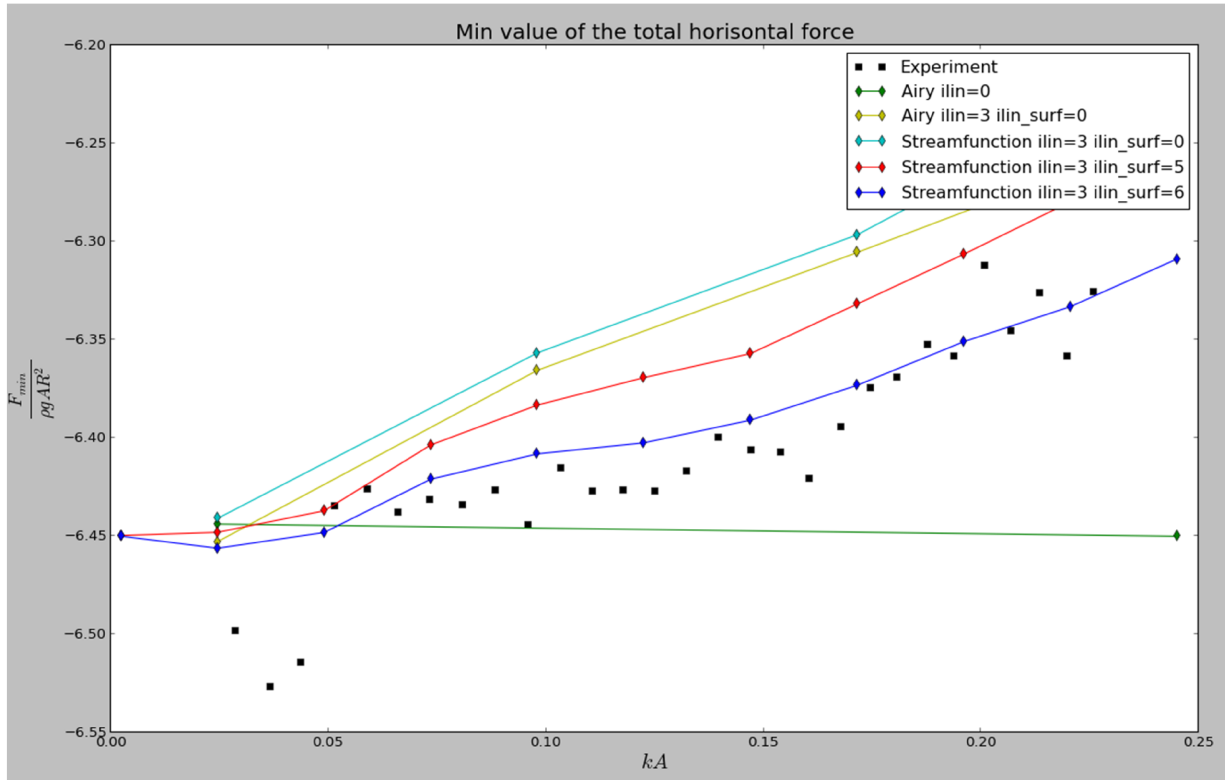
Figure 3-10 Minimum value of the dimensionless horizontal wave load on the cylinder
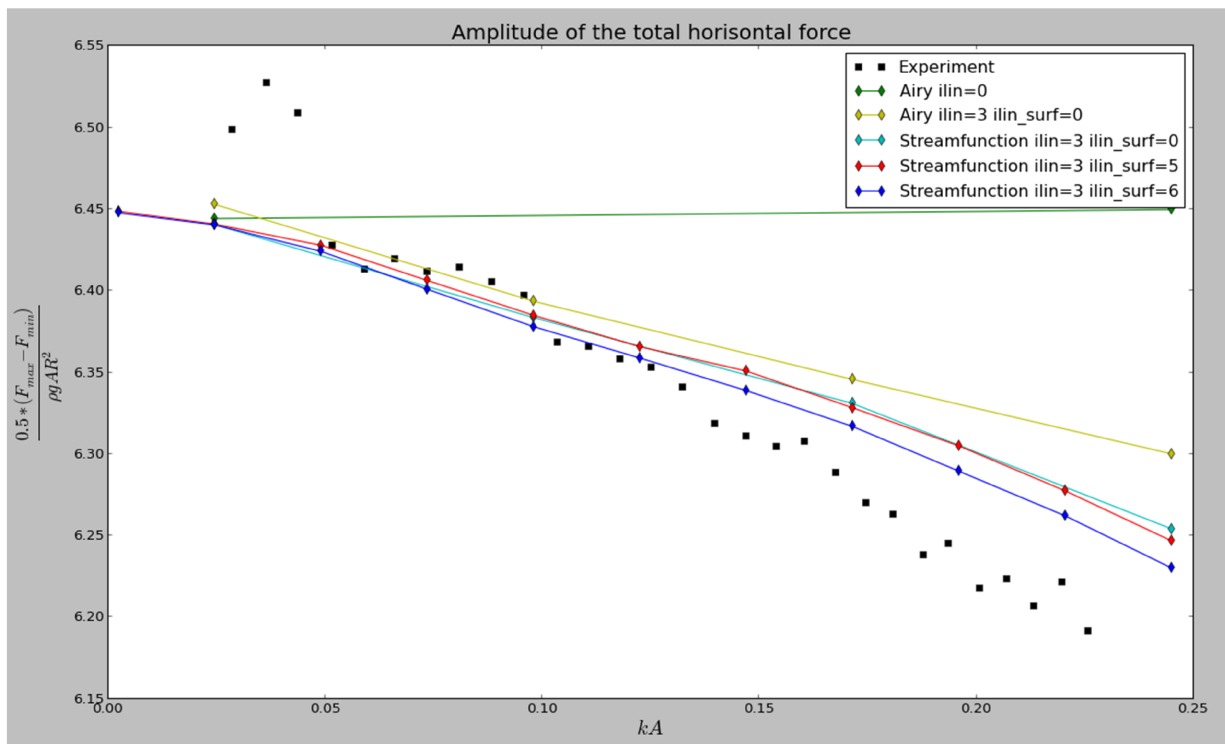

Figure 3-11 Amplitude value of the dimensionless horizontal wave load on the cylinder

which due to that linear systems with regular harmonic inputs always give regular harmonic outputs, will not give satisfying load profiles, especially when kA > 0.1 the results are too conservative. The difference of the results which due to the incident wave model is noticeable when kA>0.2 (the difference between the yellow and cyan lines).

3.4 Ship motions in steep regular waves

After we have studied the diffraction problem, it is logical to do some analysis further with a floating body so that wave radiations can be tested. Traditionally we should go for a forced oscillation analysis, i.e. a pure radiation analysis, since problems often should be spilt into components which are simpler to study. But considering the update of Wasim will be a combination of both the stream function method and the nonlinear free surface conditions, it is worth to include incident waves as excitations. In addition, a series of ship model test data, which is generated within the EC project **Extreme Seas,** is available at DNV and will be used for comparison purpose in this section, therefore the analyses will be estimation of ship motions in some steep regular waves. However, wave loads on the ship will not be studied because it requires detailed mass distribution of the ship model in Wasim, which is time consuming.

3.4.1 Ship model

The ship model used in the analyses is a LNG carrier. The following table and picture gives a description and demonstration respectively of the model.

Scale = 70	Full scale (in Wasim)	Model scale
L_{oa}	197.13 m	2.816 m
L_{pp}	186.90 m	2.670 m
B	30.38 m	0.434 m
D	18.20 m	0.268 m
d	8.40 m	0.120 m
M	35614.03 t	103.831 kg
CG_x	94.87 m	1.355 m
CG_y	0.00 m	0.000 m
CG_z	8.26 m	0.118 m
RG_x	11.27 m	0.161 m
RG_y	40.53 m	0.579 m

RG_z	40.18 m	0.574 m
Water Depth	70 m	1 m

<p align="center">Table 3-3 Main dimensions of LNG carrier</p>

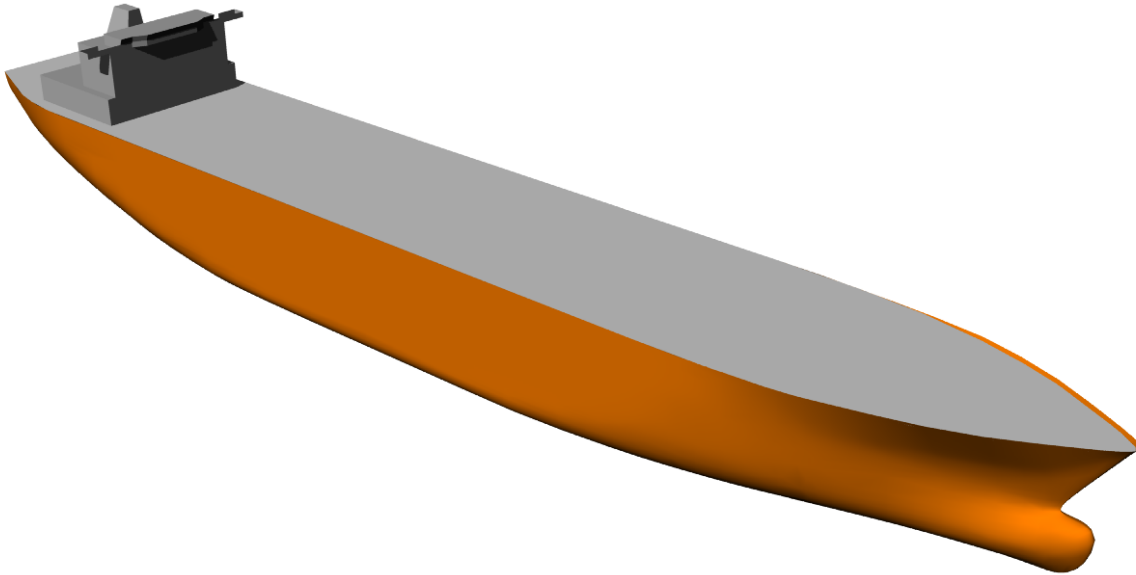

<p align="center">Figure 3-12 The LNG carrier with simplified superstructure</p>

3.4.2 Wave data

The following table includes the data of the regular waves used in the model tests. Units: [length]=meter, [time]=second, [angular frequency]=rad/second. The basin is 110 m long, with a measuring range of 90 m, the width is 8 m and the water depth is 1 m.

Wave	λ_s	λ_m	H_s	H_m	ω_s	ω_m	T_s	T_m	H/gT^2	d/gT^2	kA
1	112.14	1.6020	2	0.02857	0.7421	6.2091	8.4664	1.0119	0.00284	0.09955	0.05603
2	149.52	2.1360	2	0.02857	0.6407	5.3608	9.8062	1.1721	0.00212	0.07420	0.04202
3	168.21	2.4030	3	0.04286	0.6030	5.0448	10.4204	1.2455	0.00282	0.06571	0.05603
4	186.90	2.6700	3	0.04286	0.5698	4.7670	11.0277	1.3181	0.00251	0.05868	0.05043
5	205.59	2.9370	3	0.04286	0.5405	4.5223	11.6243	1.3894	0.00226	0.05281	0.04584
6	224.28	3.2040	4	0.05714	0.5148	4.3067	12.2062	1.4589	0.00274	0.04789	0.05603
7	261.66	3.7380	4	0.05714	0.4694	3.9269	13.3867	1.6000	0.00228	0.03982	0.04803
8	299.04	4.2720	5	0.07143	0.4313	3.6088	14.5667	1.7411	0.00240	0.03363	0.05253

9	336.42	4.8060	5	0.07143	0.3983	3.3328	15.7731	1.8852	0.00205	0.02868	0.04669
10	373.80	5.3400	6	0.08571	0.3699	3.0947	16.9870	2.0303	0.00212	0.02473	0.05043
11	411.18	5.8740	6	0.08571	0.3447	2.8836	18.2304	2.1789	0.00184	0.02147	0.04584
12	112.14	1.6020	8	0.11429	0.7598	6.3573	8.2690	0.9883	0.01193	0.10436	0.22412
13	149.52	2.1360	11	0.15714	0.6577	5.5027	9.5532	1.1418	0.01229	0.07819	0.23112
14	168.21	2.4030	12	0.17143	0.6177	5.1679	10.1723	1.2158	0.01182	0.06896	0.22412
15	186.90	2.6700	13	0.18571	0.5833	4.8804	10.7714	1.2874	0.01142	0.06150	0.21852
16	205.59	2.9370	14	0.20000	0.5532	4.6286	11.3575	1.3575	0.01106	0.05532	0.21393
17	224.28	3.2040	16	0.22857	0.5282	4.4192	11.8956	1.4218	0.01153	0.05043	0.22412
18	261.66	3.7380	18	0.25714	0.4818	4.0312	13.0404	1.5586	0.01079	0.04196	0.21612
19	299.04	4.2720	20	0.28571	0.4432	3.7077	14.1784	1.6946	0.01014	0.03550	0.21011
20	336.42	4.8060	22	0.31429	0.4103	3.4328	15.3139	1.8304	0.00956	0.03043	0.20544
21	373.80	5.3400	24	0.34286	0.3821	3.1965	16.4456	1.9656	0.00905	0.02638	0.20171
22	411.18	5.8740	25	0.35714	0.3566	2.9834	17.6203	2.1060	0.00821	0.02298	0.19101

Table 3-4 Wave data used in the model tests

The period/frequency values in the table above are different from those given in the model test report from TUB, Clauss, G & Klein, M & Dudek, M (2011). The values above are calculated by stream function method (with wave length, wave height and water depth as inputs) while the values given in the report are calculated by using $\omega^2 = kg$, i.e. by deep water assumed, which should be bad approximation for some of the waves.

These 22 waves can be divided into two series according to the wave steepness. The first wave series includes wave 1-11 which have relatively lower kA, and the rest waves are in series 2. We plot all the waves in the wave theory validity range diagram, see figure 3.13, where the horizontal axis is a measure of the water shallowness while the vertical axis is a measure of the wave steepness. The waves in series 1 are not far from the limitation of the linear wave theory, but the waves in series 2 require higher order theories. Some of the waves in series 2 are outside of the validity region of the Stokes 5th wave theory, but after tests it seems that we can still use Stokes 5th waves there without visible unphysical ''humps'' on the wave profile. In this section we will still use stream function method with 11 coefficients to generate incident waves, i.e. 11th order, so that all the waves can be handled correctly. In addition, we will also use Airy waves as bad approximation to check how the incident wave model will influence the results.
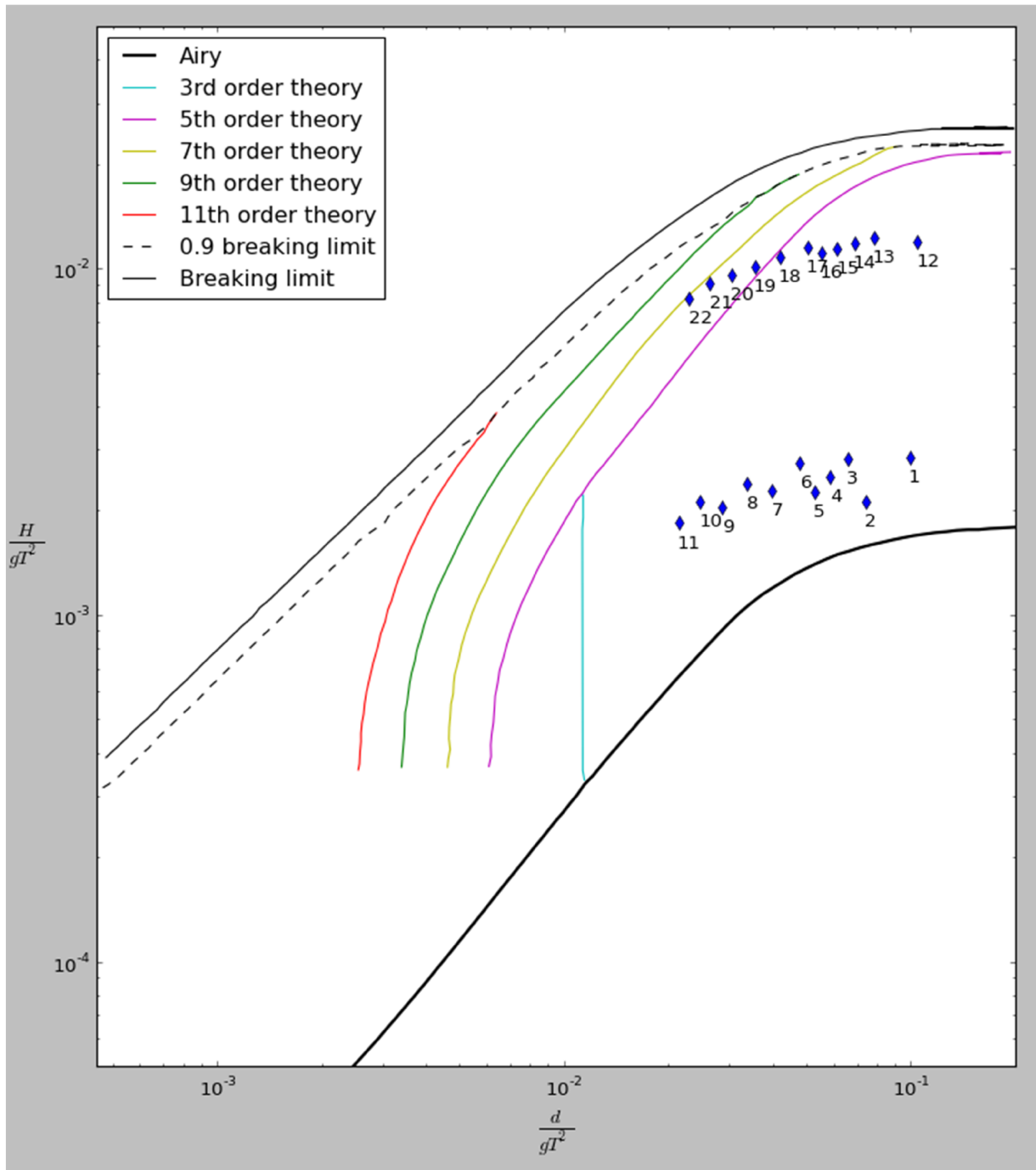
Figure 3.13 Figure 3-13 All the waves plotted in the theory validity range diagram

Since the measurement of the incident wave elevations during the model tests is also available, it is worth to investigate these data to make sure that the wave inputs to Wasim are exactly the

same as those in the experiments. The following picture is plot of the time history of wave 2. The elevations are not as steady state as expected.
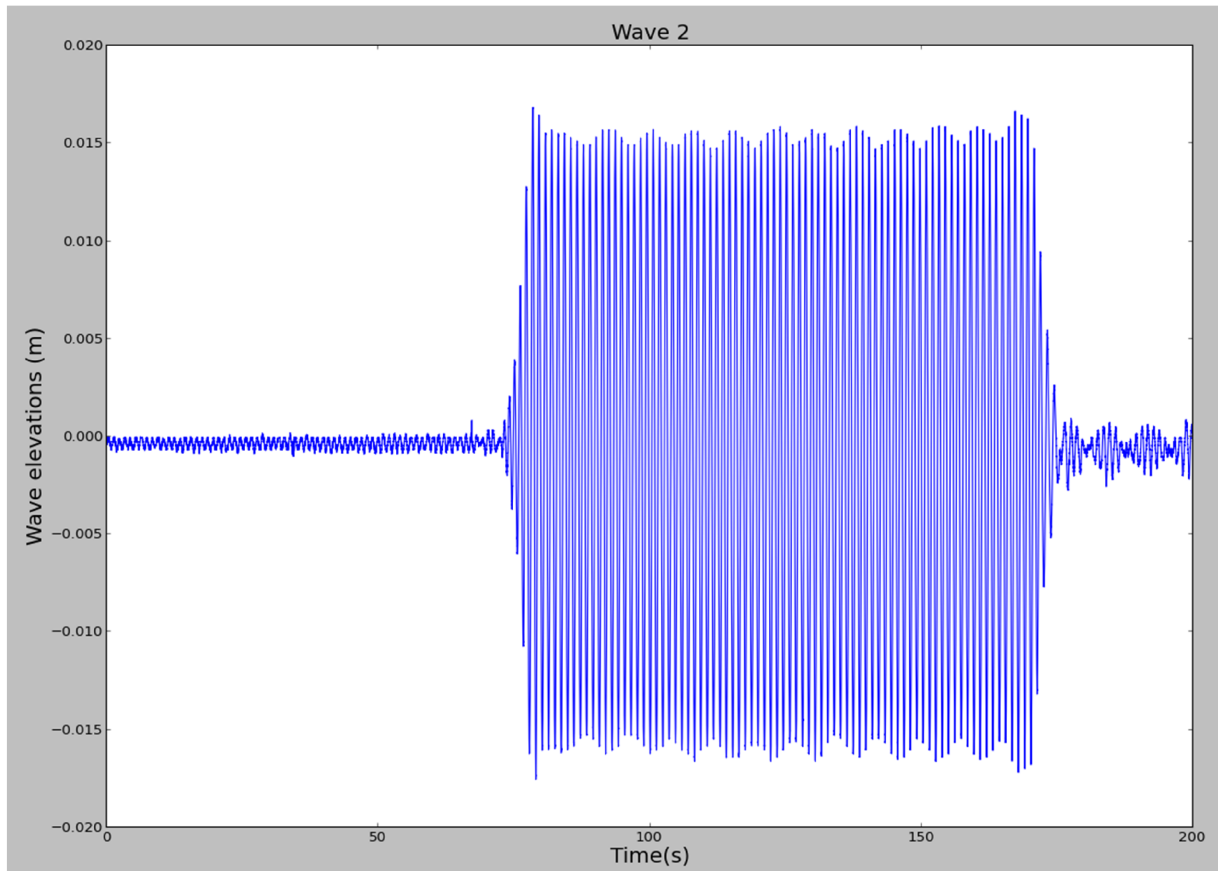

Figure 3-14 Time history of wave 2 elevations

The elevation signal is modulated by an envelop which has a frequency about 0.766 rad/s and may due to reflected waves from the basin sides. If we assume deep water condition for wave 2, it will take about 8 seconds for the wave to travel back to the ship model from the basin sides. Another considered factor which may pollute the model tests is so called seiching phenomenon, but it is less dangerous as the natural period of the basin is around 70 seconds (the basin has length/depth ratio 110, so the natural period of the basin can be evaluated by the highest natural sloshing period in shallow water).

The following table gives the mean values and standard deviations of the wave heights and wave periods calculated from the incident wave measurements. The measurements of wave 1 and wave 12 are not available.

Wave	H_{mean}	H_{std}	H_{std}/H_{mean}	T_{mean}	T_{std}	T_{std}/T_{mean}
2	0.03108	0.00065	2.0921 %	1.16963	0.00545	0.4663 %
3	0.04277	0.00022	0.5092 %	1.24045	0.00360	0.2900 %
4	0.04704	0.00026	0.5501 %	1.30770	0.00369	0.2824 %
5	0.04344	0.00060	1.3854 %	1.37150	0.00331	0.2414 %
6	0.05818	0.00028	0.4831 %	1.43278	0.00356	0.2483 %
7	0.05803	0.00058	0.9992 %	1.54771	0.00408	0.2634 %
8	0.07314	0.00047	0.6494 %	1.65402	0.00507	0.3063 %
9	0.07250	0.00082	1.1378 %	1.75386	0.00553	0.3150 %
10	0.08707	0.00027	0.3152 %	1.85050	0.00568	0.3069 %
11	0.08676	0.00028	0.3243 %	1.94111	0.00737	0.3797 %
13	0.16968	0.00349	2.0542 %	1.16958	0.01207	1.0319 %
14	0.17633	0.00343	1.9451 %	1.24150	0.01898	1.5288 %
15	0.19314	0.00203	1.0527 %	1.30714	0.01221	0.9338 %
16	0.19943	0.00307	1.5383 %	1.37313	0.01779	1.2958 %
17	0.23395	0.00470	2.0087 %	1.43558	0.01258	0.8765 %
18	0.24333	0.00248	1.0211 %	1.55000	0.03700	2.3869 %
19	0.28674	0.00424	1.4776 %	1.66227	0.02354	1.4159 %
20	0.32126	0.00461	1.4349 %	1.75950	0.02350	1.3356 %
21	0.34414	0.00472	1.3719 %	1.86075	0.03226	1.7337 %
22	0.35921	0.00518	1.4417 %	1.95528	0.02401	1.2278 %

Table 3-5 Statistics calculation of the wave parameters from the experiment measurements

The std/mean ratios are acceptable so the mean values may represent the wave conditions well. Some of the mean wave height and mean wave period values differ a certain amount from those values directly given in the model test report, i.e. the values in table 3-4. In this case, we use the mean values multiplied with the scale factor as inputs to Wasim.

3.4.3 Post-process the experiment results

One strange observation has been found before the post-processing. The heave responses are quite unsteady state while the time histories of the pitch responses seems to have better quali-ty. The following two pictures give an example.
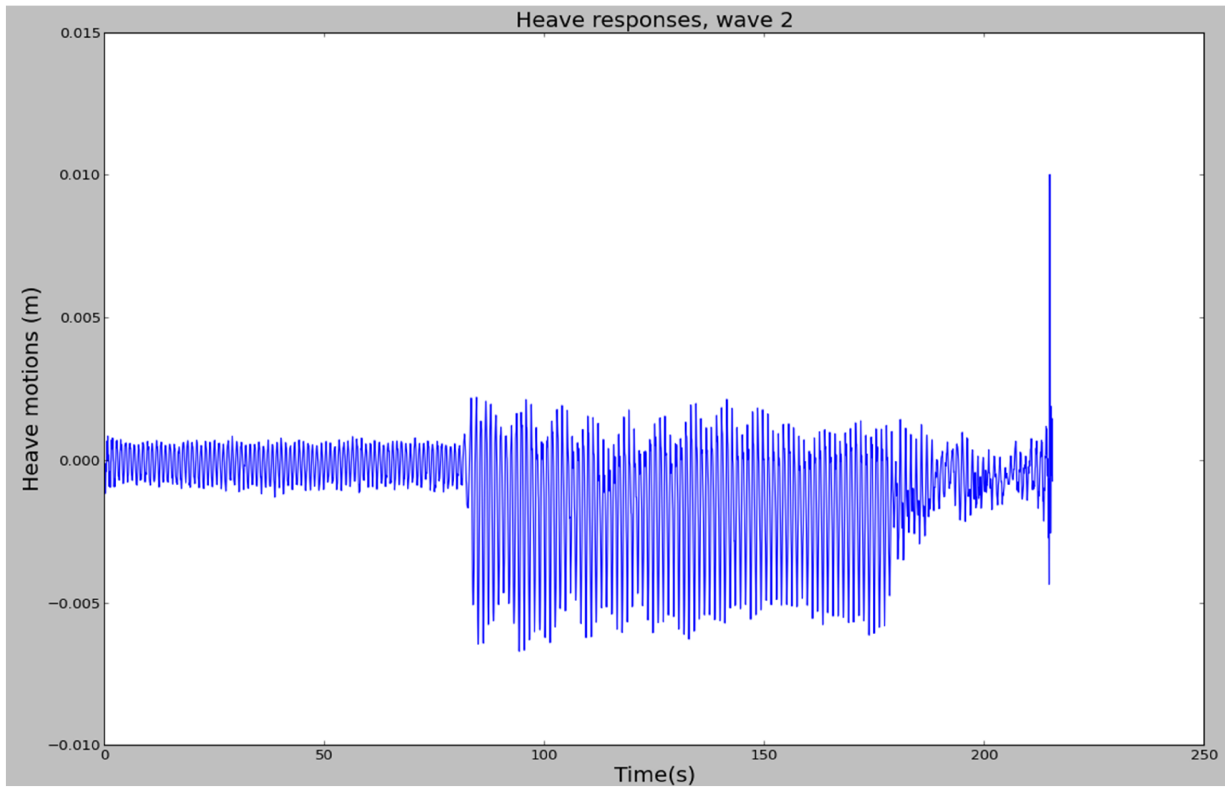
Figure 3-15 Heave responses of the ship model when incident wave is wave 2
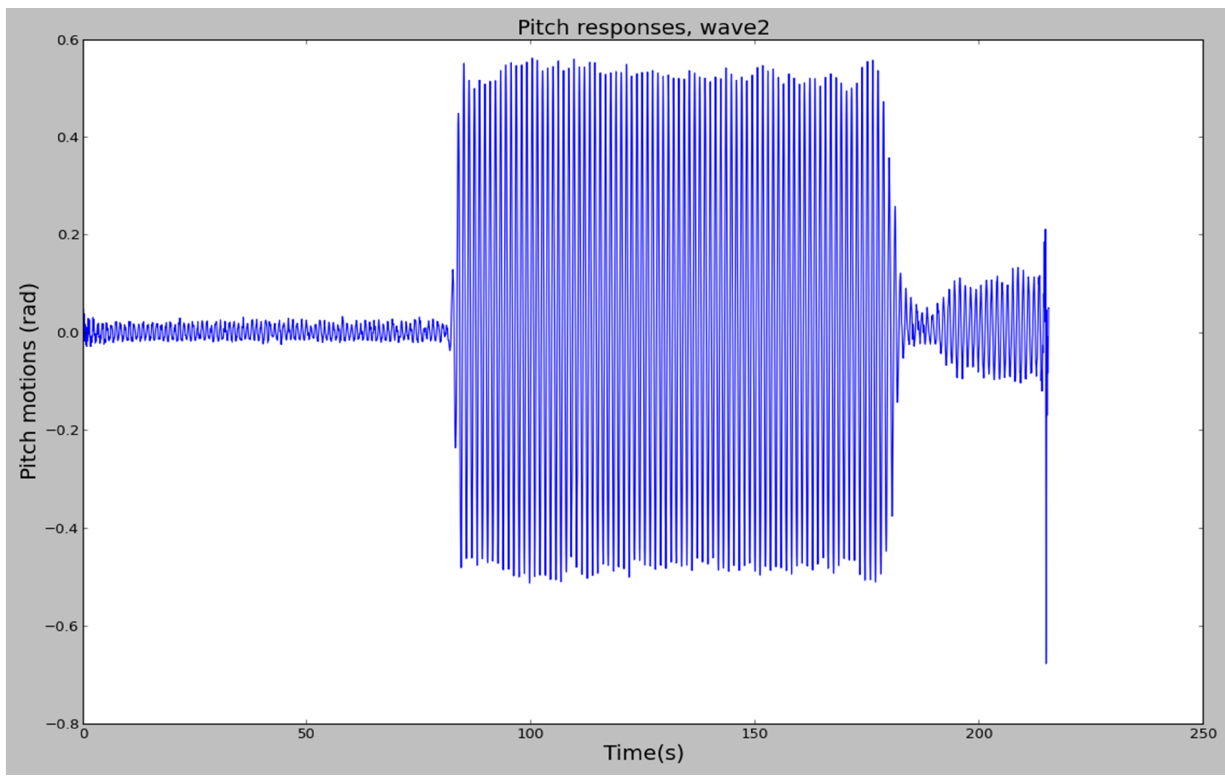

Figure 3-16 Pitch responses of the ship model when incident wave is wave 2

One possible reason is that the heave motions are not measured at the ship model's center of gravity, but then the wrongly measured heave motions should still be quite steady state as the measurement will be a linear combination of the heave and pitch motions, which both are assumed to be steady state and have the same frequency as the excitation. Another possible reason is the influence of the reflected waves from the basin sides. As mentioned earlier in the previous section, the incident wave time history is modulated by a high frequency envelop. This may cause the observed oscillation of the heave amplitudes since heave motions are most affected by wave amplitudes while pitch motions are most affected by wave slopes. Unluckily, this oscillation of the heave amplitudes makes the post-processing of the heave signal cost quite a bit of time. If we FFT the response signal and compare the 1st and 2nd order responses with the corresponding results calculated from Wasim, the comparison will not be a good assessment of the new implementations to Wasim, because ship motions calculated by Wasim are always steady state without oscillation of amplitudes when the incident waves are regular. So instead we end with to compare the mean values of the response amplitudes.

There are two approaches to calculate the mean amplitudes. We can divide the time history of responses into separate windows which has a length equals to the excitation period, and then find the extreme value among all the local maximums and minimums within each window. Figure 3.17 presents an example. Another approach is to smooth the response time histories before we calculate the mean amplitudes so that the unnecessary local maximums and minimums can be filtered out. Then we find the position of all the remaining local maximums and minimums to further calculate the mean amplitudes. The algorithm of smoothing is based on convolution of a scaled window with the signal. The mean amplitude values are still calculated from the unsmoothed data so that the error due to smoothing will not be included, see figure 3.18. Both approaches will give the same results, but the latter one is quicker as it requires less looping.
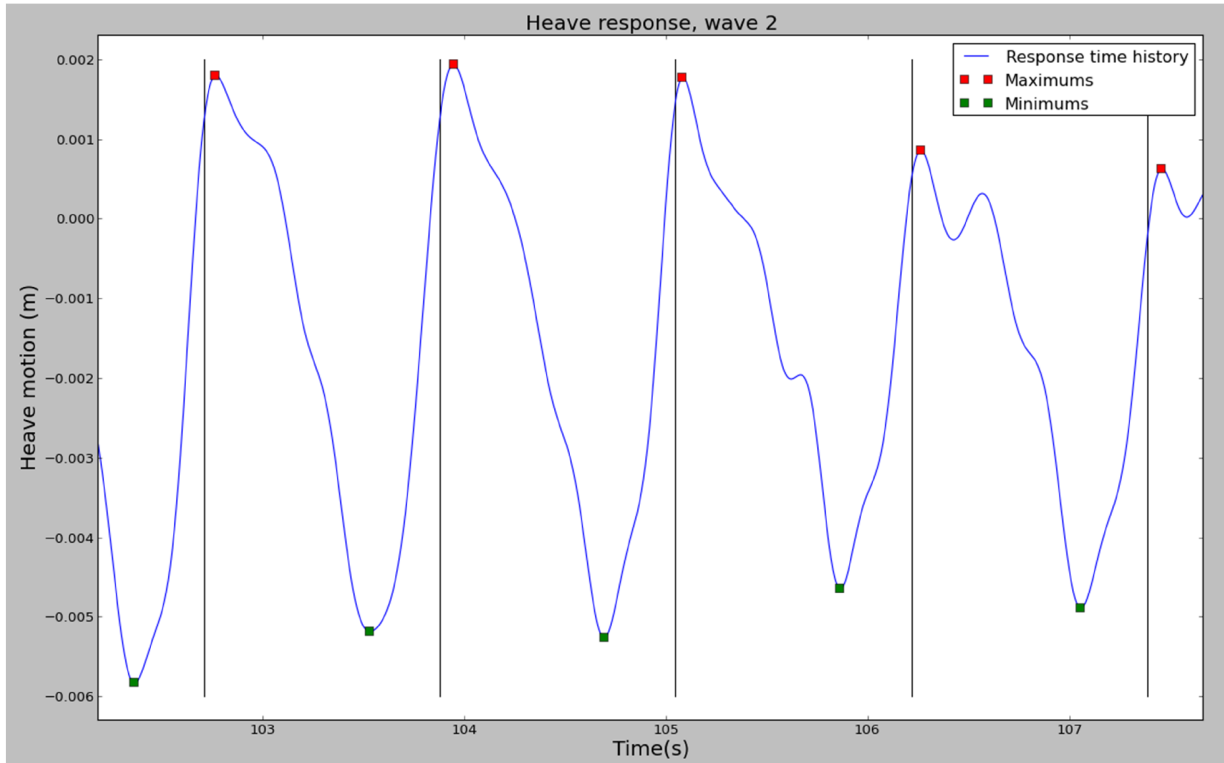
Figure 3-17 Calculate mean amplitudes by dividing the time history into separate windows
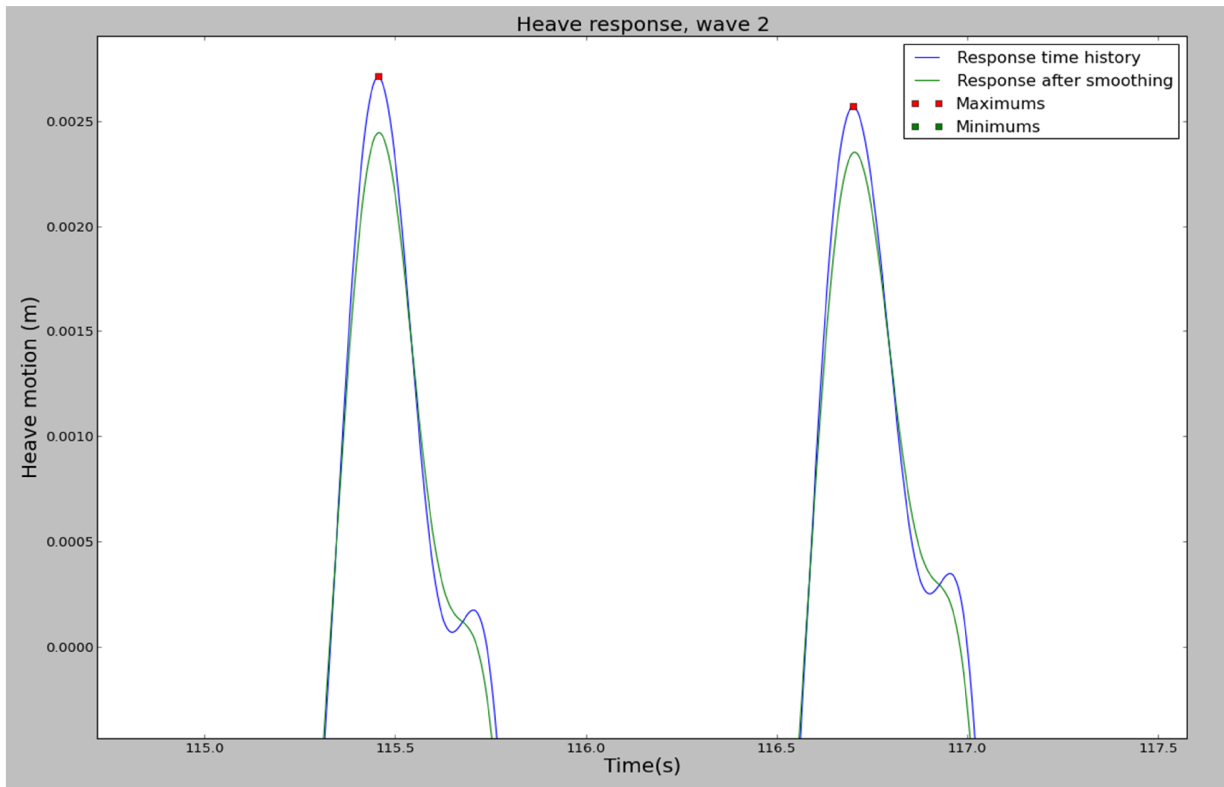

Figure 3-18 Calculate mean amplitudes by smoothing the data first

Then we calculate the mean amplitudes and the corresponding standard deviations. The standard deviation gives an estimation of error band.

Wave	$|\eta_3|_{mean}$ (m)	$|\eta_3|_{std}$	$\frac{|\eta_3|_{std}}{|\eta_3|_{mean}}$	$|\eta_5|_{mean}$ (deg)	$|\eta_5|_{std}$	$\frac{|\eta_5|_{std}}{|\eta_5|_{mean}}$	Time start (s)	Time end (s)
2	0.00276	0.00029	10.58 %	0.50821	0.01049	2.06 %	100	150
3	0.00406	0.00105	25.79 %	0.94326	0.01392	1.48 %	100	150
4	0.00510	0.00071	13.82 %	1.17830	0.01125	0.95 %	100	150
5	0.00598	0.00047	7.81 %	1.26044	0.00945	0.75 %	100	150
6	0.01002	0.00021	2.11 %	1.78074	0.00821	0.46 %	80	120
7	0.01304	0.00027	2.07 %	1.85342	0.00851	0.46 %	80	120
8	0.01877	0.00031	1.67 %	2.25561	0.00977	0.43 %	80	120
9	0.02180	0.00040	1.85 %	2.18413	0.00938	0.43 %	80	120
10	0.02853	0.00031	1.08 %	2.60883	0.00920	0.35 %	80	100
11	0.03039	0.00024	0.80 %	2.48974	0.01179	0.47 %	80	100
13	0.01129	0.00262	23.21 %	2.28477	0.08843	3.87 %	120	150
14	0.01200	0.00148	12.31 %	3.41069	0.08551	2.51 %	100	120
15	0.01821	0.00112	6.12 %	4.72382	0.06865	1.45 %	100	120
16	0.02565	0.00140	5.45 %	5.68399	0.10553	1.86 %	80	120
17	0.03874	0.00165	4.25 %	7.04654	0.13021	1.85 %	80	100
18	0.05718	0.00132	2.31 %	8.04996	0.08167	1.01 %	80	100
19	0.07865	0.00115	1.46 %	9.36943	0.10840	1.16 %	80	100
20	0.10360	0.00656	6.33 %	10.21011	0.53364	5.23 %	80	100
21	0.11915	0.01109	9.31 %	10.02668	0.48275	4.81 %	80	100
22	0.12279	0.00698	5.69 %	10.08579	0.89505	8.87 %	80	100

Table 3-6 Statistics calculation of the model responses from the experiment measurements

3.4.4 Comparison of the results

Two mesh resolutions have been applied in Wasim. The finer one gives a bit better answers according to the experiment results. Even higher resolutions have not been tested because the mentioned meshing can already predict quite accurate rigid body motions.

Mesh	Resolution on the ship boundary	Resolution on the free surface	Time step
1	44 (girthwise) × 15 (along the height)	44 (girthwise) × 119 (axial)	0.1s
2	80 (girthwise) × 30 (along the height)	80 (girthwise) × 164 (axial)	0.05s

Table 3-7 Description of the mesh resolutions

For each wave condition, a linear analysis with Airy incident wave and a nonlinear analysis with the combination of stream function incident wave plus nonlinear free surface conditions alternative 2 will be run in Wasim. The results in wave 3, 4, 5, 13 and 14 will not be presented, because these wave conditions have the same kA as some of the rest but larger standard deviations. The approach alternative 1 has not been tested, but we plan to do so if alternative 2 cannot give acceptable results. The following pictures compare the heave and pitch amplitudes calculated by Wasim with correponding mean amplitudes collected from the experiment results. The error bands are based on the standard deviations calculated earlier in table 3-6. The numbers in the pictures denote wave condition. The finer mesh is used for all the analyses.
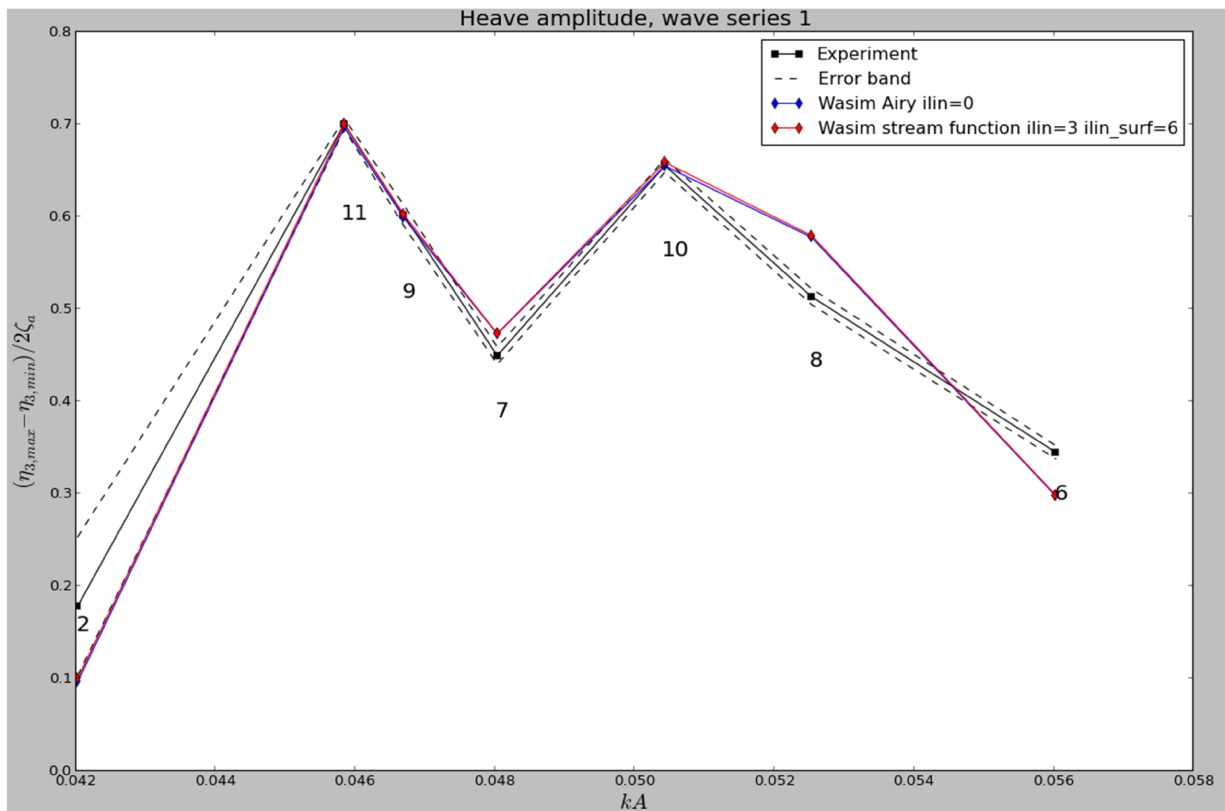

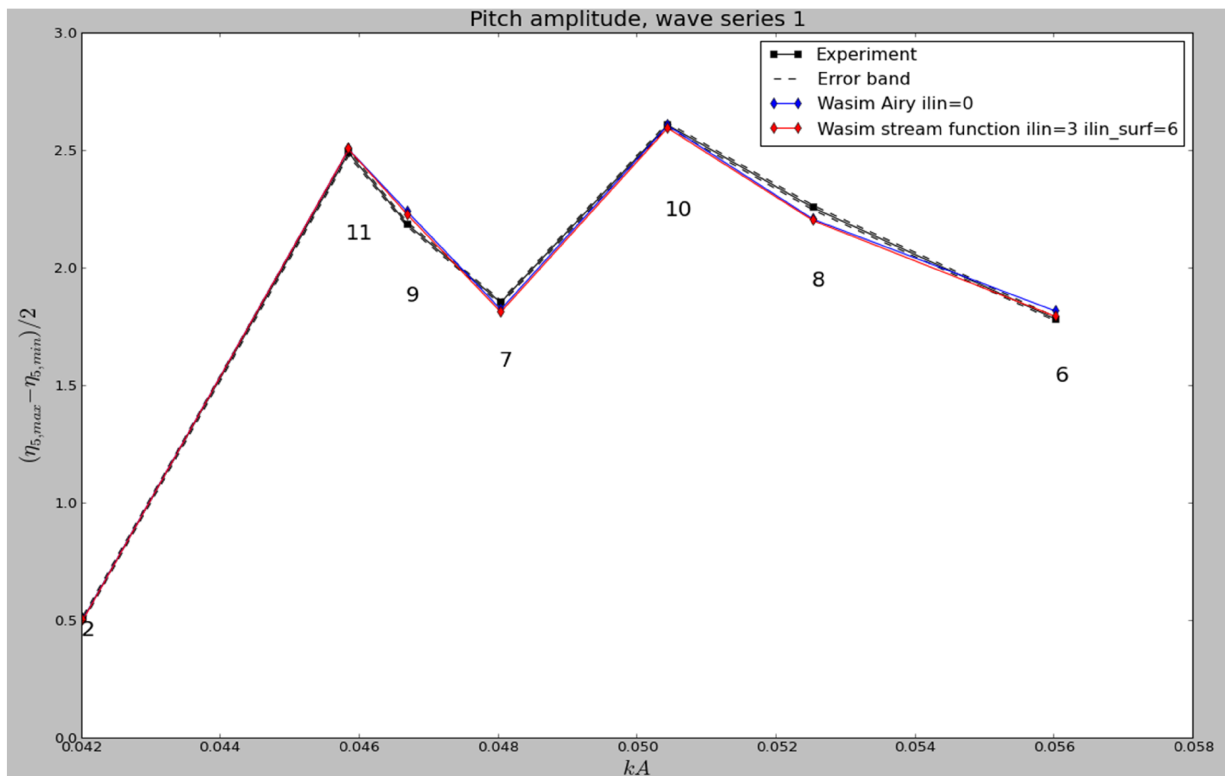**Figure 3-19 Comparison of dimensionless heave amplitudes in wave series 1**

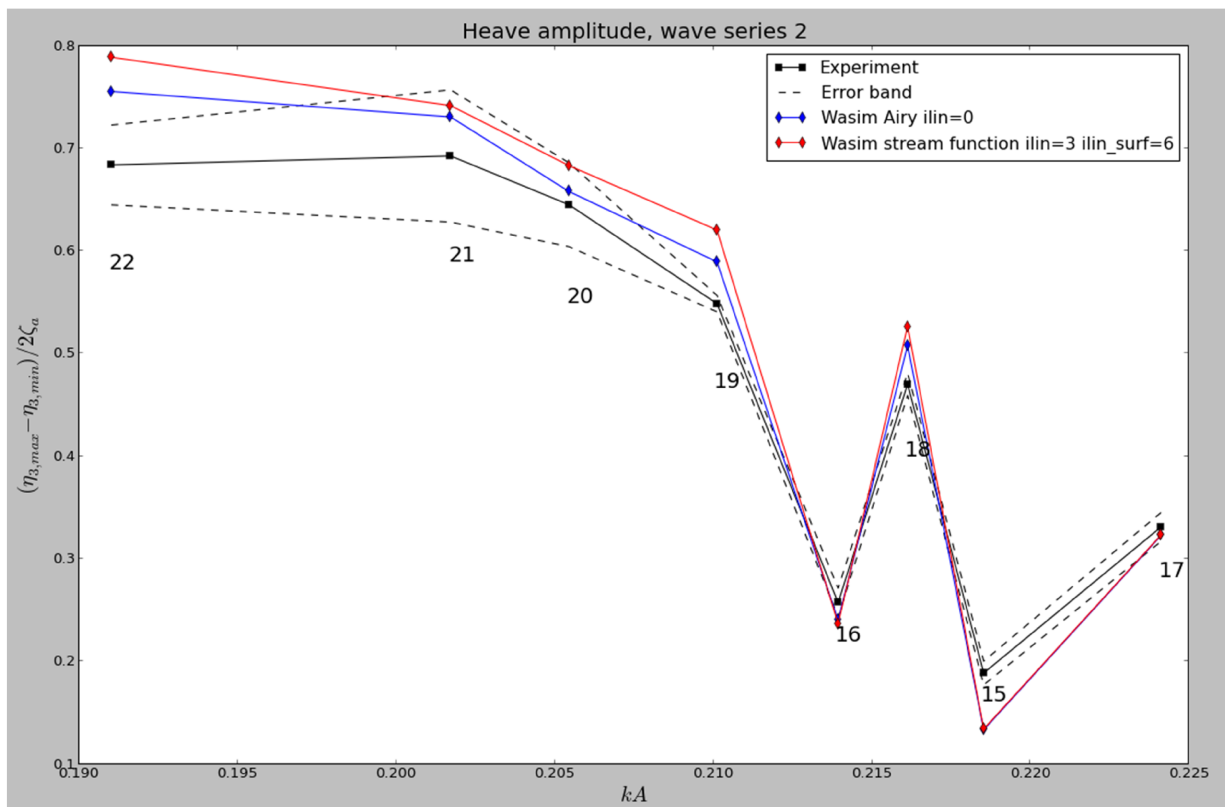**Figure 3-20 Comparison of pitch amplitudes in wave series 1**

Figure 3-21 Comparison of dimensionless heave amplitudes in wave series 2
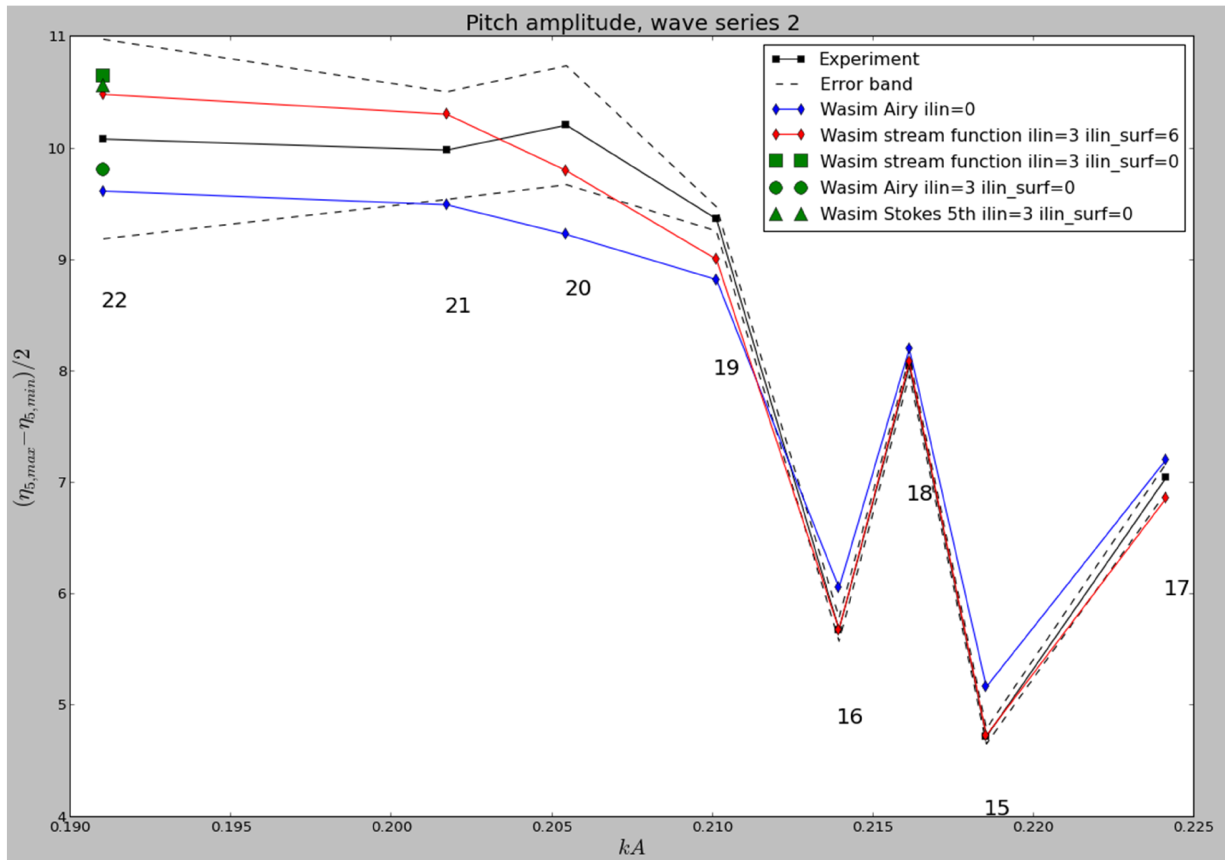
Figure 3-22 Comparison of pitch amplitudes in wave series 2

- The response is not increasing or decreasing monotonously when kA increases. This is because neither k or A remains constant in all the wave conditions, i.e. the wave conditions given does not have control variables.

- The numerical results from Wasim seems to be good when comparing with the pitch responses from the experiments, especially when the nonlinear free surface conditions alternative 2 is applied, but noticeable deviations can be observed in several waves when we compare the heave responses. Unlikely, we cannot make a concrete assessment of Wasim's accuracy of predicting heave motions since the quality of heave measurement from the experiments by itself is questionable.

- The difference between the results from the linear and nonlinear analysis is quite small overall, except in wave 22 where the responses are largest. Three extra analyses are thus made because nonlinearity seems to affect the response amplitudes by most in this

wave condition. The green rectangular is very close to the red point while the green circle is some distance away from the green triangular, which gives us an impression that the incident wave model affects the results more than the free surface conditions do. This may due to that the wave diffractions and radiations are relatively small so that the free surface conditions do not play an important role, and instead the incident wave is dominating. It is worth to mention here that whether ilin=0 or 3 is applied makes the most difference in the force responses (more details can be found in my project thesis p39), ilin=3 is mandatory if the incident wave is nonlinear.

We then plot the elevations of wave diffraction plus wave radiation, the incident wave elevations and the total wave elevations at three positions around the ship. The figure below presents only the positions so the meshing is not used in any analysis.
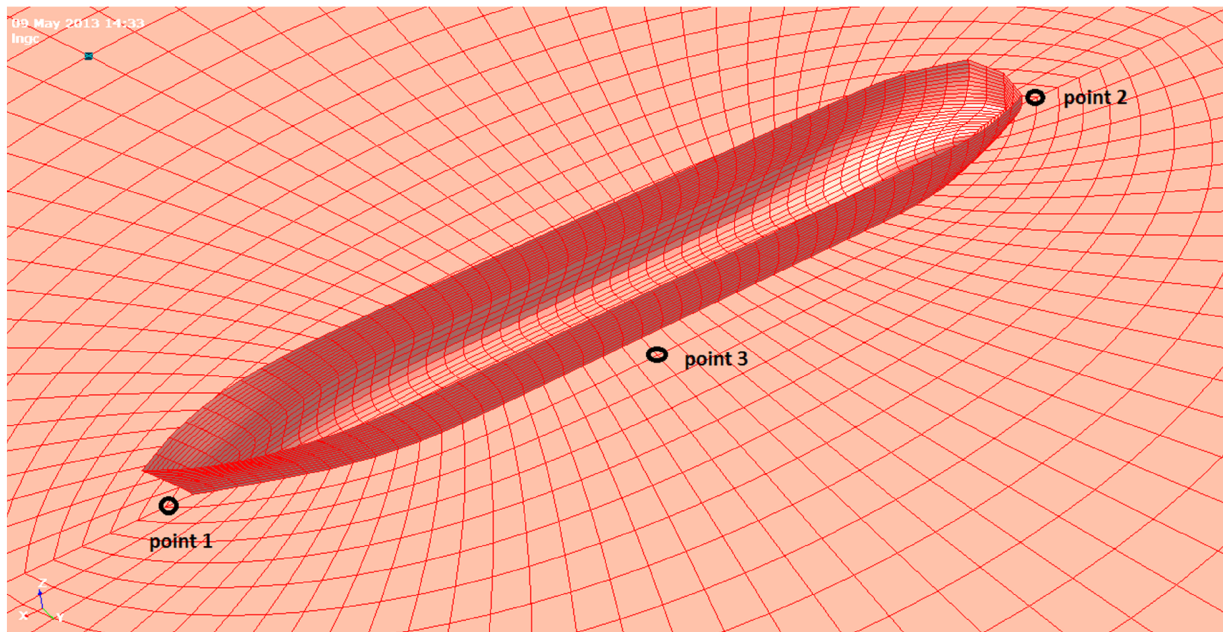
Figure 3-23 Positions where the time history of the wave elevations are plotted

The elevations in the following three pictures are collected from the nonlinear analysis at the red point in wave 22 in figure 3-22. The elevations of wave diffraction plus wave radiation are much smaller than the incident wave elevations, so whether ilin_surf=0 or 6 is applied does not affect the motion responses significantly. It is the incident wave condition and the body

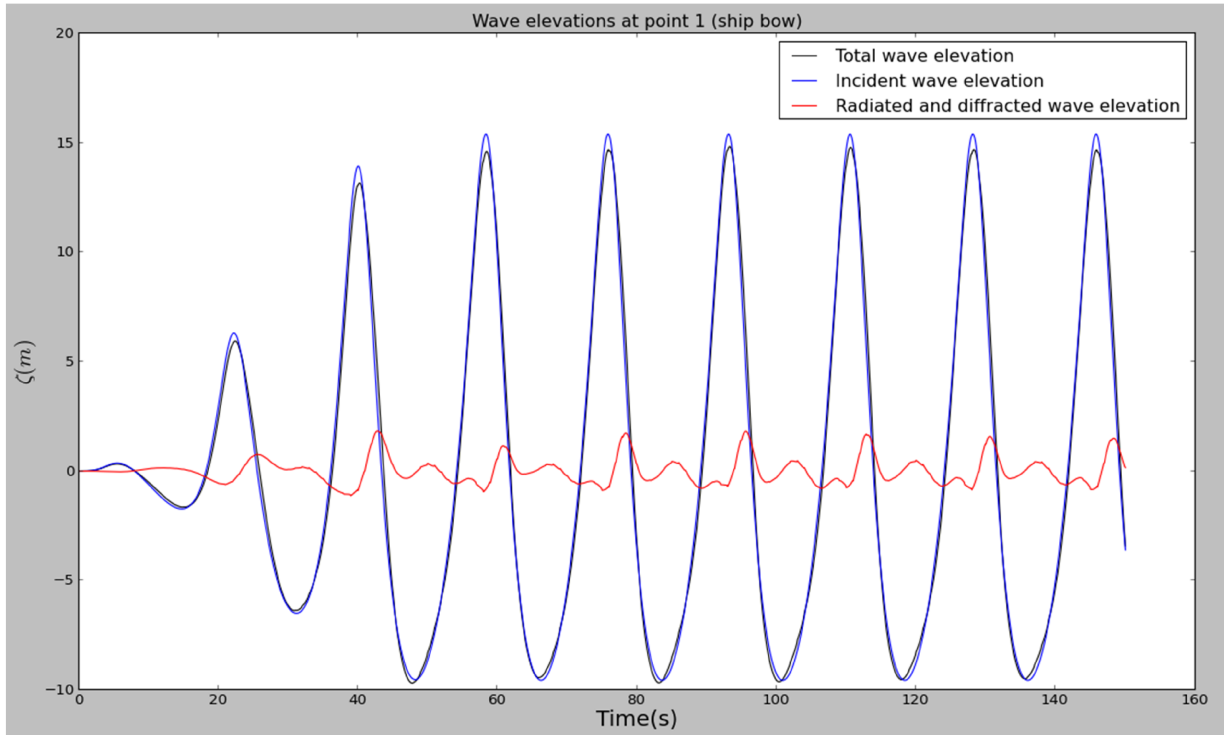**Figure 3-24 The time history of the wave elevations in front of the ship bow**
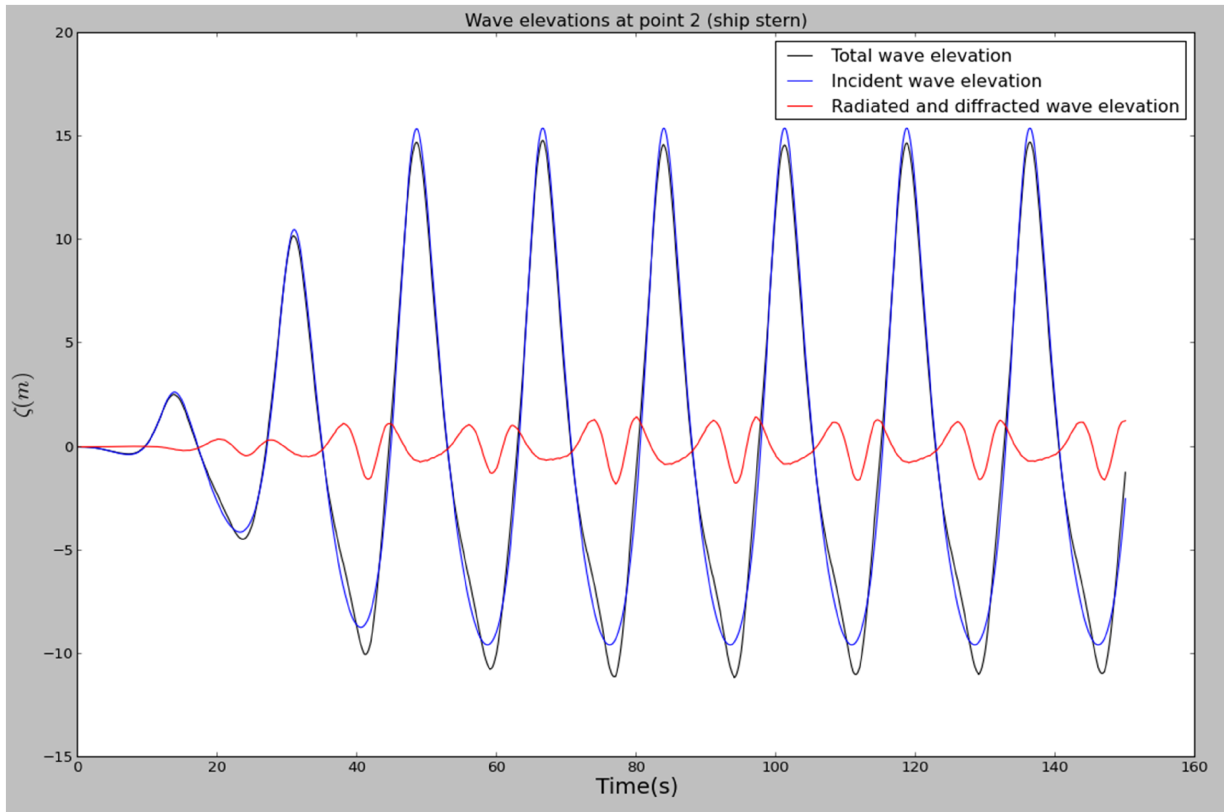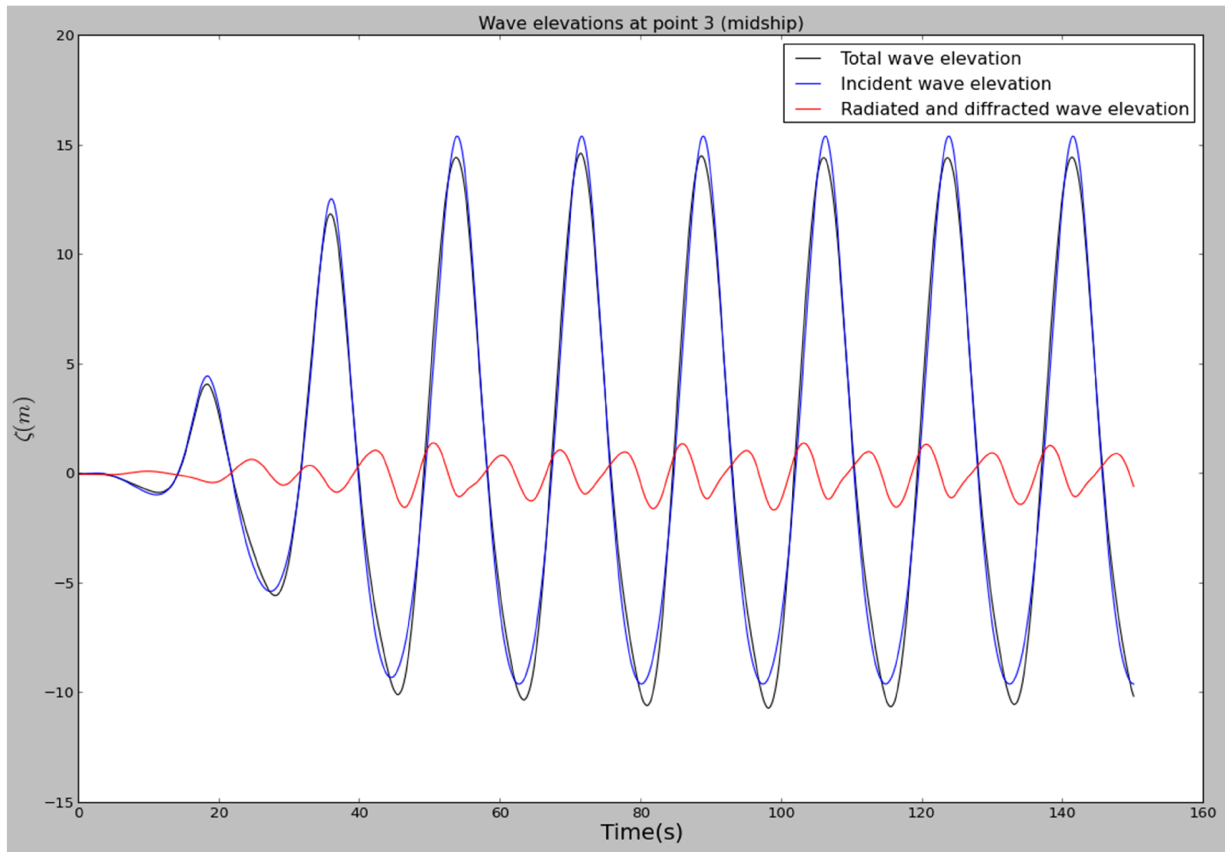

Figure 3-25 The time history of the wave elevations beside midship

Figure 3-26 The time history of the wave elevations behind the ship stern

boundary condition which decides the motion responses by most, and the body boundary condition is always evaluated at the mean position when solving memory flow. On the other side, the nonlinearity in the incident waves affects the motion amplitudes very little, except in wave condition 22 and 21 which has a period about 1.96s and 1.86s respectively (16.36s and 15.57s in full scale) close to the pitch resonance.

At last, we take the wave condition 22 where in figure 3-22 the difference between the red and blue points is largest, and keep the wave period constant while decrease the wave height to 20m, 15m, 10m, 5m and 1m respectively. The purpose is to check if the combination of the stream function method and the free surface conditions alternative 2 will gives results converging to the linear answers. The pitch responses have also been divided by wave amplitude so that the linear answers will become a horizontal line. The following two figures give evidence of the good consistence with linear theory regarding the new implementations to Wasim.
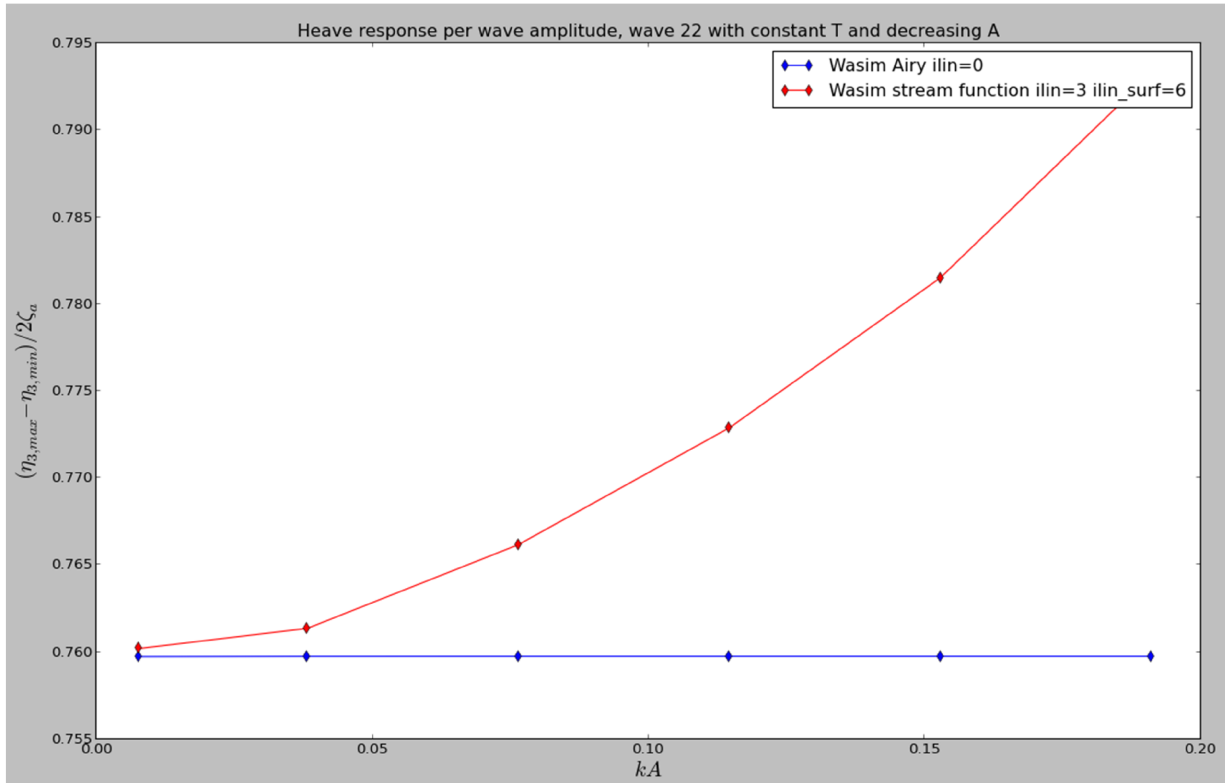
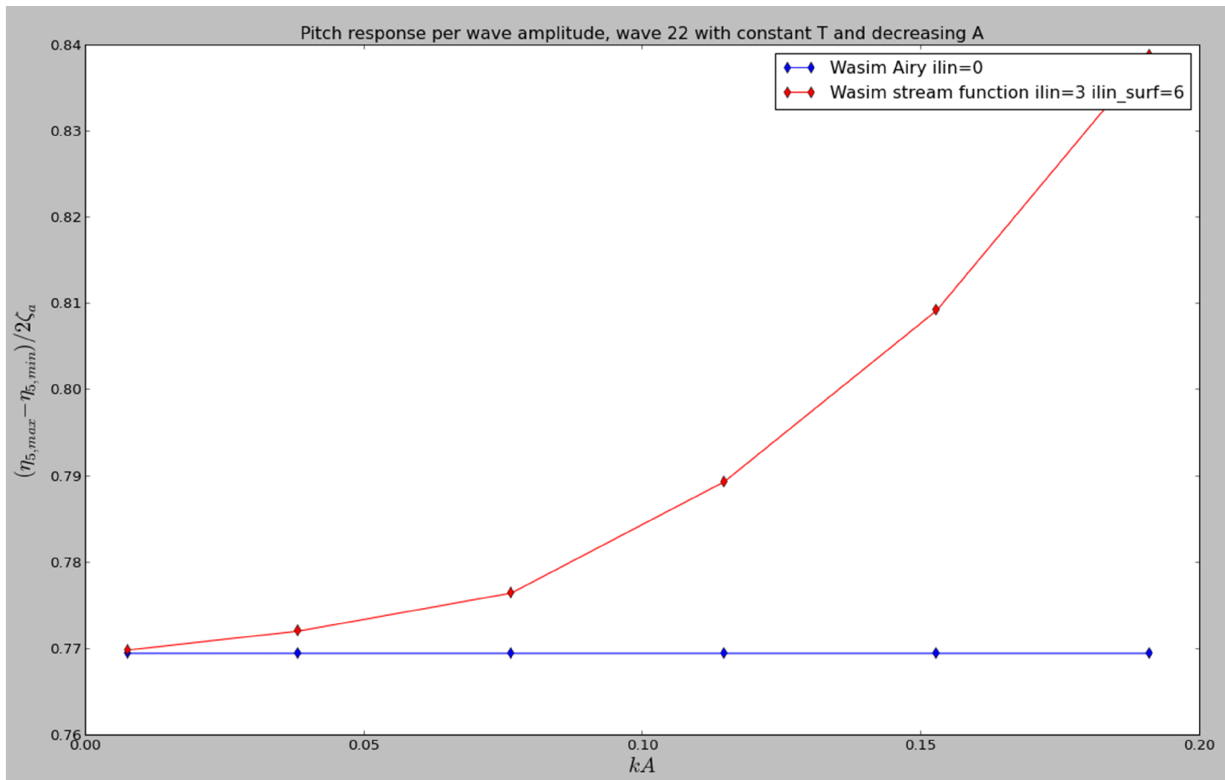**Figure 3-27 Heave responses from the nonlinear analysis converge to the linear results**

Figure 3-28 Pitch responses from the nonlinear analysis converge to the linear results

References

Clauss, G & Klein, M & Dudek, M (2011), ''model test report – LNG Carrier (TUB)'', Extreme Seas

Ferrant, Pierre (1998), ''Fully nonlinear interactions of long crested wave packets with a three dimensional body'', Twenty-Second Symposium on Naval Hydrodynamics

Greco, Marilena (2011), Lecture Notes "Sea loads", NTNU

Greco, Marilena (2001), ''A two dimensional study of green water loading'', NTNU

Huseby, M & Grue, John (2000), '' An experimental investigation of higher-harmonic wave forces on a vertical cylinder'', Journal of Fluid Mechanics

Intel® Fortran Compiler XE 12.1 User and Reference Guides

Kring, David C (1994), "Time domain ship motions by a three-dimensional Rankine panel method", MIT

McCamy, R.C. & Fuchs, R.A. (1954), ''Wave forces on a pile: A diffraction theory'', Technical memorandum No. 69

Numpy and Scipy documentation, Numpy 1.7 reference

Python 2.7.5 documentation, the python language reference

Sesam HydroD User Tutorial (2010), "Analysis of a Semi-submersible with anchors by use of Wadam and Wasim", DNV

Sesam User Manual HydroD (2011), "Wave load & stability analysis of fixed and floating structures", DNV

Sesam User Manual Wasim (2011), "Wave Loads on Vessels with Forward Speed", DNV

Sun, Hui (2012), D-4.1-DNV, DNV

Vada, Torgeir (1994), DNV Research Report NO.94-2030, DNV

Vada, T. & Nakos, D.E. (1993), ''Time marching schemes for ship motion simulations'', 8th International Workshop on Water Waves and Floating Bodies

4 Summary and comments

Generation of incident waves by stream function method is now available in Wasim and verified. The method not only covers the Stokes 5th, but also extends the validity range for possible wave inputs. This will be an important update for Wasim considering nonlinear analyses in shallow water. But the use of Dalrymple's approach is still not perfect due to the disadvantage when handling extremely long waves, so further implementation of Fenton's approach may be reasonable.

The stream function method and the free surface conditions alternative 2 seems to cooperate well through several verification analyses. Although not all the tests are in shallow water due to limited public references available to be compared with, we assume that the water shallowness affects mainly the nonlinearity in waves by more asymmetry forming in the wave profile when potential theory is applied. We focus thus by most at how the nonlinearity will change the response results.

In the wave diffraction problem, nonlinear free surface conditions are quite necessary to predict accurate load response when kA gets value larger than 0.1. As we assume that the body boundary condition remains the same in both linear and nonlinear analyses, then the free surface conditions rule how waves will be diffracted, which is directly associated with the dimension of wetted surface on the body, i.e. how the free surface conditions are implemented is the most essential factor to force integration. The nonlinearity in the incident wave, on the other side, determines the asymmetry of the incident wave profile which further determines the instantaneous wave kinematics impacting on the body. This nonlinearity may give a vertical translation to load responses, but it will not change the load amplitudes so much until kA increases to 0.2. According to the comparisons, the nonlinear free surface conditions alternative 2 combined with stream function method gives the most satisfying results.

In the "body motion" problem, the wave diffractions and radiations are so small that we cannot throw a concrete vote to the nonlinear free surface conditions, though the results are a bit more compatible to the experiment results when the nonlinear free surface conditions are applied. Whether this superiority will rise up with growing wave diffractions and radiations cannot

be decided at present without further testing. The nonlinearity in the incident wave affects the motion amplitudes very little except for the excitations approaching to body's resonance frequency.

After all, I need to say that this master thesis is very interesting, and I have learned a lot from both literature and practical sides. Actually it is a great combination of theories and implementations. In addition, I also want to mention some of my impressions and several comments by the following.

- It may take much longer for verification and evaluation than to implement some theory or method when we consider both stability and accuracy.
- When comparing with experiment results, we should not always trust these numbers as reference. It is worth to keep a critical mind and make sure that they are in good quality.
- Post-processing plays also an important role as the results may be sensitive to the process algorithm. Fourier analysis is a traditional way and can be the first choice to handle the result signal. FFT may be the best for signals which have some random parameter while harmonic analysis suits better for regular signals. But we should pay attention if the regular signal has a horizontal asymmetric profile. To choose a proper algorithm will be time saving if there are huge amounts of data, e.g. to find every local maximums can be realized by several approaches: by looping through all the values, by differentiating the signal, and can also be done by some fancy approach such as genetic algorithm.
- HydroD (the housing of Wasim, which provides GUI for some pre- and post-process functionality) can generate the mesh of free surface automatically, and the size of free surface is determined based on the dimension of the body. But this may lead to too small free surface area for some shallow water analysis, i.e. the radius of free surface is shorter than the wave length, because slender bodies are dominating in shallow water and relatively long waves become frequent. The limited free surface area will act as a tank and cause oscillations due to reflected waves. Therefore it would be better if the size of free surface is determined based on the wave length instead when the program detects a small water depth.

- Considering long crested waves, Airy wave, Stokes 5th wave and stream function wave are now available in Wasim. It would be nice to include also pre-established or measured wave time history as input to Wasim. This may extend the program from prediction by idealized modeling to kind of postmortem analysis.

Appendix A   Linearization of free surface conditions for 3D wave body interaction

i) The kinematic free surface condition:

$$\left(\frac{D}{Dt} + \nabla\phi_{tot} \cdot \nabla\right) \cdot [z - \zeta] = 0 \text{ , and introduce Galilean transform } \frac{D}{Dt} = \frac{\partial}{\partial t} - \overrightarrow{W} \cdot \nabla$$

$$\Rightarrow \left(\frac{\partial}{\partial t} - \overrightarrow{W} \cdot \nabla + \nabla\phi_{tot} \cdot \nabla\right) z = \left(\frac{\partial}{\partial t} - \overrightarrow{W} \cdot \nabla + \nabla\phi_{tot} \cdot \nabla\right) \zeta$$

L.H.S: $\frac{\partial z}{\partial t} = 0$ since z is only coordinate of a certain point on the free surface and it does not follow a water particle, so it is not a function of time.

$\overrightarrow{W} \cdot \nabla z = 0$ since $\nabla z = (0,0,1)$ and $\overrightarrow{W}$ has no k-component.

$$\nabla\phi_{tot} \cdot \nabla z = \frac{\partial\phi_{tot}}{\partial z}$$

R.H.S= $\left(\frac{\partial}{\partial t} - \overrightarrow{W} \cdot \nabla\right) \zeta + \nabla\phi_b \cdot \nabla\zeta$ since $\phi_l, \phi_m, \zeta = O(\epsilon)$

$$\Rightarrow \frac{\partial\zeta}{\partial t} - \left(\overrightarrow{W} - \nabla\phi_b\right) \cdot \nabla\zeta = \frac{\partial}{\partial z}(\phi_b + \phi_l + \phi_m) \text{ on } z = \zeta$$

Apply Taylor expansion for small ζ about z=0 for all z-dependent terms, e.g.

$$\left(\frac{\partial\phi_b}{\partial z}\right)_{z=\zeta} \approx \left(\frac{\partial\phi_b}{\partial z}\right)_{z=0} + \frac{\partial}{\partial z}\left(\frac{\partial\phi_b}{\partial z}\right)_{z=0} \cdot \zeta + O(\epsilon^2)$$

$$\left(\frac{\partial\phi_m}{\partial z}\right)_{z=\zeta} \approx \left(\frac{\partial\phi_m}{\partial z}\right)_{z=0} + O(\epsilon^2)$$

Since $\frac{\partial\phi_b}{\partial z} = 0$ on $z = 0$

$$\Rightarrow \frac{\partial\zeta}{\partial t} - \left(\overrightarrow{W} - \nabla\phi_b\right) \cdot \nabla\zeta = \frac{\partial^2\phi_b}{\partial z^2} \cdot \zeta + \frac{\partial}{\partial z}(\phi_l + \phi_m) \text{ on } z = 0$$

Now we consider only the memory flow and introduce ϕ_i and ζ_i due to incident wave.

$$\Rightarrow \frac{\partial(\zeta+\zeta_i)}{\partial t} - \left(\vec{W} - \nabla\phi_b\right) \cdot \nabla(\zeta + \zeta_i) = \frac{\partial^2\phi_b}{\partial z^2} \cdot (\zeta + \zeta_i) + \frac{\partial}{\partial z}(\phi_i + \phi_m + \phi_l)$$

And further we introduce the linear kinematic free surface condition for the incident wave.

$$\frac{\partial\phi_i}{\partial z} = \frac{D\zeta_i}{Dt} = \left(\frac{\partial}{\partial t} - \vec{W} \cdot \nabla\right)\zeta_i$$

$$\Rightarrow \frac{\partial\zeta}{\partial t} - \left(\vec{W} - \nabla\phi_b\right) \cdot \nabla\zeta = \frac{\partial^2\phi_b}{\partial z^2} \cdot (\zeta + \zeta_i) + \frac{\partial(\phi_m + \phi_l)}{\partial z} - \left(\nabla\phi_b \cdot \nabla\zeta_i\right)$$

ii) Dynamic free surface condition:

$$\frac{D\phi_{tot}}{Dt} = -g\zeta - \frac{1}{2}(\nabla\phi_{tot})^2 \text{ , and introduce Galilean transform } \frac{D}{Dt} = \frac{\partial}{\partial t} - \vec{W} \cdot \nabla$$

$$\Rightarrow \left(\frac{\partial}{\partial t} - \vec{W} \cdot \nabla\right)(\phi_b + \phi_l + \phi_m) = -g\zeta - \frac{1}{2}\left(\nabla(\phi_b + \phi_l + \phi_m)\right)^2, \text{ keep the linear terms}$$

$$\Rightarrow \left(\frac{\partial}{\partial t} - \left(\vec{W} - \nabla\phi_b\right) \cdot \nabla\right)(\phi_l + \phi_m) = -g\zeta + \vec{W} \cdot \nabla\phi_b - \frac{1}{2}(\nabla\phi_b)^2 \text{ on } z = \zeta$$

Apply Taylor expansion for small ζ about $z = 0$ for all z-dependent terms, e.g.

$$\left(\vec{W} \cdot \nabla\phi_b\right)_{z=\zeta} \approx \vec{W} \cdot (\nabla\phi_b)_{z=0} + \vec{W} \cdot \frac{\partial}{\partial z}(\nabla\phi_b)_{z=0} \cdot \zeta + O(\epsilon^2)$$

since $\frac{\partial}{\partial z}(\nabla\phi_b)_{z=0} = \left(\frac{\partial^2\phi_b}{\partial z\partial x}, \frac{\partial^2\phi_b}{\partial z\partial y} \cdot \frac{\partial^2\phi_b}{\partial z^2}\right) = \left(\frac{\partial^2\phi_b}{\partial x\partial z}, \frac{\partial^2\phi_b}{\partial y\partial z} \cdot \frac{\partial^2\phi_b}{\partial z^2}\right) = \left(0,0,\frac{\partial^2\phi_b}{\partial z^2}\right)$

$$\Rightarrow \vec{W} \cdot \frac{\partial}{\partial z}(\nabla\phi_b)_{z=0} \cdot \zeta = 0$$

$$\Rightarrow \left(\vec{W} \cdot \nabla\phi_b\right)_{z=\zeta} \approx \vec{W} \cdot (\nabla\phi_b)_{z=0}$$

$$(\nabla\phi_b \cdot \nabla\phi_b)_{z=\zeta} \approx (\nabla\phi_b \cdot \nabla\phi_b)_{z=0} + \frac{\partial}{\partial z}(\nabla\phi_b \cdot \nabla\phi_b)_{z=0} \cdot \zeta + O(\epsilon^2)$$

since $\frac{\partial}{\partial z}(\nabla\phi_b \cdot \nabla\phi_b) = \frac{\partial}{\partial z}\left(\left(\frac{\partial\phi_b}{\partial x}\right)^2 + \left(\frac{\partial\phi_b}{\partial y}\right)^2 + \left(\frac{\partial\phi_b}{\partial z}\right)^2\right) = 2 \cdot \frac{\partial\phi_b}{\partial x} \cdot \frac{\partial^2\phi_b}{\partial z\partial x} + 2 \cdot \frac{\partial\phi_b}{\partial y} \cdot \frac{\partial^2\phi_b}{\partial z\partial y} + 2 \cdot$

$\frac{\partial\phi_b}{\partial z} \cdot \frac{\partial^2\phi_b}{\partial z^2} = 0$

$$\Rightarrow (\nabla\phi_b \cdot \nabla\phi_b)_{z=\zeta} \approx (\nabla\phi_b \cdot \nabla\phi_b)_{z=0}$$

$$\Rightarrow \left(\frac{\partial}{\partial t} - \left(\vec{W} - \nabla\phi_b\right) \cdot \nabla\right)(\phi_l + \phi_m) = -g\zeta + \vec{W} \cdot \nabla\phi_b - \frac{1}{2}(\nabla\phi_b)^2 \text{ on } z = 0$$

Now we consider only the memory flow and introduce ϕ_i and ζ_i due to incident wave.

$$\Rightarrow \left(\frac{\partial}{\partial t} - \left(\vec{W} - \nabla\phi_b\right) \cdot \nabla\right)(\phi_i + \phi_m) = -g(\zeta + \zeta_i) + \vec{W} \cdot \nabla\phi_b - \frac{1}{2}(\nabla\phi_b)^2$$

And further we introduce the linear dynamic free surface condition for the incident wave.

$$\frac{D\phi_i}{Dt} + g\zeta_i = 0 \Rightarrow \left(\frac{\partial}{\partial t} - \vec{W} \cdot \nabla\right)\phi_i + g\zeta_i = 0$$

$$\Rightarrow \left(\frac{\partial}{\partial t} - \left(\vec{W} - \nabla\phi_b\right) \cdot \nabla\right)\phi_m = -g\zeta + \vec{W} \cdot \nabla\phi_b - \frac{1}{2}(\nabla\phi_b)^2 - (\nabla\phi_b \cdot \nabla\phi_i)$$